universität wien

MASTERARBEIT

Titel der Masterarbeit

INVESTIGATION OF THE 2A PROTEASE OF HUMAN RHINOVIRUS 1A AND 14

Martina Aumayr, BSc

angestrebter akademischer Grad

Master of Science (MSc)

Wien, 2012

Studienkennzahl lt. Studienblatt:	A 066 830
Studienrichtung lt. Studienblatt:	Master Molekulare Mikrobiologie und Immunbiologie
Betreuerin / Betreuer:	Ao. Univ.-Prof. Dr. Timothy Skern

ACKNOWLEDGEMENT

It is a pleasure to thank all those who supported me during this thesis:

In particular I would like to thank my supervisor Prof. Tim Skern for giving me the chance to work in his lab on this fascinating topic and for all the important advices throughout my work.

I would also like to express my gratitude to David Neubauer for his introduction into laboratory work and his help and guidance whenever I needed it. I am also very grateful to my other lab mates Jutta Steinberger, Sofiya Fedosyuk, Tomas Sara and Flàvia Leite for providing a great atmosphere in the lab and for accompanying me through good and bad times. Furthermore, I would like to thank Irene Gösler for introducing me to cell culture and for the help concerning cells and virus.

Special thanks go to my family, in particular to my parents for their unconditional love, guidance, patience, and support in any respect throughout my life. Thanks, that you always encouraged me to study the subject of my choice. Moreover, I would like to say thank you to my brothers, Christian and Lukas, for the questions concerning my work and for their entertainment throughout the last year.

In addition, I would like to thank all of my friends for providing friendship, joy and support that I needed. Finally, I would like to say thank you to Markus Gunacker for the patience, motivation and endless support throughout my studies. Thanks for always listening to all my scientific stories and for believing in me.

TABLE OF CONTENTS

ABSTRACT

Human rhinoviruses (HRV), belonging to the family *Picornaviridae*, are small, non-enveloped viruses with an icosahedral capsid and are one of the main causative agents of the common cold. After infection, the single-stranded RNA genome of positive sense containing one large open reading frame is directly translated into a polyprotein, which is subsequently processed to yield mature viral proteins. The first cleavage event is performed by the chymotrypsin-like proteinase $2A^{pro}$ in HRVs which cleaves between the C-terminal of the preceding protein VP1 and its own N-terminus.

Here, we investigate the different substrate specificities of the $2A^{pro}$ of HRV1A and HRV14, two human rhinoviruses from the different genetic groups, A and B, that show a great variation in the amino acid sequence at the cleavage site of the $2A^{pro}$.

Initially, we analyzed the effect of mutations in the cleavage site on the self-processing. We found that HRV1A $2A^{pro}$ is not able to accept the full HRV14 $2A^{pro}$ cleavage site *in vitro* as monitored by translation in rabbit reticulocyte lysates (RRL). It was further shown that these multiple mutations also severely impair the self-processing *in vivo*, as no viral offspring could be generated after the transfection of corresponding RNA in HeLa cells. Subsequently, we demonstrated that substitutions on both side of the cleavage junction are necessary to stop proteolytic processing *in vitro*. Mutating residues on only one side of the $2A^{pro}$ cleavage junction resulted only in a slightly delayed self-processing *in vitro*.

In the next step, we tried to find the minimal number of HRV14 residues required to abrogate proteolytic activity of HRV1A $2A^{pro}$. We showed that changing residues P2, P1 (threonine and alanine) and P2' (proline) at the $2A^{pro}$ cleavage junction of HRV1A with corresponding residues of HRV14 (serine, tyrosine and leucine, respectively) was enough to prevent the HRV1A $2A^{pro}$ from processing. This sub-optimal cleavage site was introduced into a HRV1A full length clone and HeLa cells were transfected with viral RNA. We were able to identify several representatives of two different escape mutants in response to this cleavage site. Most escape mutants had changed tyrosine at P1 to cysteine, which was rather surprising, as tyrosine was normally very well accepted at this position in the wild-type HRV2 $2A^{pro}$ (HRV1A is closely related to that of HRV2) cleavage (Sommergruber et al., 1992). Another response was to mutate leucine, at P2', back to the wild type proline.

In addition, we exchanged the highly conserved glycine at position P1' with the slightly larger amino acid alanine which also completely stopped the self-processing reaction of the HRV1A $2A^{pro}$ *in vitro*. All escape mutants isolated had reverted alanine back to the wild type glycine. These *in vivo* experiments demonstrate that glycine is the only amino acid accepted at this position in the *cis* cleavage reaction of HRV1A $2A^{pro}$. In our model, the HRV2 $2A^{pro}$ tyrosine 85, which is rotated after the binding of the substrate to the enzyme, and the subsequent formation of a hydrogen bond between

threonine at position P2 (substrate) and serine 83 (enzyme) would block the access of any bulkier molecule at the P1' site other than glycine. Any residue bigger than alanine would also be blocked by leucine 19; however, alanine would be small enough to not be blocked by leucine 19.

As previous results have suggested that the activity of the $2A^{pro}$ is influenced by the neighboring protein 2B *in vitro* (Kirkegaard and Neubauer, both pers.comm.), we aimed to transfect HeLa cells with the RNA containing the mutation I94N in the 2B in order to possibly be able to isolate escape mutants. However, we showed that the activity of the HRV14 $2A^{pro}$ is not influenced *in vivo* by the 2B I94N mutation. We could not detect any difference *in vivo* neither in regard to plaque phenotypes nor to growth kinetics compared to wild type HRV14. We further isolated two escape mutants having an additional mutation in the $2A^{pro}$ (M17T and P4H). These second site revertants showed reduced growth kinetics compared to wild type HRV14 and single HRV14 2B I94N mutant. Therefore, we concluded that these mutations were probably introduced incidentally by the error-prone RNA polymerase.

Furthermore, previous experiments have shown that HRV14 $2A^{pro}$ is not able to accept an arginine (in place of a tyrosine) in the P1 position of the cleavage site (Sousa et al., 2006). We therefore again tried to transfect HeLa cells with RNA containing the mutation Y289R in the VP1 in order to search for escape mutants. Here, we showed that the activity of the HRV14 $2A^{pro}$ is influenced *in vivo* by the VP1 Y289R mutation also. Much smaller plaques were observed when transfecting cells with the VP1 Y289R mutant than with the wild type HRV14. In addition, viral growth was not only delayed but did also not reach the same amount of maximum yield. However, the difference was only about 1 log, which does not explain the very small plaque sizes of this mutant. We therefore assume that this mutation might lead to a defect in spreading or lysis as it affects the sequence of the capsid protein VP1.

The work in this thesis shows that exchanging combinations of residues on both side of the cleavage junction are necessary to inhibit the intramolecular cleavage of the HRV1A $2A^{pro}$. However, the replacement of one side is enough to recover proteolytic activity of this enzyme. We show that cysteine at the position P1 of the cleavage junction is accepted by the HRV1A $2A^{pro}$ *in vivo*. Although the VP1 Y289R mutation was shown to inactivate the HRV14 $2A^{pro}$ *in vitro*, we demonstrate that is not the case *in vivo*. However, a small plaque phenotype can be observed which might be due to the presence of arginine at the P1 position of the cleavage junction of HRV14 $2A^{pro}$. We conclude that it is further necessary to investigate substrate specificity of both HRV1A and HRV14 $2A^{pro}$. However, from what we can say so far, both proteases display distinct substrate specificities; thus, specific inhibitors will be necessary for each protease if they are to be used to treat the common cold.

ZUSAMMENFASSUNG

Humane Rinoviren (HRV), welche zu der Gruppe der Picornaviridae gehören, sind die Erreger die Schnupfen und Erkältung beim Menschen erzeugen. Die sehr kleinen Viren besitzen keine Lipidschicht als Hülle und weisen die Symmetrie eines Ikosaeders auf. Als genomisches Material besitzen sie eine einzelsträngige RNA mit positiver Polarität, die nur einen offenen Leserahmen besitzt. Von diesem wird ein langes Polyprotein abgelesen, das sogleich von viralen Proteasen prozessiert wird um fertig entwickelte, virale Proteine zu erhalten. In HRV wird der erste Schritt dieser Prozessierung von der Chymtrypsin-ähnlichen Protease $2A^{pro}$ durchgeführt, die sich selbst in einer intramolekularen Reaktion zwischen dem C-Terminus des vorrangehenden Proteins VP1 und ihrem eigenen N-Terminus abspaltet.

In dieser Arbeit wird die unterschiedliche Substrat-Spezifität von HRV1A und HRV14, zwei aus unterschiedlichen genetischen Gruppen stammenden HRV (A und B), untersucht. Die Aminosäuresequenz der Spaltungsstelle der $2A^{pro}$ dieser beiden HRVs ist besonders unterschiedlich.

Am Anfang analysieren wir den Effekt unterschiedlicher Mutationen in der Schnittstelle auf die Selbstprozessierungsreaktion. Dabei finden wir heraus, dass die $2A^{pro}$ von HRV1A nicht in der Lage ist, die Schnittstelle der $2A^{pro}$ von HRV14 zu akzeptieren, wenn sie gänzlich ausgetauscht wird. Wir beobachten den Spaltungsprozess während der Translation mit Hilfe von Kaninchen Retikulozytenlysaten. Weiters zeigen wir, dass diese vielen Mutationen in der Spaltungsstelle nicht nur die Selbst-Prozessierung *in vitro* stark beeinflussen, sondern auch kein viraler Nachkomme nach der Transfektion der entsprechenden RNA in HeLa Zellen generiert werden kann. Im Rahmen dessen, demonstrieren wir, dass Veränderungen auf beiden Seiten der Spaltungsstelle notwendig sind, um die proteolytische Aktivität *in vitro* zu stoppen. Wenn man nur eine Seite rechts oder links des Spaltungspunktes austauscht erhält man lediglich eine zeitverzögerte Selbst-Prozessierung *in vitro*.

Im nächsten Schritt, versuchen wir die minimale Anzahl an Aminosäuren, welche notwendig sind um die proteolytische Aktivität der $2A^{pro}$ von HRV1A zu stoppen, herauszufinden. Wir zeigen, dass die Veränderung von den Aminosäuren an den Stellen P2, P1 (Threonin und Alanin) und P2‘ (Prolin) der HRV1A $2A^{pro}$ Prozessierungsstelle, wenn sie durch die entsprechenden Aminosäuren der HRV14 $2A^{pro}$ an diesen Stellen (Serin, Tyrosin und Leucin) ausgetauscht werden, ausreichen um die Selbst-Prozessierung zu inhibieren. Diese nicht-optimale Spaltungsstelle wird in den kompletten HRV1A Klon eingefügt. Daraufhin werden HeLa Zellen mit dieser viralen RNA transfiziert. Es gelingt uns zwei unterschiedliche Arten von sogenannten Fluchtmutanten als Antwort auf die Spaltungseinschränkung der veränderten Spaltungsseite, zu isolieren. Die meisten Fluchtmutanten haben anstelle des Tyrosins an der P1 ein Cystein. Dies ist durchaus erstaunlich, da in vorangegangenen Studien ein Tyrosin an dieser Stelle der Spaltungsseite der HRV2 $2A^{pro}$, die sehr

ähnlich wie die HRV1A $2A^{pro}$ ist, von dieser ausgezeichnet akzeptiert wurde (Sommergruber et al., 1992). In anderen Mutanten konnten wir eine Rückänderung von Leucin zur ursprünglichen Aminosäure, dem Proline, beobachten.

Zusätzlich vertauschen wir das stark konservierte Glycin an der Stelle P1‘ mit der nächst größeren Aminosäure, dem Alanin. Auch diese Veränderung verhindert die Spaltungsreaktion der $2A^{pro}$ von HRV1A *in vitro*. Alle isolierten Fluchtmutanten haben dieses Alanin zurück zu Glycin gewandelt. Diese *in vivo* Experimente demonstrieren, dass Glycin die einzig akzeptierte Aminosäure an dieser Stelle in der intramolekularen Spaltung der $2A^{pro}$ von HRV1A ist. In unserem Model dreht das Tyrosin an der Stelle 85 in der HRV $2A^{pro}$, nach der Bindung des Substrats und der darauf folgenden Bildung einer Wasserstoffbrücke zwischen dem Threonin an der Stelle P2 des Substrats und dem Serin an der Stelle 83 des Enzyms hinaus und blockiert somit irgendeine umfangreichere Aminosäure als Glycin an der P1‘ Stelle. Eine größere Aminosäure als Alanin wird zusätzlich auch von Leucin an der Stelle 19 blockiert. Jedoch wäre Alanin klein genug um nicht von diesem Leucin blockiert zu werden.

Darüber hinaus beschäftigen wir uns auch mit der $2A^{pro}$ von HRV14, da vorrangegangene Ergebnisse zeigen, dass die Aktivität der $2A^{pro}$ von dem benachbarten Protein 2B *in vitro* beeinflusst wird (Kirkegaard und Neubauer, pers.comm.). Wir erhofften uns, durch die Transfektion dieser RNA, welche die Mutation I94N im 2B Protein erhielt, Fluchtmutanten isolieren zu können, welche uns einen Hinweis auf strukturell wichtige Aminosäuren geben. Wir zeigen jedoch, dass die Aktivität dieser $2A^{pro}$ *in vivo* nicht von der Mutation im 2B Protein (I94N) beeinflusst wird. Wir können keinen Unterschied zwischen dieser Mutante und dem HRV14 Wildtyp feststellen, weder in Zusammenhang mit den Erscheinungsformen der viralen Plaques noch im Wachstums. Jedoch können wir zwei Fluchtmutanten isolieren. Da aber auf der einen Seite kein Wachstumsdefekt der Einzel-2B-Mutante festgestellt werden kann, und auf der anderen Seite die Fluchtmutanten eine reduzierte Wachstumsrate aufweisen, schließen wir daraus, dass diese Mutationen aufgrund der natürlichen Evolution eingefügt wurden und nichts mit unserer eingefügten Mutation zu tun haben.

Außerdem haben weitere Experimente gezeigt, dass die HRV14 $2A^{pro}$ ein Arginin (anstatt Tyrosin) an der Stelle P1 der Spaltungsstelle nicht akzeptiert (Sousa et al., 2006). Daher untersuchen wir die Beeinflussung dieser Mutation (Y289R in VP1) *in vivo* und versuchen erneut Fluchtmutanten zu isolieren. Ein Unterschied in der Größe der Plaques nach der Transfektion kann festgestellt werden. Diese Mutante zeigt deutlich kleinere virale Plaques als der HRV14 Wildtyp. Zusätzlich ist die Wachstumsrate nicht nur etwas verzögert, es kann auch nie die maximale Ausbeute an Virus erreicht werden. Da jedoch der Unterschied nur ein Log beträgt, kann dies nicht vollständig den äußerst kleinen Durchmesser der Plaques erklären. Wir vermuten allerdings, dass diese Mutation zu einem zusätzlichen Defekt in der viralen Ausbreitung oder der Lyse führt.

Die Ergebnisse dieser Arbeit zeigen, dass es notwendig ist beide Seiten der HRV1A $2A^{pro}$ Spaltungsstelle auszutauschen um die intramolekulare Spaltung zu inhibieren. Jedoch ist es *in vivo* ausreichend nur eine Seite zu verändern, um die proteolytische Aktivität der HRV1A $2A^{pro}$ wiederherzustellen. Wir zeigen außerdem, dass ein Cystein an der Stelle P1 von der HRV1A $2A^{pro}$ *in vivo* akzeptiert wird. Obwohl die Mutation im VP1 Protein (Y289R) *in vitro* zu einer Inaktivierung der HRV14 $2A^{pro}$ geführt hat, zeigen wir dass die HRV14 $2A^{pro}$ mit dieser Mutation *in vivo* aktiv ist. Jedoch können wir eine Veränderung der Plaquegröße feststellen, die wir auf das Vorhandensein von Arginin anstelle des Tyrosins an der Stelle P1 zurückführen. Daraus folgern wir, dass weitere Erforschungen bezüglich der Substratspezifität der $2A^{pro}$ von HRV1A und HRV14 notwendig sind. Bis jetzt kann man allerdings sagen, dass beide Proteasen eine unterschiedliche Substratspezifität aufweisen, und man wahrscheinlich spezifische Inhibitoren gegen jede dieser Proteasen herstellen wird müssen um den Schnupfen zu behandeln.

1 INTRODUCTION

1.1 PICORNAVIRUSES

The family *Picornaviridae* derives its name from the greek word *pico* meaning very small and RNA referring to their single-stranded positive-sense RNA (Semler and Wimmer, 2002). Indeed, picornaviruses are small viruses with a 28-30 nm diameter of their non-enveloped icosahedral capsid, which encloses one naked molecule of positive sense single-stranded RNA ranging from 7.2-8.5 kilobases (kb). Well-known picornaviruses include poliovirus, human hepatitis A virus, human rhinovirus and foot-and-mouth disease virus. They cause a variety of diseases in human and animals, including poliomyelitis, hepatitis, the common cold and foot-and-mouth disease (Semler and Wimmer, 2002; Racaniello, 2007).

According to the most recent taxonomy, the international committee on taxonomy of viruses (ICTV, 2009; Knowles et al., 2011), the family *Picornaviridae* contains 12 genera. These genera are: *Aphthovirus*, *Avihepatovirus*, *Cardiovirus*, *Enterovirus*, *Erbovirus*, *Hepatovirus*, *Kobuvirus*, *Parechovirus*, *Sapelovirus*, *Senecavirus*, *Teschovirus* and *Tremovirus*. Each genus is further divided into species containing one or more antigenically distinct serotypes ((ICTV, 2009; Knowles et al., 2011). The high similarity of sequence and genome organization has led the former genera Rhinovirus and Enterovirus to be recently (2009) re-classified together into the genus of Enterovirus.

1.2 HUMAN RHINOVIRUS

This thesis deals with the substrate specificity of the proteinase $2A^{pro}$ of human rhinovirus (HRV); therefore, the introduction is based on the Enterovirus genus.

One of the most frequent infectious diseases in humans, the common cold, is caused by human rhinoviruses (Makela et al., 1998). Although HRVs make up about 30% of all common colds (Monto and Sullivan, 1993), little progress in the generation of vaccines or anti-viral compounds for the treatment of HRVs has been made (Papi and Contoli, 2011). HRV are transmitted via the respiratory-salivary route and are able to infect the upper as well as the lower respiratory tract (Savolainen et al., 2003). Infection of the lower respiratory tract can cause more severe diseases such as asthma (Nicholson et al., 1993) and chronic obstructive pulmonary disease (COPD) exacerbations (Johnston, 2005).

The current taxonomy (ICTV, 2009; Knowles et al., 2011) classifies HRV in the *Enterovirus* genus of the *Picornaviridae* family and distinguishes between three different species: *HRV*-A, *HRV*-B and *HRV*-C (Palmenberg et al., 2010). The *HRV*-C species was identified in 2006 (Lamson et al., 2006; Kistler et al., 2007). Several studies reveal that HRV-C types induce more severe illnesses in children (Lee et al., 2007) and are highly prevalent and widely circulating worldwide (Renwick et al., 2007; Lau et al., 2009). 77 serotypes have as yet been identified to belong to the species HRV-A, 25 serotypes to HRV-B and 49 serotypes to the species HRV-C (http://www.picornaviridae.com/).

HRV serotypes are classified into one of the three groups A, B and C based on genetic relationships. One way to cluster the serotypes A and B is according to sequence homologies in the viral capsid proteins VP1 and VP4 (Laine et al., 2006). Classification into HRV-C was done recently by sequence comparison of the VP4/VP2 region (Simmonds et al., 2010). Secondly, the A and B serotypes can be classified according to the receptor used for attachment and entry. Two receptors have been identified so far. Major group viruses, to which about 90% of all A and B serotypes belong to, use the intercellular adhesion molecule 1 (ICAM-1) as receptor for attachment and as catalyst for the subsequent viral uncoating during cell entry (Staunton et al., 1989; Rossmann, 1994; Bella and Rossmann, 1999). The minor group of rhinoviruses uses the low-density lipoprotein receptor (LDLR) as their receptor for cell entry (Hofer et al., 1994). The minor group of rhinoviruses is exclusively HRV-A serotypes. HRV-Cs probably use a unique cellular receptor, as propagation in cell culture is not very successful at present (Palmenberg et al., 2009).

1.3 VIRION STRUCTURE

1.3.1 CAPSID

Picornaviruses have a simple structure with a spherical shape of only about 28-30 nm of diameter. The genomic material is tightly packed into an icosahedral capsid, consisting of an arrangement of 60 identical asymmetric subunits (protomers) arranged as 12 pentamers (Janner, 2006). Each protomer consists of one copy of four structural proteins, viral protein (VP) 1, VP2, VP3 and VP4. During maturation of the viral particle, the precursor VP0 is cleaved autocatalytically to yield VP2 and VP4 (see chapter 1.4.2). These four proteins are arranged in a T=3 icosahedron displaying 20 threefold axes and 12 fivefold axes (Racaniello, 2007). Figure 1 shows the structure of a typical picornaviral capsid and a representation of the packing of viral proteins into the icosahedral shell. Capsid proteins VP1-VP3 form the external surface whereas VP4 is located in the interior and is associated by a distributed network of contacts with VP1-VP3 within a protomer (Rossmann et al., 1985; Flint et al., 2009).

Although the amino acid sequences of VP1-VP3 show no identity, they share the same general structure. Each protein consists of an eight stranded, antiparallel β-sheet or β-barrel jelly roll. This β-barrel forms a wedge-shaped structure. Tight protein packing allows the formation of a dense, rigid protein shell, that is further stabilized by the N-termini of VP1-VP4, which are covered in the interior of the capsid (Smyth and Martin, 2002). The C-termini of structural proteins protrude outside the capsid shell.

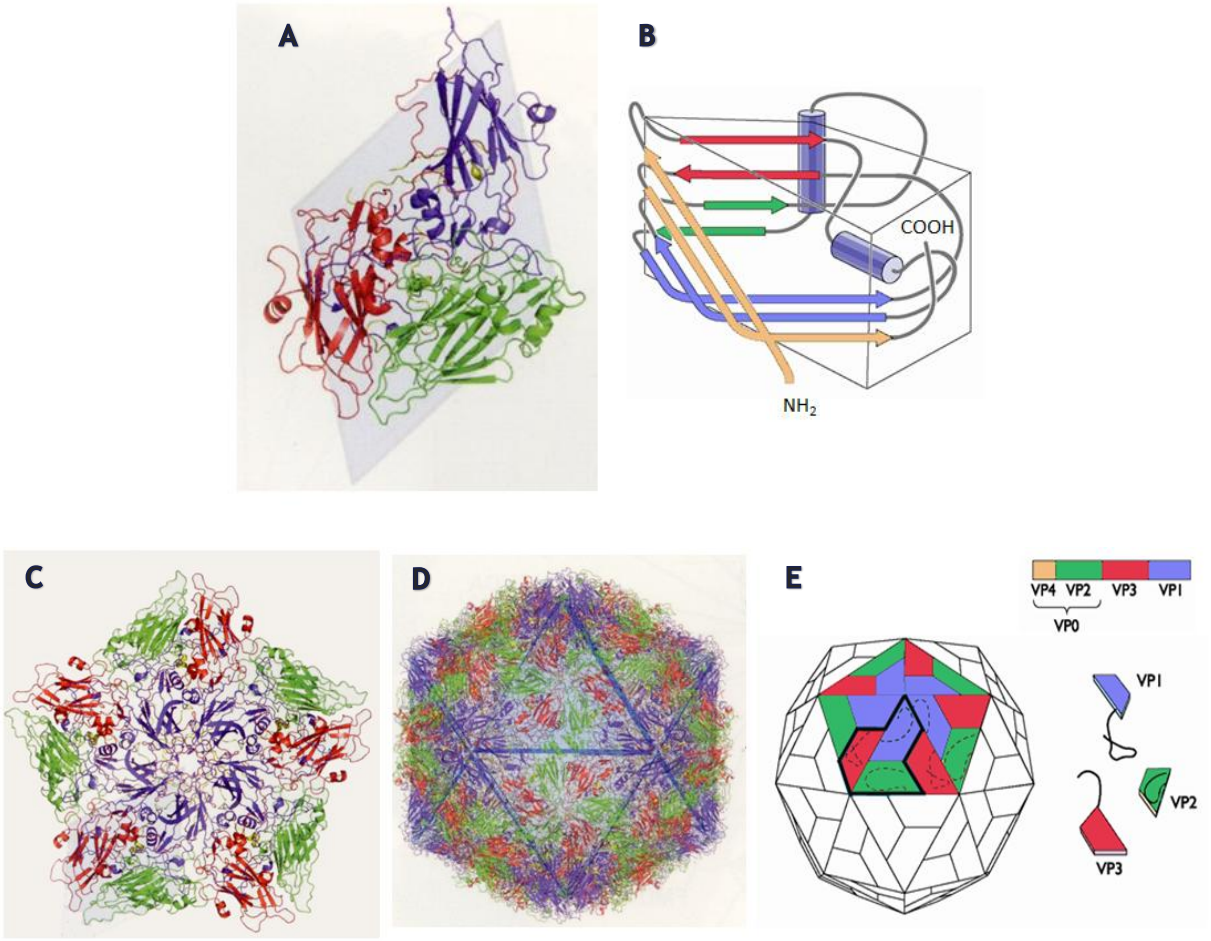

Figure 1 Structure of picornaviruses. Picornaviral capsids consist of 60 protomer subunits. A) Each protomer subunit is formed by 4 structural proteins: VP1 (blue), VP2 (green) and VP3 (red) and VP4 (yellow). VP1-VP3 form the external surface, whereas VP4 is located on the inner surface (Ehrenfeld et al., 2010) B) Core β-barrel architecture of picornaviral structural proteins forming a wedge shaped β-barrel. C) One pentamer consists of 5 protomer subunits (Ehrenfeld et al., 2010). D) Ribbon diagram of complete capsid containing of 12 pentamer subunits (Ehrenfeld et al., 2010). E) Schematic representation of complete capsid. Protomer is surrounded by black lines. VP4 is not shown as it lies on the inner surface of the protein shell and can be considered as extension of VP2 (Flint et al., 2009). Pictures taken from Flint et al., 2009 and modified with Photoshop.

The crystal structure of HRV1A was determined by Kim et al. (Kim et al., 1989) and shows a great difference in charge distribution of amino acid residues in the “canyon”, the putative receptor binding site of HRV14. This difference in amino acids is probably the explanation why major group viruses (e.g. HRV14) and minor group viruses (e.g. HRV1A) bind different receptor groups

(Verdagauer et al., 2004). Although HRV1A is similar to HRV2, it is not able to bind to the human low-density lipoprotein receptor but recognizes the murine protein, whereas HRV2 binds to both homologues (Reithmayer et al., 2002). A Glu residue was determined to be important for HRV1A recognition by exchanging parts of the human receptor with the murine homologue and monitoring virus binding efficiency (Herdy et al., 2004).

These highly organized viral capsids are not only vital for the protection of the viral genome from the surrounding, but also play a substantial role in the recognition of cell receptors on the host cell, entry and release of the RNA genome (Rossmann, 1994; Flint et al., 2009).

1.3.2 ENTEROVIRAL GENOME ORGANIZATION

Enteroviral genomes are composed of a single stranded RNA molecule of positive sense and belong therefore to class IV of Baltimore's classification system. Figure 2 shows the three parts of the enteroviral RNA: the 5' UTR (untranslated region), the coding region and the UTR at the 3' end. Both UTRs contain important structural motifs.

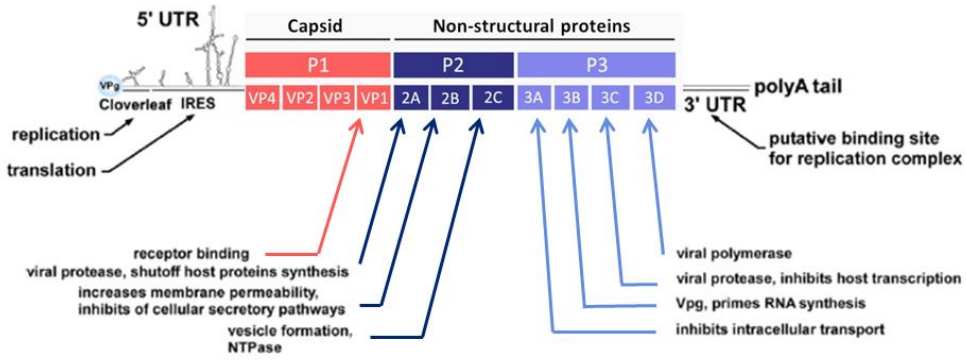

Figure 2 Structure of an enteroviral genome. The structural proteins (VP4, VP2, VP3 and VP1) are shown in red. The non-structural proteins (P2-P3) are shown in dark and light blue. P2 contains the protease $2A^{pro}$ and the accessory proteins 2B and 2C. P3 consists of the accessory proteins 3A and 3B, the protease $3C^{pro}$ and the polymerase $3D^{pol}$. Picture adapted from (Lin et al., 2009).

The 5' end (0.6-1.2 kb) of the viral genome is covalently connected to a small protein, called viral protein genome linked or VPg (Flanegan et al., 1977; Lee et al., 1977) through a Tyr residue, a conserved residue in the VPg. It has been shown that VPg plays a vital role in genome replication (Paul et al., 1998). *Cis* responsive elements (cre) are RNA sequences that regulate expression of genes located on the same strand. They are often present in the 5' UTR, but can also be found within the coding region and have been identified to be involved in replication and translation of viral RNA (Steil and Barton, 2009). It has been shown that cres are involved in VPg uridylylation which is assumed to serve as primer for the viral polymerase 3D in RNA synthesis (Cordey et al., 2008).

Another highly conserved element in the 5' UTR is the internal ribosomal entry site (IRES) type I, which promotes initiation of translation from the uncapped viral genome (Rohll et al., 1994; Borman et al., 1995). A cloverleaf structure is also found at the 5' end. Replication of RNA of the viral genome is promoted by the binding of 3CD precursor protein to the cloverleaf (Gamarnik and Andino, 1998)

The coding region contains one single open reading frame (ORF) so that translation produces only one polyprotein. The open reading frame consists of three regions P1, P2 and P3. P1 harbors the structural proteins VP1-VP4. All non-structural proteins are derived from P2 and P3. The P2 region codes for the protease $2A^{pro}$ and for accessory proteins 2B and 2C. The protease $3C^{pro}$, the polymerase $3D^{pol}$ and accessory proteins 3A and 3B are encoded on the P3 region. Viral proteases cleave the polyprotein into mature proteins (Racaniello, 2007). To the rather short 3' UTR (47 bp in HRV), a polyA tail is attached (Kitamura et al., 1981).

1.4 ENTEROVIRAL REPLICATION CYCLE

The replication cycle is divided into several steps: attachment to and entry into the host cell, decoding of genetic information and subsequent synthesis of new genomes, followed by the assembly and the release of the virion particle. The picornaviral replication cycle takes place in the cytoplasm of an infected cell and is schematically depicted and explained in Figure 3.

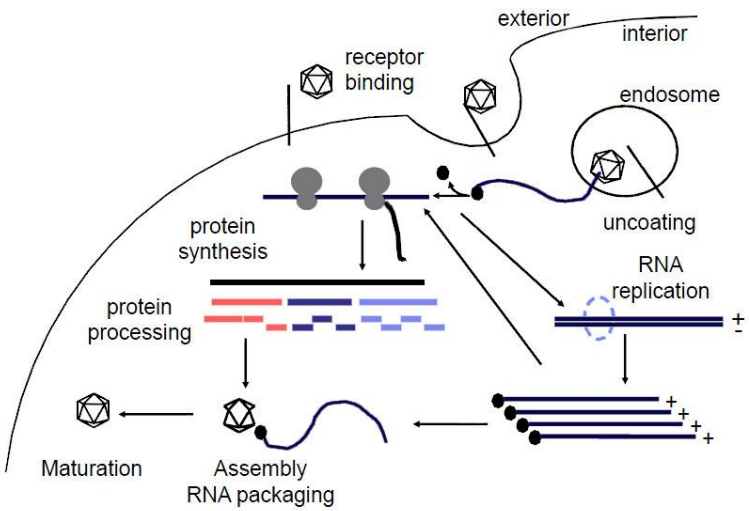

Figure 3 Schematic representation of the HRV2 replication cycle. Attachment of the native virion to the plasma membrane of a host cell leads to the internalization and entry of the virus particle in an early endosome. During the development to a late endosome, the pH inside the endosome drops which leads to the release of viral RNA into the cytoplasm. RNA is translated into a polyprotein that is co-translationally processed into mature viral proteins. Apart from the self-cleavage, several host factors are also cleaved which lead to the shut-off of host-cell translation. During RNA synthesis, the (+) strand RNA is copied into full length (-) strand RNA which is used to produce additional (+) strand RNA. In early infection, this RNA is mainly used for further translation, whereas during late infection it is packed into viral particles. Capsid proteins (VP1-VP4) are produced during translation (not shown). The viral particles exit the cell upon lysis. Picture taken from Skern's lecture on virology [1]

1.4.1 ATTACHMENT AND CELL ENTRY

Picornaviral infection of a cell starts with the attachment of a virion to the plasma membrane of a cell. Several surface molecules have been identified to serve as cellular receptors for picornaviruses. The two species of human rhinoviruses HRV-A and HRV-B bind either the intercellular adhesion molecule 1 (Greve et al., 1989) and belong to the major group of human rhinoviruses or bind to members of the low-density lipoprotein receptor (LDLR) and belong to the minor group of human rhinoviruses (Hofer et al., 1994). The receptor used by the third, recently discovered species HRV-C, is not known until now.

ICAM-1 was identified by isolating the receptor protein from susceptible cells by using monoclonal antibodies directed against the cellular binding site (Greve et al., 1989). It is an integral membrane protein that is a member of the immunoglobulin (Ig) superfamily of proteins and highly expressed on various surfaces of tissues, including the nasal epithelium, which is the entry site for rhinoviruses (Bella and Rossmann, 2000; Racaniello, 2007). ICAM-1 penetrates into the canyon of the major group viruses which encircles the fivefold axis (Olson et al., 1993). Some major group viruses can also use heparan sulphate as receptor (Racaniello, 2007).

The LDLR normally mediates the transport of macromolecules into cells by receptor-mediated endocytosis. Differences in structure and sequence of major and minor group rhinoviruses give a hint why they recognize different receptors. Recent investigations have shown that minor group rhinoviruses contain a conserved Lys residue at position 224 of VP1 that is thought to interact with the negatively charged cluster of the LDLR (Vlasak et al., 2003; Verdaguer et al., 2004). Although several minor group rhinoviruses possess a canyon, it is thought that it is not directly involved in the binding of the receptor. Instead the minor group receptors bind close to the fivefold axis on the star-shaped dome that is surrounded by the canyon (Hewat et al., 2000).

The uncoating process probably differs for major and minor group viruses. While ICAM-1 interactions facilitate direct RNA transfer through the membrane by initiating conformational changes in the capsid protein, minor group viruses are internalized into endosomes after attachment to the host cell. The vesicle formed proceeds to an early endosome and matures to a late endosome. This maturation process is associated with a decrease of the pH followed by a conformational change of the receptor and the virus. This leads to the release of the RNA from the viral capsid into the cytoplasm (Prchla et al., 1994).

1.4.2 TRANSLATION AND POLYPROTEIN PROCESSING

The plus (+) strand RNA serves as both the genome and the viral mRNA and is therefore infectious. Immediately after the release of the viral RNA genome into the cytoplasm of the host cell,

translation takes place. Most (+) strand RNA viruses do not carry a RNA dependent RNA polymerase with them, but encode it on their genome. Therefore viral proteins, including the viral RNA polymerase, have to be generated before RNA replication can take place.

Picornaviruses do not have a cap-structure at the 5' end and therefore require a cap-independent mechanism to initiate synthesis of their proteins. This different mechanism of translation initiation to synthesize host cell proteins (cap-dependent) or viral proteins will be relevant for the host cell shut-off during later viral infection (see chapter 1.5). A protein is found at the 5' end of picornaviruses, the VPg. This virus-encoded protein acts as a primer for transcription for positive and negative strand RNA synthesis and is probably not involved in translation as it was shown to be cleaved off before translation initiation in poliovirus (Ambros and Baltimore, 1980).

Cap-independent translation is stimulated by the internal ribosomal entry site (IRES) which facilitates binding of the 40 S subunit of the ribosome (Rohll et al., 1994). Human rhinoviruses and enteroviruses use a type I of IRES (Borman et al., 1995). IRES structure of different type share an AUG codon just downstream of an oligopyrimidine tract of about 25 nucleotides (nt). However, in type I IRES initiation sites for polyprotein synthesis are found further downstream at about 35 nt in rhinoviruses (Jackson and Kaminski, 1995; Kaminsky et al., 2010).

The 240-250 kDa long polyprotein is cleaved by viral proteases to give rise to functional proteins (Palmenberg, 1990). Polyprotein processing of *Enteroviruses* is shown in Figure 4A. Proteolytic processing is performed co-translationally (Toyoda et al., 1986).

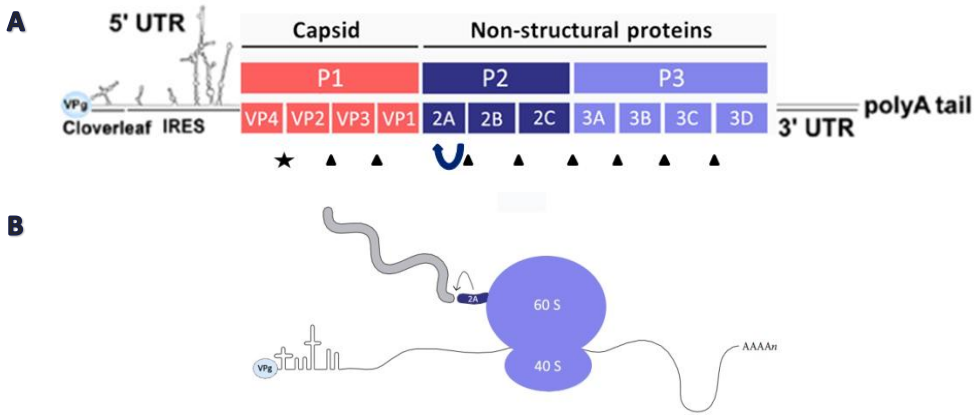

Figure 4 Cleavage events during polyprotein processing performed by picornaviral 2A^{pro} and 3C^{pro}. A) After translation from a single open reading frame, the polyprotein is processed by viral proteases. Co-translationally, the 2A^{pro} cleaves itself off from the polypeptide chain, separating it into structural and non-structural proteins. This is indicated by a blue arrow. Most other cleavage events are performed by the 3C^{pro} and are indicated by a triangle. The final cleavage step, which takes place already in the newly assembled particle, is indicated by a star. The agent is unknown. Picture adapted from (Lin et al., 2009). B) Co-translational *cis* cleavage event performed by the 2A^{pro} during polyprotein synthesis. The 2A^{pro} cleaves itself between its own N-terminus and the C-terminus of the preceding capsid protein VP1. Picture adapted from Castello et al., 2011.

In *Enteroviruses,* the first proteolytic cleavage event that separates the structural from the non-structural proteins is performed by the 2A^{pro} in *cis*, implying an intramolecular reaction

mechanism (Figure 4B). Cleavage occurs between its own N-terminus and the C-terminus of the preceding protein VP1 (Toyoda et al., 1986). The $2A^{pro}$ of different enteroviruses seem to recognize quite different cleavage sites. HRV1A $2A^{pro}$ recognizes and cleaves the amino acid sequence T I T T A * A P S D whereas the cleavage site of HRV14 $2A^{pro}$ consists of the amino acid sequence D I K S Y * G L G P. The $2A^{pro}$ is also responsible to cleave a variety of cellular proteins leading amongst others to the inhibition of host cell translation.

Some picornaviruses, such as the foot-and-mouth disease virus (FMDV), use a different protease to initiate the first cleavage event: the leader protease or L^{pro}, a papain-like cysteine protease (Strebel and Beck, 1986). The FMDV L^{pro} precedes the P1 region and frees itself from the polyprotein by cleaving between its own C-terminus and the N-terminus of the subsequent protein (VP4). FMDV encodes a 2A protein, which is only 18 amino acids in length but lacks proteolytic activity. Nevertheless, the 2A protein frees itself from the neighboring 2B protein by a ribosomal skip during translation (Donnelly et al., 2001).

The remaining cleavages to yield mature proteins are performed by the chymotrypsin-like cysteine protease $3C^{pro}$ (Palmenberg, 1990; Porter, 1993; Malcolm, 1995). The $3C^{pro}$ exists as a $3CD^{pro}$ precursor, which interacts with the protease specificity to accelerate cleavage (Jore et al., 1988), but is also thought to act as a molecular switch that facilitates viral persistence (Buenz and Howe, 2006). Proteolytic cleavage of substrates by the $3C^{pro}$ or $3CD^{pro}$ occurs between the amino acids Gln and Gly. However, it seems that Gln and Gly are not the only substrate requirements, as not all Gln*Gly junctions are cleaved in the PV polyprotein (Kitamura et al., 1981; Hanecak et al., 1982). Substances cleaved seem to have an Ala at position P4 and a Pro at position P2 of the cleavage site (Norder et al., 2011). Enteroviral $3C^{pro}$ play also a vital role in host translation inhibition by cleaving the polyA-binding protein (Kuyumcu-Martinez et al., 2002; Kuyumcu-Martinez et al., 2004).

During early infection, structural proteins are cleaved into VP0 (an immature capsid precursor), VP3 and VP1. The final maturation step is much later in infection when the new virion particle is already assembled. During this final step in polyprotein processing, VP0 is cleaved into VP4 and VP2. The mechanism of this cleavage event remains yet to be determined (Holland and Kiehn, 1968; Basavappa et al., 1994).

1.4.3 VIRAL REPLICATION

A cloverleaf structure in the 5’ UTR controls the switch between translation and replication. The viral precursor 3CD binds to this structure and to the cellular poly-C binding protein and thereby represses RNA translation and enhances replication (Gamarnik & Andino 1998).

Efficient viral replication requires modification of cellular proteins and structures which induces rearrangement of intracellular membranes into characteristic vesicles. Proteins 2B and its precursor 2BC are thought to play a role in membrane alteration by inducing membrane permeabilization (Aldabe et al., 1996). Picornaviral replication occurs in such complexes associated with the cytoplasmic membranes and involves various picornaviral non-structural proteins, as well as host proteins (Bienz et al., 1992; Egger et al., 2000) .

The major component of the replication machinery is the viral encoded RNA dependent RNA polymerase $3D^{pol}$. The 3AB precursor anchors the VPg (3B) to the virally induced membranes. A *cis*-acting replication element (cre) is involved in the attachment of two uridine residues to a conserved Tyr region at position 3 in VPg. VPg itself acts as a primer for the RNA polymerase in positive and negative RNA synthesis (Cordey et al., 2008). *Cis*-acting elements and other structural elements help in recruiting the viral RNA to the replicative complex (Cameron et al., 2009). Positive strand RNA is used to generate a negative strand RNA intermediate. Negative strand RNA is never found as a free strand but exists always as a replicative intermediate complex (positive and negative RNA) which is used as a template for the production of thousands of new positive strands (Crowder and Kirkegaard, 2005). These newly synthesized positive strand RNAs can either be used for translation of viral proteins or for the generation of new viral RNA.

1.4.4 VIRUS ASSEMBLY AND RELEASE

In the final step of the infection cycle, when sufficient newly synthesized genomic viral RNA and capsid proteins have been produced, encapsidation starts. This highly specific process is schematically depicted in Figure 5. Only positive sense RNA which contains a VPg at its 5' UTR is encapsidated (Novak and Kirkegaard, 1991).

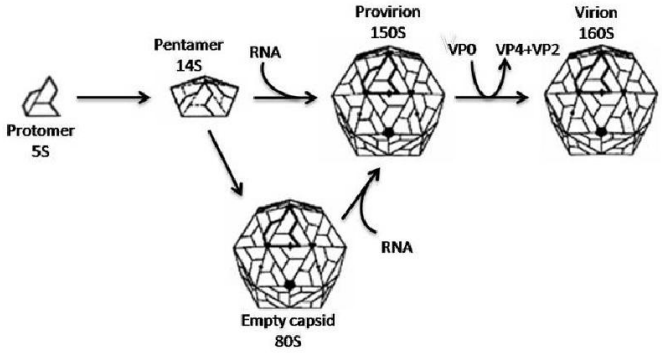

Figure 5 Assembly of the viral particle. One copy of the structural proteins VP0, VP3 and VP1 are assembled to form the 5S protomer. This further builds the 14S pentamer. Currently there are two mechanisms possible: RNA is internalized after the formation of an empty 80S capsid. Or there is a direct interaction between the 14S pentamers and the RNA leading to the 150 provirion. The final step is the maturation cleavage of VP0 into VP4 and VP2 yielding in the mature 160S virion (Rotbart, 1995).

The structural proteins are separated from the non-structural already co-translational by the $2A^{pro}$. Cleavage by the $3C^{pro}$ leads to the capsid products VP0, VP3 and VP1. One copy of each capsid protein, the precursor VP0, VP3 and VP1, is assembled to form the 5S protomers. Then five protomers assemble to form a 14S pentamer (Palmenberg, 1982; Verlinden et al., 2000). There are two possible models of how assembly is performed. On suggests that, after the formation of an empty 80S capsid, the RNA is inserted into it (Jacobson and Baltimore, 1968). The second model suggests that the 14S pentamer directly interacts with the RNA, thereby forming the 150S provirion with the already encapsidated RNA (Nugent and Kirkegaard, 1995). In the presence of viral RNA, the final step of assembly is performed, namely the cleavage of VP0 into VP2 and VP4 resulting in the mature 160S virion (see chapter 1.4.2). The mechanism of this proteolytic cleavage is not known. However, it is thought to play a role in stability of the virion and acquisition of infectivity (Basavappa et al., 1994). Picornaviruses are released from the cell upon cell lysis (Leong et al., 2002; Flint et al., 2009).

1.5 HOST CELL SHUT OFF

In the early infection, viral mRNA must compete with their host counterparts for the protein synthesis machinery (especially for the eukaryotic translation initiation factors). During viral protein synthesis in an infected cell, translation of cellular proteins is subsequently shut down. Host cells therefore lose their ability to produce their own proteins whereas viral protein production is even enhanced leading to the take-over of the host cell (Etchison et al., 1982; Etchison and Fout, 1985; Gingras et al., 1999). The key aspect of the inhibition of host cell translation inhibition lies in the manipulation of the process itself, rather than in the disruption of cellular mRNA.

The 7-methyl-guanosine capped structure at the 5' end of eukaryotic mRNA is an important feature in cellular translation. This cap structure is important to initiate translation as it recruits the so called 43S pre-initiation complex (containing the 40S ribosomal subunit, the ternary complex Met-tRNA and eIF2-GTP) to the mRNA. This recruitment involves several eukaryotic translation initiation factors (eIFs). The cap-binding protein or eIF4E recognizes and binds the 5' cap structure on the mRNA (Sonenberg et al., 1978; Svitkin et al., 2005). Additionally, it also binds the N-terminal domain of eIF4G which itself acts as central scaffold protein for the initiation complex. The other C-terminal domain of eIF4G binds eIF4A and eIF3. The polyA-binding protein (PABP) which attaches to the poly-A tail on the 3' UTR is also linked to the eIF4G leading to a circularization of the complex (Imataka et al., 1998). After the assembly of this eIF4F complex (eIF4A, 4G and 4E), the 43S pre-initiation complex binds and scans along the 5' UTR until an AUG initiation codon is encountered, which leads to an

abrogation of the scanning and to hydrolysis of the bound GTP of eIF2. Thereby, the pre-initiation factors dissociated from the small subunit and the large ribosomal subunit is bound leading to the start of protein synthesis (Pain, 1996; Borman et al., 1997). Figure 6A shows a schematic representation of the cap-dependent translation initiation complex.

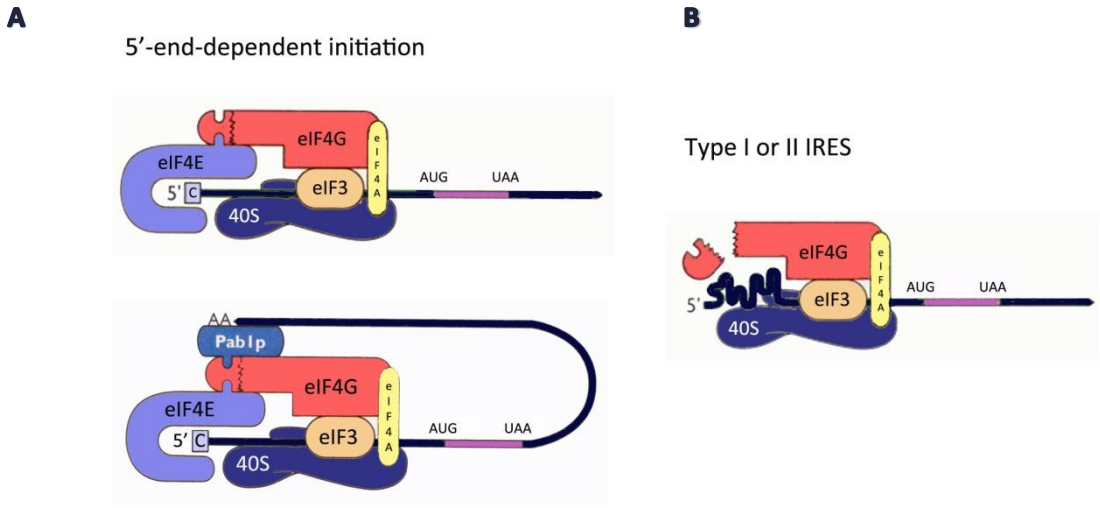

Figure 6 Cap-dependent and cap-independent translation initiation. A) Intact eIF4G is the scaffold protein which brings the 43S subunit to the cellular mRNA. In the course of viral infection, eIF4G is cleaved by the $2A^{pro}$ in HRVs leading to the abrogation of cellular protein synthesis and enhancement of cap-independent translation. Binding of polyA tail by the PABP leads to a circularization. B) Viral translation is not effected as it is not cap-dependent, but viral mRNA contains an IRES structure important for translation initiation (Flint et al., 2009).

During picornaviral infection, the scaffold protein eIF4G is cleaved by virally encoded proteases (enteroviral $2A^{pro}$ or FMDV L^{pro}) inhibiting the binding of the ribosome to cellular mRNA. Picornaviruses translate their proteins in a cap-independent way via an IRES structure present in the 5' UTR of the viral genome. This IRES structure facilitates ribosomal recruitment and requires also almost all cellular eukaryotic initiation factors used in cap-dependent translation. However, after the cleavage of eIF4G enteroviral protein synthesis works even more efficiently than in presence of intact eIF4G (Borman and Kean, 1997). Figure 6B shows a schematic representation of enteroviral translation via an IRES structure.

In HRV, the enzyme responsible for this host cell shut off is the $2A^{pro}$ in HRV, which is able to cleave eIF4G directly (Figure 7). There are two homologues of eIF4G present in eukaryotic cells, eIF4G I and II (Gradi et al., 1998; Lloyd, 2006). Gradi et al. have shown that both types of eIF4G have to be cleaved to lead to host-cell shut off. It has been shown that HRV2 $2A^{pro}$ cleaves the sites L S T R * G P P R on eIF4GI (Lamphear et al., 1993) and L L N V * G S R R at eIF4GII (Gradi et al., 2003). However, by site directed mutagenesis, it was also shown that the binding and cleavage sites on eIF4GI differ. In these experiments, the $2A^{pro}$ is able to bind eIF4GI fragments which lack the cleavage site amino acids Arg*Gly in eIF4GI and are therefore not able to perform cleavage (Foeger et al., 2000; Foeger et al., 2002).

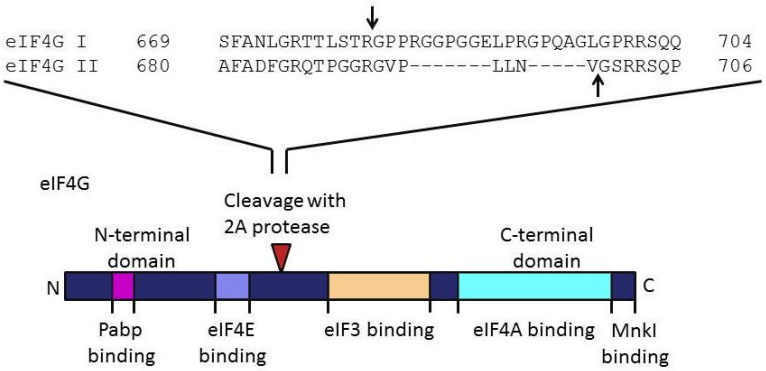

Figure 7 Overview of the eIF4G scaffold protein and 2A^{pro} cleavage site. 2A^{pro} of HRV cleaves eIF4G I and II during infection. Arrows indicated cleavage sites in eIF4G I and II for enteroviral 2A^{pro}. eIF4G binding domains for PABP, eIF4E, eIF3 and eIF4A and Mnk are shown as well. Picture from (Flint et al., 2009).

1.6 2A PROTEINASE (2A^{PRO})

1.6.1 FUNCTION

In *Enteroviruses,* the 2A^{pro} is essential for viral translation as it separates the structural from the non-structural proteins by cleaving the polyprotein (Toyoda et al., 1986). The 2A^{pro} cleaves between its own N-terminus and the C-terminus of the preceding protein VP1. This initial cleavage event is performed co-translationally and only in *cis*, implying an intramolecular reaction mechanism. As mentioned in chapter 1.5, it also plays a very important role during host cell shut-off as it cleaves the two homologues of eIF4G leading to an abrogation of cellular protein synthesis. In addition, 2A^{pro} of different picornaviruses cleave several other cellular proteins, such as the polyA-binding protein PABP, which was shown to be cleaved by PV 2A^{pro} and 3C^{pro} (Joachims et al., 1999) and CV B3 2A^{pro} (Kerekatte et al., 1999), dystrophin, which was shown to be cleaved by the CVB3 2A^{pro} (Badorff et al., 1999) and cytokeratin 8, which was shown to be cleaved by the 2A^{pro} of HRV2 (Seipelt et al., 2000). The 2A^{pro} of HRV2 also alters RNA and protein trafficking between the nucleus and the cytoplasm by proteolysis of several nucleoporins (Gustin and Sarnow, 2001; Park et al., 2008; Park et al., 2010). Table 1 summarizes this data.

Protein	Cleaved by
PolyA Binding Protein	PV 2A^{pro} and 3C^{pro} CV-B3 2A^{pro}
Dystrophin	CV-B3 2A^{pro}
Cytokeratin 8	HRV 2A^{pro}, CV-B4 2A^{pro}
Nup 62	HRV 2A^{pro}
Nup 98	HRV 2A^{pro}
Nup 153	HRV 2A^{pro}

Table 1 Cellular proteins cleaved by enteroviral 2A^{pro}.

Crowder and Kirkegaard showed that PV bearing a mutation that makes the $2A^{pro}$ enzyme inactive can also act as a dominant negative inhibitor of wild-type growth (Crowder and Kirkegaard, 2005). Co-infection of cells with wt PV and PV containing a mutation in the $2A^{pro}$ that inhibits $2A^{pro}$ activity showed that intracellular growth was inhibited also for the wt virus. As the cleavage between VP1 and $2A^{pro}$ is exclusively intramolecular (Toyoda et al., 1986), and therefore wild type structural products are produced, it was postulated that uncleaved VP1-$2A^{pro}$ can assembly with wild type VP0 and VP3 to form non-functional capsids, and thereby preventing viral growth (Crowder and Kirkegaard, 2005).

1.6.2 STRUCTURE

The enteroviral $2A^{pro}$ is a protein composed of 142 – 149 amino acids that belong to the cysteine protease group (Konig and Rosenwirth, 1988) with a chymotrypsin-like fold (Bazan and Fletterick, 1988). At the moment, two structures of $2A^{pro}$ are available: the crystal structure from HRV2 (Petersen et al., 1999) and the NMR structure from coxsackievirus B4 (Baxter et al., 2006). In Figure 8, the crystal structure of HRV2 $2A^{pro}$ is shown.

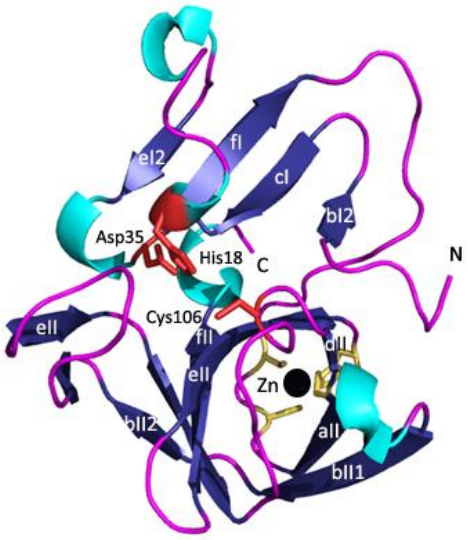

Figure 8 Structure of HRV2 $2A^{pro}$. The catalytic triad residues His18, Asp35 and Cys106 are shown in red. The residues Cys52, Cys54, Cys112 and His114 that coordinate the zinc ion (black) are shown in yellow. The β-strands are highlighted in dark blue, α-helices in light blue and loops in violet. Created with Pymol (DeLano, 2002) using the PDB ID code 2HRV2.

In comparison to chymotrypsin, a prototypic serine proteinase, the $2A^{pro}$ exhibits some unique characteristics in its structure. Instead of a serine as the active site nucleophile, it contains a cysteine. As in chymotrypsin, the $2A^{pro}$ contains a N-terminal and a C-terminal domain which is connected by an interdomain loop. However, the N-terminal domain is made up of four β-strands forming an antiparallel β-sheet, whereas the N-terminus of chymotrypsin is built from 8 β-strands. The C-

terminus of the $2A^{pro}$ is made of 6 β-strands forming a β-barrel. For the formation of an active enzyme, a zinc ion coordinated by Cys52, Cys54, Cys112 (via sulfur) and His114 (via nitrogen) was shown to be required. This tightly bound zinc ion is thought to be essential for the stability of the protein, presumably by compensating the truncation of the N-terminal domain (Sommergruber et al., 1994; Voss et al., 1995; Petersen et al., 1999). However, it seems not to be involved in functionality of the $2A^{pro}$, as it rather far away from the active site (> 20 Å) and not accessible to other ligands.

The catalytic triad which is located at the junction of the N- and C-terminal domains is formed by the nucleophile Cys106, the general base His18 and Asp35 as determined by mutational analysis and confirmed by the crystal structure (Yu and Lloyd, 1991; Sommergruber et al., 1997; Petersen et al., 1999). Figure 9A shows the catalytic triad. Although actives site residues in other chymotrypsin-related serine proteinases are normally rather rigid, His18 shows an unusual flexibility. This structure is stabilized by Asp35. Asp35 itself is fixed by a well-established hydrogen bonding network involving several other residues.

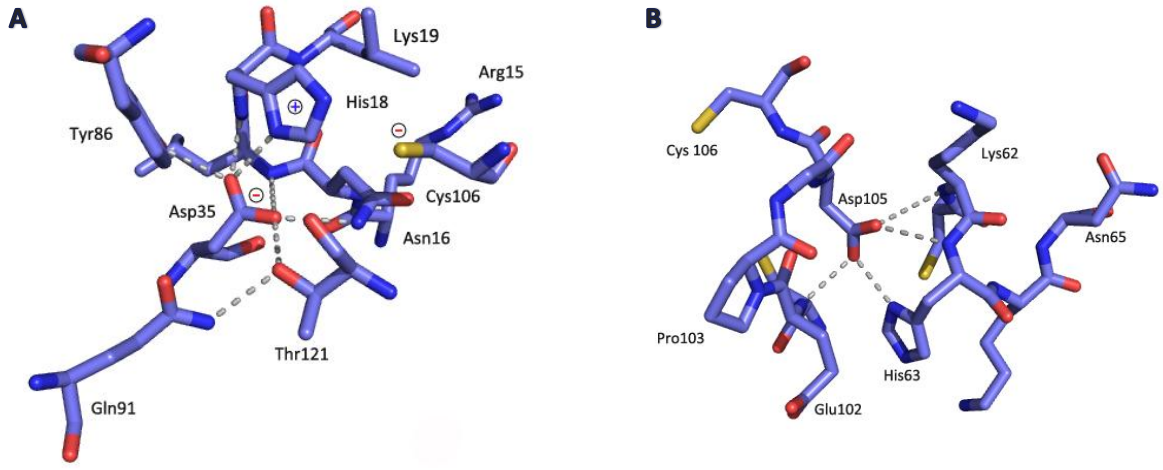

Figure 9 Important hydrogen bonding networks stabilizing the active site of HRV2 $2A^{pro}$. A) Active site residues His 18, Asp35 and Cys106 are shown. Asp35 is part of a hydrogen bonding network stabilizing itself and the rather unusual flexible His18. B) Oxyanion hole stabilizing the negative charge in the substrate binding site. Created with Pymol (DeLano, 2002) using the PDB ID code 2HRV2.

Cleavage of the peptide bond is a two-step reaction. In the first step, a covalent bond between the C1-atom of the substrate (at position P1) and the sulfhydryl group of the reactive Cys residue of the enzyme is formed. The His provides a general base and accepts a proton from the sulfhydryl group of the reactive Cys, which leads to the formation of an intermediate. During the formation of this intermediate, a negative transition state intermediate is formed where the bonds of the C1 of the substrate have tetrahedral geometry in contrast to the planar triangular geometry in the peptide group. A structure called the “oxyanion hole”, which is part of the enzyme, stabilizes the negative charge of the oxygen atom attached to the C1-atom (at position P1). Stabilization is achieved by a hydrogen bonding network formed by Asp105 with various residues and is shown in Figure 9B. After

the breakage of the peptide bond, one cleavage product is released, whereas the second is still attached to the enzyme. This product-enzyme is then hydrolyzed by a water molecule to release the second cleavage product and the enzyme. This process again proceeds through a negative tetrahedral transition state (Branden and Tooze, 1999; Sarkany et al., 2000).

1.6.3 SUBSTRATE SPECIFICITY

Most experiments made on the substrate specificity of $2A^{pro}$ have been done on PV-1 (Hellen et al., 1992) and HRV2 (Sommergruber et al., 1992; Petersen et al., 1999). As HRV1A belongs to the same group as HRV2 and the cleavage sites of HRV2 and HRV1A $2A^{pro}$ are rather similar, the substrate specificity of HRV2 is discussed here.

The $2A^{pro}$ cleavage site for self-processing reactions, consisting of 5 residues of the C-terminal part of VP1 (also designated as P site) and 4 residues of the N-terminal part of the $2A^{pro}$ (also designated as P' site), is recognized by the $2A^{pro}$ and cleaved. The nomenclature of Schechter and Berger was used to describe the residues of the cleavage site (Schechter and Berger, 1967). In Figure 10 and 11, a substrate was modeled into the binding cleft of HRV2 $2A^{pro}$. For substrate recognition, residues at position P1', P2 and P4 seem of great importance. Indeed, the only absolutely conserved residue in the cleavage site of $2A^{pro}$ is the Gly at position P1' indicating the strong requirement for this residue. The presence of Glu, Lys, Thr and Trp at this site were shown to inhibit the self-cleavage reaction (Skern et al., 1991). Petersen et al. (Petersen et al., 1999) explain the absolute requirement of Gly at P1' to be due to Leu19 that blocks the access of any residues other than Gly to the S1' site.

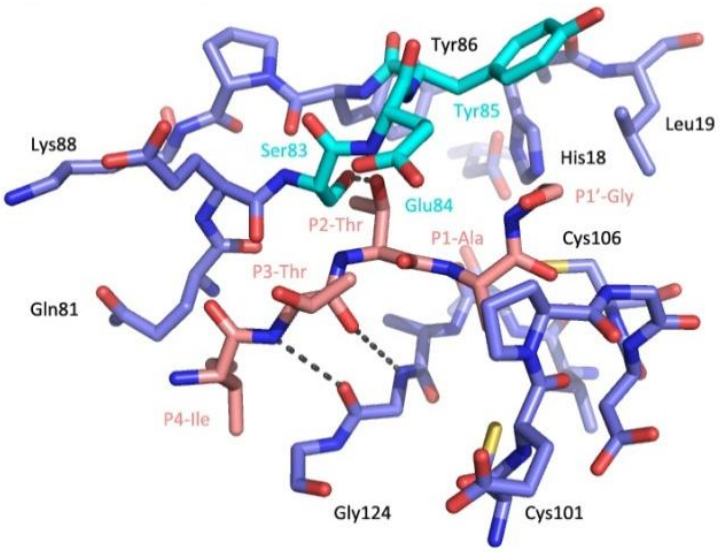

Figure 10 Model of substrate binding in HRV2 $2A^{pro}$. A peptide (P4-P1') was modeled into the binding cleft of the HRV2 $2A^{pro}$ structure. The important hydrogen bond of Ser83 with Thr at position P2 is shown and Tyr85 has been rotated out in order to form an S2 site. Created with Pymol (DeLano, 2002) as described by Petersen et al., 1999. A brief description of how this model was generated is given in chapter 5.2.

At P2, a Thr is found in HRV2 (and HRV1A). However, binding of a substrate with a Thr residue at P2 requires a rotation of Tyr85 away from its original position, stacked upon His18, so that Thr at P2 can form a hydrogen bond with Ser83. This hydrogen bond seems to compensate for this rotation (Petersen et al., 1999). Peptides with a Val at position P2 are not cleaved due to the inability to form a hydrogen bond. However, HRV2 $2A^{pro}$ does process Thr, Asn, Ser at the P2 position of the cleavage site. By exchanging the P2 position of HRV14, which originally contains a Ser, with Thr, a 5-fold more efficient cleavage of oligopeptides by the HRV14 $2A^{pro}$ can be observed (Sommergruber et al., 1992).

Hydrophobic residues such as Leu or Ile are found at the P4 site due to their flexibility of the side chains as the S4 site is a rather narrow but deep pocket (Petersen et al., 1999).

The other positions of the substrate binding site can be rather diverse. For instance, the cleavage site of wild type HRV2 $2A^{pro}$ contains an Ala at P1 position. However, it accepts a variety of amino acids such as Met, Leu, Tyr, Phe, Thr, and Arg as well and even shows higher cleavage efficiency with Met or Tyr at this site. This can be explained by the narrow and flat character of the S1 pocket formed by the eII strand and the oxyanion hole and is mainly filled by the side chains of Cys101 and Glu102 at the bottom of the pocked providing a negative charge. Residues with long and flexible side chains, such as Met, can fit in the S1 site more easily, as well as residues with positive side chains, as Arg and Lys. Negative charged substrates containing Asp and Glu were not cleaved at all (Skern et al., 1991; Sommergruber et al., 1992). P2' can also accept several other amino acids such as Phe, Thr, Asn and Lys, however, compared to wild type cleavage of HRV2 with Pro at position P2', cleavage was reduced to about two to five folds (Sommergruber et al., 1992).

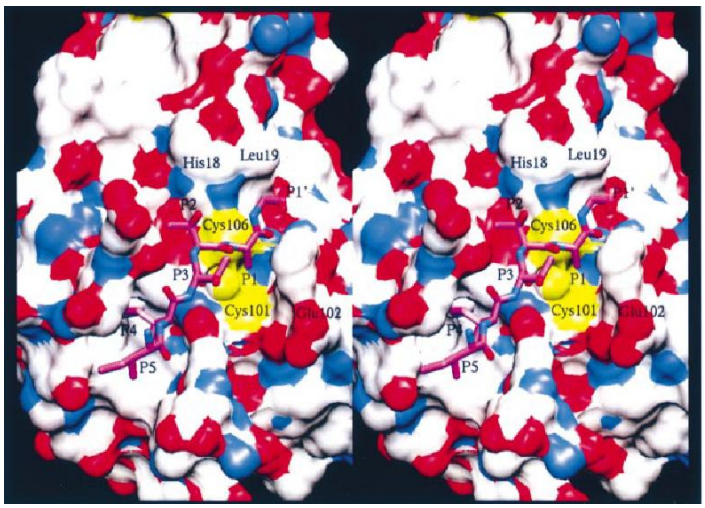

Figure 11 Surface model of the substrate binding cleft of HRV2 $2A^{pro}$. The narrow and flat S1 pocket formed by Cys101 and Glu102 is shown. Residues 82-89 from the dityrosine flap have been removed. Picture taken from (Petersen et al., 1999).

The specificity of the HRV1A and HRV14 $2A^{pro}$ appear to be different. Figure 12 shows the cleavage sites for different enteroviral $2A^{pro}$ enzymes. These cleavage sites have only a few residues in common, as only residues at position P4, P2 and P1' are identical.

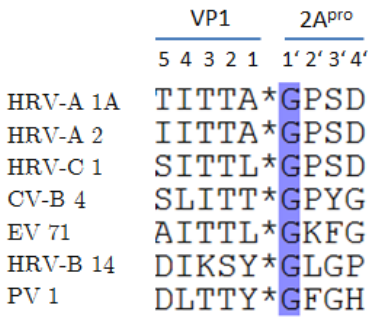

Figure 12 Comparison of the 2A^{pro} cleavage sites of different picornaviruses. Sequence alignment of selected picornaviruses: HRV human rhinovirus, CV coxsackievirus, EV enterovirus, PV poliovirus; The P site represents the C-terminus of VP1 and the P' site the N-terminus of 2A^{pro}. Numbers indicate the position of amino acid residues relative to the scissile bond between the VP1 and the 2A^{pro}, which is indicated by an asterisk. The sequences have been taken from the database www.ncbi.nlm.nih.gov. Sequence IDs: AY458604 (HRV-A 1a), Xo2316.1 (HRV-A 2), X01087 (HRV-B 14), EF582387.1 (HRV-C 026) ABV60422 (PV 1), DQ480420 (CV-B 4), U22521.1 (EV 71). Sequence alignment was made online using ClustalW (http://www.ebi.ac.uk/Tools/ msa/clustalw2/) and edited with the programme BioEdit.

For this work the difference in cleavage site residues of HRV1A 2A^{pro} and HRV14 2A^{pro} is the most important. Identical residues are the Ile at position P4 and the Gly at position P1'. Similar residues are located at position P2 (Thr, Ser in HRV1A, HRV14 respectively). Thr and Ser are both able to make hydrogen bonds, and are maybe involved in forming a hydrogen bond with Ser83 as it was shown in HRV2 (see chapter 1.6.3). In contrast, different residues are found at position P5, P1, P2' and P4'. Wang et al. showed that HRV14 2A^{pro} cleaves poorly a peptide with its wild type cleavage site poorly *in vitro* and showed that when HRV14 residue Leu at position P2' was mutated to Pro (as in HRV1A) or Ser at position P2 was mutated to Thr resulted in a 12 fold higher cleavage efficiency than with the wild type residues (Wang et al., 1998).

The cleavage site on eIF4G recognized by the 2A^{pro} contains T L S T R * G P P R (Lamphear et al., 1993). It shows a similar substrate binding motif: a hydrophobic amino acid at P4, Thr at P2 and Gly at P1'. Although eIF4G is cleaved directly by the 2A^{pro}, its cleavage efficiency *in vitro* is not very high, but is significantly improved when it is part of the eIF4F complex (Haghighat et al., 1996). This suggests that after binding of eIF4E to eIF4G, there is a change in conformation of eIF4G in narrowness allowing a better binding and cleavage of the 2A^{pro} (Petersen et al., 1999).

Sousa et al. showed that HRV14 2A^{pro} was not able to carry out self-processing when the wt cleavage site was replaced by that of eIF4GI. In contrast to that HRV2 2A^{pro} is able to perform self-processing. Site-directed mutagenesis showed that the Arg at position P1 was responsible for the cleavage inhibition of HRV14 2A^{pro}. This result indicated that HRV14 2A^{pro} might cleave at a different site on eIF4G than HRV2. By solely replacing the Tyr at position P1 with an Arg cleavage of HRV14 2A^{pro} was also inhibited (Sousa et al., 2006).

2 AIM OF THE WORK

This thesis focuses on the substrate specificity of the $2A^{pro}$ of HRV1A and HRV14. Understanding protease substrate specificities is of crucial importance in developing antiviral inhibitors specifically targeting the $2A^{pro}$, a highly conserved protease in *Enteroviruses*.

During the course of this work, the first cleavage reaction in picornaviruses, which is executed by the $2A^{pro}$, is monitored by using an *in vitro* system employing rabbit reticulocyte lysates (RRL). This *in vitro* system is used to investigate the intramolecular cleavage between the C-terminus of the preceding protein VP1 and its own N-terminus. Although a crystal structure of HRV2 $2A^{pro}$ is available, we performed our experiments with HRV1A, another group A human rhinovirus, as the transfection efficiency of HRV2 RNA in HeLa cells is very low compared to that in HRV1A RNA. A high transfection efficiency is necessary for our experiments in order to be able to isolate compensatory mutants later.

Which are the crucial residues of $2A^{pro}$ required to recognize the substrate at the VP1-$2A^{pro}$ junction? Although this *cis* cleavage is a highly conserved, co-translational process in different *Enteroviruses*, the residues in the cleavage site are rather diverse. Several studies have been performed to identify important residues in the $2A^{pro}$ cleavage sites (Skern et al., 1991; Sommergruber et al., 1992). During the course of this work, we aimed to exchange residues at the VP1-$2A^{pro}$ junction of HRV1A with those from HRV14 in order to identify which residues in the cleavage junctions are not accepted by the $2A^{pro}$ and which are exclusively required to carry out this important self-cleavage process. Subsequently, cleavage site residues identified as being sub-optimal for this cleavage were to be introduced into a HRV1A full length clone in order to be able to transfect HeLa cells with viral RNA containing the desired mutations. From the viral offspring, we will try to isolate virus with second site revertants. This should help us to identify structurally important amino acids in various positions of the $2A^{pro}$ enzyme or cleavage site. We further tried to determine why glycine at position P1' is absolutely required for performing this *cis*-cleavage event.

Is the activity of the $2A^{pro}$ influenced by the sequence of the neighboring proteins? In another set of experiments, the protease activity of the HRV14 $2A^{pro}$ was to be monitored. The influence of mutations in the protein VP1 (Y289R) and in the 2B (I94N) was to be investigated as both mutations had been shown to prevent the $2A^{pro}$ from performing self-processing (Sousa et al., 2006; Neubauer et al., 2009) Again, viral RNA carrying the desired mutations was transfected into HeLa cells and we tried to isolate second site revertants that might have recovered the biological activity of the $2A^{pro}$. We hypothesize that such mutations identified could shed light on the specificity and mechanism of the $2A^{pro}$.

3 MATERIALS AND METHODS

3.1 PLASMIDS AND CONSTRUCTS

For *in vitro* experiments the pCITE vector (Novagen), containing a cap-independent translation enhancer (CITE) sequence, that derived from the encephalomyocarditis virus (EMCV) and facilitates internal initiation of protein synthesis was used. This vector also contains a T7 promoter before the CITE that allows *in vitro* transcription by T7 RNA polymerase. The pCITE vector containing the HRV2 VP1-2A^{pro}, containing a *Nco*I and *BamH*I restriction site before and after the coding sequence of the viral proteins, was kindly provided by David Neubauer. The HRV2 VP1-2A^{pro} was exchanged by HRV1A cDNA encoding the VP1-2A^{pro} (Figure 13A). Therefore *Nco*I and *BamH*I restriction sites were introduced before and after the cDNA of HRV1A VP1-2A^{pro} via standard PCR and used to exchange the HRV2 VP1-2A^{pro} with the corresponding fragment of HRV1A VP1-2A^{pro}. All plasmids used throughout the experiments code for a gene that gives resistance to ampicillin, which was used to screen for bacterial clones that carried the plasmid.

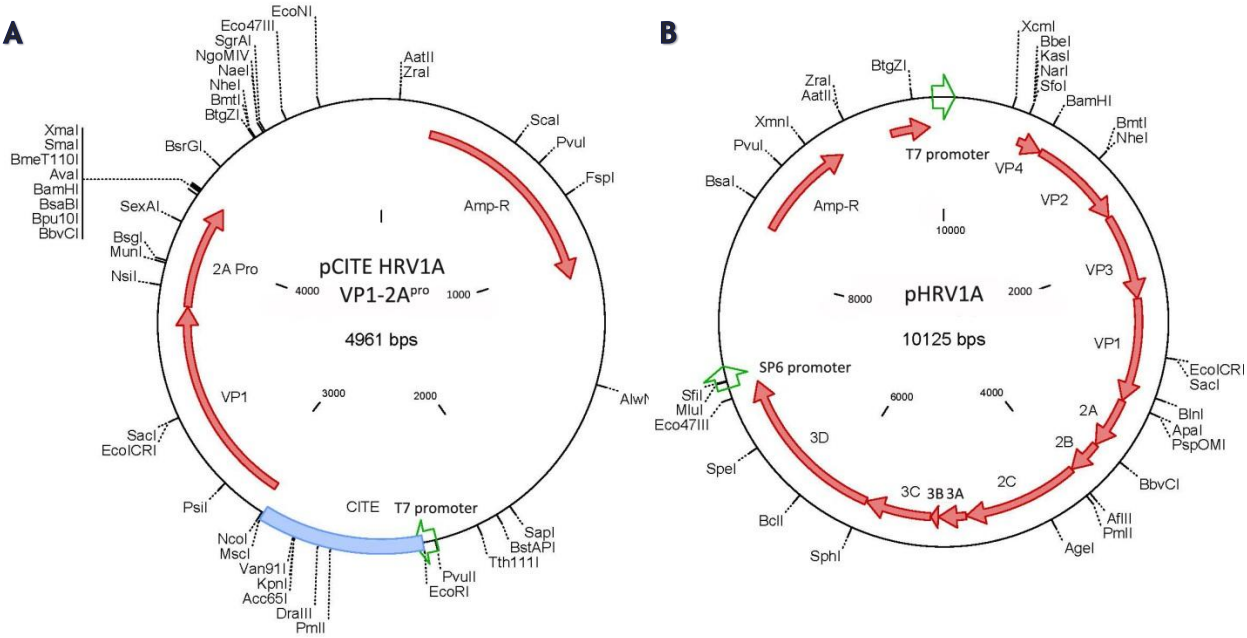

Figure 13 HRV1A plasmids used without modifications. A) pCITE HRV1A VP1-2A^{pro}. B) pHRV1A containing the full HRV1A genome. Single restriction sites available are shown. Pictures made with CloneManager.

The HRV1A VP1-2A^{pro} was used for monitoring wild type HRV1A cleavage of the 2A^{pro}. Further on cleavage site residues of the HRV1A 2A^{pro} were exchanged by introducing the restriction sites *BsiW*I and *BstE*II via silent mutations around the cleavage junction of the 2A^{pro} (55 bp apart from each

other) by standard PCR. Phosphorylated primer containing mutated residues were used to modify the cleavage site via cassette cloning. Prior to *in vitro* transcription plasmids were linearized with *BamH*I.

For transfection experiments in HeLa cells full length HRV1A mRNA was used (Figure 13B). The plasmid pHRV1A, containing the cDNA of the complete HRV1A genome was kindly provided by McKnight. Unfortunately no whole sequence map was available, but the plasmid was sequenced on both sides, upstream and downstream from the coding sequence. Sequence results showed that the plasmid belongs to the family of pGEM vectors – probably pGEM13-Zf(+). The plasmid pHRV1A is 10125 bp in size and also contains a T7 promoter, an IRES and a gene coding for ampicillin resistance. *BsiW*I and *BstE*II restriction sites were introduced around the cleavage junction of the $2A^{pro}$ via PCR mutagenesis and the cleavage site was again modified by introducing phosphorylated primers containing mutated residues via cassette cloning. Prior to *in vitro* transcription the plasmid was linearized with *Mlu*I.

In vivo experiments with HRV14 were performed with a plasmid containing full length HRV14 cDNA (Figure 14). This pHRV14 as3f contained either a mutation in the VP1 protein (Y289R) or in the 2B protein (I94N), which were both thankfully provided by David Neubauer.

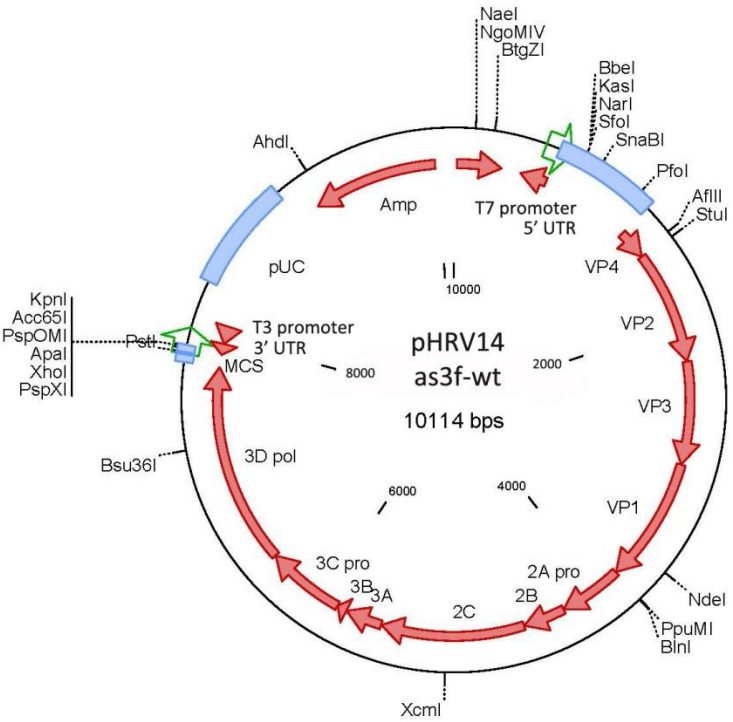

Figure 14 HRV14 plasmid used without modifications. Single restriction sites available are shown. Picture made with CloneManager.

3.2 OLIGONUCLEOTIDES

Oligonucleotides were purchased from Eurofin MWG Operon.

3.2.1 PRIMERS USED FOR SITE DIRECTED PCR MUTAGENESIS

Primer	Sequence (orientation 5` to 3`)	Description
Tim 1849	5' CCACAACCATGGTAGAAAACTACATTGATGAAG 3'	Sense primer for the introduction of a NcoI restriction site into pCITE HRV1A VP1-2A^{pro}
Tim 1850	5'CCCGGGGGATCCTTATCATTGTTCCTCAGCACAGTGA AATTG 3'	Antisense primer for the introduction of a BamHI restriction site into pCITE HRV1A VP1-2A^{pro}
Tim 1851	5'CGTGACAACAGCCATCGTACGCAGAAACACTATAACA ACTG 3'	Sense primer for the introduction of a BsiWI restriction site (silent mutation) into pCITE HRV1A VP1-2A^{pro} and into pHRV1A full length clone
Tim 1852	5'CAGTTGTTATAGTGTTTCTGCGTACGATGGCTGTTGTC ACG 3'	Antisense primer for the introduction of a BsiWI restriction site (silent mutation) into pCITE HRV1A VP1-2A^{pro} and into pHRV1A full length clone
Tim 1853	5'CTATATGTGCATGTAGGTAACCTAATATATAGAAACTT ACATCTG 3'	Sense primer for the introduction of a BstEII restriction site (silent mutation) into pCITE HRV1A VP1-2A^{pro} and into pHRV1A full length clone
Tim 1854	5'CAGATGTAAGTTTCTATATATTAGGTTACCTACATGCA CATATAG 3'	Antisense primer for the introduction of a BstEII restriction site (silent mutation) into pCITE HRV1A VP1-2A^{pro} and into pHRV1A full length clone
Tim 1887	5' GTGTTTTGTTTCTGCATGTAAAG 3'	Sense primer for the introduction of BsiWI/ BstEII restriction site (silent mutation) into the pHRV1A full length clone
Tim 1888	5' ATGTAACACTTGAAACCATTTGG 3'	Antisense primer for the introduction of BsiWI/ BstEII restriction site (silent mutation) into the pHRV1A full length clone

Table 2 Oligonucleotides used for site directed PCR mutagenesis. Restriction sites are shown underlined..

3.2.2 OLIGONUCLEOTIDES FOR CASSETTE CLONING

Primer	Sequence (orientation 5` to 3`)	Description
Tim 1859	5'GTACGCAGAAACGATATCAAATCCTATGGTTTAGGAC CTCTATATGTGCATGTAG 3'	Introduction of the cleavage site DIKSY*GLGP into pCITE HRV1A VP1-2A^{pro} and pHRV1A full length clone (silent mutation: *EcoR*V)
Tim 1860	5'GTTACCTACATGCACATATAGAGGTCCTAAACCATAGG ATTTGATATCGTTTCTGC 3'	

Tim 1861	5'GTACGCAGAAACGATATCAAATCCTATGGGCCCAGTG ATCTATATGTGCATGTAG 3'	Introduction of the cleavage site DIKSY*GPSD into pCITE HRV1A VP1-2A^{pro} and pHRV1A full length clone (silent mutation: *Eco*RV)
Tim 1862	5'GTTACCTACATGCACATATAGATCACTGGGCCCATAGG ATTTGATATCGTTTCTGC 3'	
Tim 1863	5'GTACGCAGAAACACTATAACAACAGCTGGTTTAGGAC CTCTATATGTGCATGTAG 3'	Introduction of the cleavage site TITTA*GLGP into pCITE HRV1A VP1-2A^{pro} and pHRV1A full length clone (silent mutation: *Pvu*II)
Tim 1864	5'GTTACCTACATGCACATATAGAGGTCCTAAACCAGCTG TTGTTATAGTGTTTCTGC 3'	
Tim 1867	5'GTACGCAGAAACACTATAAAATCCTATGGCCTAAGCG ATCTATATGTGCATGTAG 3'	Introduction of the cleavage site TIKSY*GLGP into pCITE HRV1A VP1-2A^{pro} and pHRV1A full length clone (silent mutation: *Bpu10*I)
Tim 1868	5'GTTACCTACATGCACATATAGATCGCTTAGGCCATAGG ATTTTATAGTGTTTCTGC 3'	
Tim 1869	5'GTACGCAGAAACACTATAACATCCTATGGCCTAAGCG ATCTATATGTGCATGTAG 3'	Introduction of the cleavage site TITSY*GLGP into pCITE HRV1A VP1-2A^{pro} and pHRV1A full length clone (silent mutation: *Bpu10*I)
Tim 1870	5'GTTACCTACATGCACATATAGATCGCTTAGGCCATAGG ATGTTATAGTGTTTCTGC 3'	
Tim 1871	5'GTACGCAGAAACACTATAACAACAGCTGCACCCAGTG ATCTATATGTGCATGTAG 3'	Introduction of the cleavage site TITTA*APSD into pCITE HRV1A VP1-2A^{pro} and pHRV1A full length clone (silent mutation: *Pvu*II)
Tim 1872	5'GTTACCTACATGCACATATAGATCACTGGGTGCAGCTG TTGTTATAGTGTTTCTGC 3'	

Table 3 Oligonucleotides used for cassette cloning. Cleavage sites are shown underlined.

3.2.3 PRIMERS USED FOR SEQUENCING

Primer	Sequence (orientation 5` to 3`)	Description
Tim 1797	5' GCACTACCCTACACATCAATAGG 3'	Sense primer for sequencing of cDNA from HRV14 plaques
Tim 1798	5' CCTGTGTTGGATTCGAGATATGC 3'	Antisense primer for sequencing of cDNA from HRV14 plaques
Tim 1922	5' CCCTTACACACATAGTCATGTG 3'	Sense primer for sequencing of cDNA from HRV1A plaques
Tim 1923	5' ATTTCACATTTGATTTTCTCTTG 3'	Antisense primer for sequencing of cDNA from HRV1A plaques
Tim 1928	5' ATCCATTCAAGACCACGTGCAG 3'	Antisense primer for sequencing of 2B of cDNA from HRV1A plaques

Table 4 Oligonucleotides used for sequencing.

3.2.4 PRIMERS USED FOR RT-PCR OF VIRAL RNA

Primer	Sequence (orientation 5` to 3`)	Description
Tim 1795	5' GGCAAAGTGCTTCAAACC 3'	Sense primer for PCR amplification of cDNA of HRV14 plaques
Tim 1796	5' GCCATTGGAGGCAAGAAATC 3'	Antisense primer for PCR amplification of cDNA of HRV14 plaques
Tim 1915	5' TTTTATGATGGATATGATGG 3'	Sense primer for PCR amplification of cDNA of HRV1A plaques
Tim 1921	5' GTAACACTTGAAACCATTTGG 3'	Antisense primer for PCR amplification of cDNA of HRV1A plaques

Table 5 Oligonucleotides used to reverse transcribe and amplify viral mRNA isolated from plaques.

3.3 DNA METHODS

3.3.1 AMPLIFICATION OF DNA FRAGMENTS BY PCR (POLYMERASE CHAIN REACTION)

3.3.1.1 Introduction of mutations by site directed PCR mutagenesis

For the introduction of mutations of one or a few base pairs into plasmid DNA, complementary primers containing the mismatches were designed. To ensure proper hybridization to the template, regions of exact homology to the template were included on both sides around the mutated site.

A standard PCR reaction of 50 µl consists of:

0.5 µl	DNA
1.0 µl	Sense primer (1 µg/µl)
1.0 µl	Antisense primer (1 µg/µl)
2.5 µl	dNTPs (2.5 mM) (Invitrogen)
5.0 µl	10x Pfu Buffer (Promega)
1.0 µl	Pfu Polymerase (3 u/µl) (Promega)
39.0 µl	dH_2O
50.0 µl	

PCR was performed on a Perkin Elmer DNA Thermal Cycler 480 with the following conditions:

Temperature [°C]		Time [min]	Step
95 °C		2 minutes	1.Initial denaturation
95°C	30 cycles	1 minute	2. Denaturation
x °C		1 minute	3. Annealing
72°C		4-20 minutes	4. Extension
72°C		5 minutes	5. Final extension
4°C		∞	6. Storage

Table 6 PCR reaction conditions, steps 2-4 were repeated 30 times. Annealing temperature (x) depends on the melting temperature of the primers. Usually annealing temperatures were 5-10°C lower than the calculated melting temperature of the primers. Extension time depends on the length of the DNA template. Normally per 1000 bp of sequence length two minutes are needed for extension.

Template DNA in the PCR mix contains methylated adenines, which allow digestion with *Dpn*I. 10 µl of the PCR reaction were kept as undigested control, whereas the remaining part was digested with 1 µl *Dpn*I (New England Biolabs, 20 u/µl) and 4.5 µl NE Buffer 4 for 5 h at 37°C. 10 µl of the template-free PCR reaction and 10 µl of the undigested control were analyzed on a 1% agarose gel (see chapter 3.3.6.1). For the transformation in competent *E. coli* Top 10 cells 10 µl of digested DNA was used (see chapter 3.3.3).

3.3.1.2 Manipulation of cleavage sites by cassette cloning

For replacing a small DNA fragment (up to 50 nucleotides) at the cleavage site of the $2A^{pro}$ with a new fragment, bearing the desired mutations, cassette cloning was applied. Two primers complementary to each other, containing the desired mutations and the same restriction sites (correct sticky ends) used to digest the vector, were phosphorylated on the 5' end (see chapter 3.3.7.3) and ligated into a digested and dephosphorylated vector (see chapter 3.3.7.1, 3.3.7.2 and 3.3.7.4). The plasmid bearing the desired mutation was then transformed into *E.coli* Top10 cells (see chapter 3.3.3).

3.3.1.3 Generation of cDNA by RT- PCR

The process of RT-PCR (reverse transcription – polymerase chain reaction) was carried out in two separate steps; the initial production of cDNA from the isolated RNA using SuperScript® III Reverse Transcriptase (Invitrogen, 200 u/µl), and the subsequent amplification of the synthesized cDNA by PCR. Mutant viruses were isolated by picking plaques from cell culture plates. After three rounds of plaque purification, viral RNA was resuspended in 100 µl PBS, freeze/thawed three times and centrifuged at 6500 rpm for 5 minutes, separating the virus (in the supernatant) from dead cells.

First strand cDNA synthesis is performed in a total volume of 20 µl composed of:

11 µl	Virus supernatant
2 µl	1 µM antisense primer
1 µl	2.5 mM dNTPs (Invitrogen)
2 µl	10x first strand buffer
1 µl	RNasin® RNase Inhibitor (Promega, 40 u/µl)
1 µl	SuperScript® III Reverse Transcriptase (Invitrogen, 200 u/µl)
2 µl	dH_2O
20 µl	

Negative controls with *in vitro* transcribed RNA with or without SuperScript® III Reverse Transcriptase were performed as well. Synthesis of cDNA from an RNA template was performed on a Perkin Elmer DNA Thermal Cycler 480 with the following conditions:

Temperature [°C]	Time [min]	Step
55 °C	10 minutes	
40°C	60 minute	Reverse Transcription
70°C	15 minutes	Inactivation of RT

Table 7 Conditions for reverse transcription reaction.

The created cDNA can then be used as template for amplification in PCR:

2.5 µl	cDNA (from first-strand reaction)
1.0 µl	Sense primer (1 µg/µl)
1.0 µl	Antisense primer (1 µg/µl)
2.5 µl	dNTPs (2.5 mM) (Invitrogen)
5.0 µl	10x Pfu Buffer (Promega)
1.0 µl	Pfu Polymerase (3 u/µl) (Promega)
37.0 µl	dH_2O
50.0 µl	

PCR was performed on a Perkin Elmer DNA Thermal Cycler 480 with the following conditions:

Temperature [°C]		Time [min]	Step
95 °C		2 minutes	1.Initial denaturation
95°C	30 cycles	1 minute	2. Denaturation
37 °C		1 minute	3. Annealing
72°C		4 minutes	4. Extension
72°C		5 minutes	5. Final extension
4°C		∞	6. Storage

Table 8 PCR reaction conditions for amplification of cDNA after reverse transcriptase. Steps 2-4 were repeated 30 times.

The synthesized cDNA was checked on an agarose gel (see chapter 3.3.6.1), concentration was determined using the NanoDrop (see chapter 3.3.10) before sending it for sequencing (see chapter 3.3.11).

3.3.2 PREPARATION OF CHEMICALLY COMPETENT CELLS

A 3 ml overnight culture of competent *E.coli* TOP10 cells was grown in 2x TY medium overnight at 37°C with rotation at 220 rpm. On the following day 100 ml of 2x TY medium was inoculated with the overnight culture and grown at 37°C for 2-3 hours until an OD_{600} of 0.45-0.55 was reached. Cells were then incubated on ice for 15 minutes, before centrifuging them for 15 minutes at 2500 rpm at 4°C. The pellet was resuspended in 33 ml RF1 suspension and incubated for 15 minutes on ice and centrifuged as described before. The pellet was taken up in 8 ml RF2 suspension and the bacterial solution was then divided in 200 µl aliquots, snap frozen in liquid nitrogen and stored at -80°C.

Solutions:

2x TY medium (1l)	RF1 solutions	RF2 solution
16 g Tryptone 10 g Yeast extract 5 g NaCl Adjusted with NaOH to a pH 7	100 mM KCl 100 mM MnCl2 30 mM K-Acetate 10 mM CaCl2 15% (w/v) Glycerol Adjusted with HCl to a pH 5.8	10 mM MOPS 10 mM KCl 75 mM CaCl2 15% (w/v) Glycerol Adjusted with KOH to a pH of 6.08

3.3.3 BACTERIAL TRANSFORMATION BY HEAT SHOCK

Throughout all cloning experiments *E.coli* TOP10 bacterial cells were used to amplify plasmids in order to make larger quantities of it.

In order to make the bacterial cells "competent" to take up DNA, the procedure of heat shock is applied. Bacterial cells, which were suspended in a solution containing high concentration of calcium, were thawed on ice and DNA (0.1 µl of plasmid DNA or 10 µl of a ligation) was added. Cells and DNA were together incubated on ice for 15°C, placed at 42°C (heat shock) for 50 seconds and put back on ice briefly. 400 µl of LB medium was added and the cells were incubated at 37°C for 30 minutes. Cells were then plated out on antibiotic containing media and incubated overnight at 37°C.

3.3.4 OVERNIGHT CULTURE

Bacteria, picked directly from petri dishes or taken from frozen cultures, were incubated in 4 ml LB media for mini-preps or in 100 ml LB media for midi-preps with antibiotics and incubated overnight at 37°C under aerobe conditions.

Solutions:

LB Medium	Ampicillin sodium salt (Sigma)
10 g/l Tryptone 5 g/l Yeast extract 10g/l NaCl Adjusted to pH 7.0	Dissolved in H_2O 100 mg/ml

3.3.5 ISOLATION OF PLASMID DNA FROM BACTERIA

3.3.5.1 DNA miniprep

Small-scale isolation of plasmid DNA from bacteria is performed for screening and analysis of plasmid DNA in cloning experiments. A single colony was taken from the transformation plate and used to inoculate 4 ml of LB medium containing ampicillin (Sigma, 100 mg/ml) and incubated

overnight at 37°C. Bacteria from the overnight culture were harvested by centrifugation at 5000 g for 5 minutes at 4°C. The pellet of bacterial cells was carefully resuspended in 100 µl re-suspension buffer S1 (Solutions from Nucleobond Midipreparation kit). Cell lysis was performed by adding 200 µl lysis solution S2 to the cells, inverting the tube and incubating it for two minutes. 150 µl pre-cooled neutralization buffer S3 was added to the suspension, again inverting the tube and incubating it for 5 minutes. Separation of the DNA from cell debris was performed by centrifugation at 13200 rpm for 10 minutes at 4°C. Supernatant, containing the plasmid DNA was transferred to a new tube and DNA was precipitated by addition of 1 ml ice-cold 70% ethanol. After centrifugation at 13200 rpm for 5 minutes at 4°C, the pellet was resuspended in 200 µl 1x TE buffer and 200 µl 5 M LiCl to precipitate remaining RNA and centrifuged at 13200 rpm for 5 minutes at 4°C. Again the supernatant was transferred to a new tube and DNA was precipitated as described above. After centrifugation, the pellet was dried for 10-15 minutes and DNA was resuspended in 50 µl dH_2O. This plasmid quality is suitable for analytical digestions.

Solutions:

Re-suspension buffer SI	**Lysis buffer SII**	**Neutralization buffer SIII**	**1x TE buffer**
50 mM Tris/HCl, pH 8.0 10 mM EDTA 100 µg/ml RNase A	20 mM NaOH 1% (w/v) SDS	2.8 M potassium-acetate pH5.1	10 mM Tris pH 8.0 (adjusted with NaOH) 1 mM EDTA

3.3.5.2 DNA midiprep

For preparative digestions and sequencing higher amounts of pure plasmid DNA were needed and were obtained with the Nucleobond AX plasmid Midi Kit (Macherey-Nagel) used according to the instructions of the manufacturer.

Additional solutions to miniprep:

Equilibration buffer N2	**Wash buffer N3**	**Elution buffer N5**
100 mM Tris 15% ethanol 900 mM KCl 0.15% Triton X-100 Adjusted to pH 6.3 with H_3PO_4	100 mM Tris 15% ethanol 1.15 M KCl adjusted to pH 6.3 with H_3PO_4	100 mM Tris 15% ethanol 1.15 M KCl adjusted to pH 8.5 with H_3PO_4

3.3.6 AGAROSE GEL ELECTROPHORESIS

For the separation and analysis of DNA agarose gel electrophoresis was used. The purpose of the gel might be to look at the DNA, to quantify it (see chapter 3.3.6.1) or to isolate a particular band (see chapter 3.3.6.2).

Solutions:

0.5 x TAE buffer	10 x Loading buffer	Marker	Ethidium bromide
20 mM Tris base 5 mM Sodiumacetate 1 mM EDTA	1 mM EDTA 0.1% Orange G 10% Ficoll in 0.5 x TAE	1 µg of *Hind*III digested λ-DNA (Promega)	10^{-4}% Ethidium bromide in 0.5 x TAE

3.3.6.1 DNA separation on agarose gels

Agarose was melted in 1x TAE buffer by boiling. Under normal conditions a 1% agarose gel was made. After cooling the gel for some minutes it was poured into a gel rack with a comb. When the gel was fully polymerized it was put into a tank containing 0.5x TAE buffer.

Samples, which were loaded on the gel consisted of 2 µl DNA, 2 µl loading buffer and 16 µl H_2O. The lid and power leads are placed on the apparatus, and current is applied. As DNA molecules are negatively charged, they migrate from the negative to the positive pole. Smaller fragments move faster than larger ones, thus the DNA fragments are separated according to their size. DNA fragment separation normally was performed at 110 V using the Biorad power pack basic. The distance the DNA has migrated can be visualized by staining with ethidium bromide, which intercalates between bases of DNA and RNA, on an ultraviolet transilluminator.

3.3.6.2 Extraction of DNA from agarose gels

Desired fragments were cut out from the gel under UV light and isolated and purified from the gel using the "Wizard® Gel and PCR Clean up system" by Promega (see 3.3.8.1).

3.3.7 ENZYMATIC REACTIONS

3.3.7.1 Restriction digestions of DNA

Digestion of DNA was performed using restriction endonucleases and 10x reaction buffers purchased from New England BioLabs according to the manufacturers protocols. Depending on the enzymes used, the temperature and the time of incubation was chosen. For efficient analytical digestions 5 – 10 µg of DNA were used in a total volume of 100 µl normally composed of:

x	µl DNA
10	µl NE buffer (1-4)
1	µl enzyme
y	µl dH_2O
100	µl

Preparative digestions were performed with 1-2 µg of DNA in a total volume of 20 µl:

x	µl DNA
2	µl NE buffer (1-4)
0.5	µl enzyme
y	µl dH_2O
20	µl

3.3.7.2 Removal of 5' phosphate groups from DNA with calf intestinal phosphatase

In order to prevent re-ligation of the vector and thereby increase ligation efficiency, the cut vector was subjected to dephosphorylation of the 5' phosphates of the vector by CIP (calf intestinal alkaline phosphatase, New England Biolabs). The restricted and purified vector was eluted in 53 µl dH_2O and incubated with 1 µl CIP (10 u/µl) and 6 µl NEB 3 (New England Biolabs) at 37°C for 60 minutes. Afterwards, the reaction mixture was purified using the Clean-Up System (see chapter 3.3.8.1).

3.3.7.3 Phosphorylation and annealing of oligonucleotides

Phosphorylation of 5' ends was carried out using the T4 polynucleotide kinase (PNK, New England BioLabs, 10 u/µl). Phosphorylation reactions were performed in a total volume of 20 µl composed of:

1 µl	Tim XXX (1 µg/µl)
1 µl	Tim XXX (1 µg/µl)
2 µl	100 mM ATP
2 µl	10 x Polynucleotidekinase (PNK) buffer (New England BioLabs)
1 µl	T4 PNK (New England BioLabs, 10 u/µl)
13 µl	dH_2O
20 µl	

A single cycle of incubation was performed on a Perkin Elmer DNA Thermal Cycler 480 with the following conditions:

Temperature [°C]	Time [min]	Step
37 °C	30 minutes	Phosphorylation
90°C	30 seconds	Inactivation
37°C	5 minutes	

Table 9 Conditions for kinasing of 5' ends of primers.

3.3.7.4 Ligation of DNA fragments with T4 DNA ligase

To estimate the DNA concentration prior to ligation dephosphorylated vector and insert were loaded on an agarose gel. Ideal ratio of vector to insert concentration was about 1:3. Ligation reaction were either performed at RT for 2 hours or at 16°C overnight in a total volume of 20 µl composed of:

50 ng	vector
150 ng / 1 µl	insert / phosphorylation mix
2 µl	10 x ligase buffer (New England BioLabs)
0.5 µl	T4 DNA ligase (New England BioLabs, 400 u/µl)
x µl	dH_2O
20 µl	

3.3.8 DNA PURIFICATION

3.3.8.1 Wizard SV Gel and PCR Clean-Up System (Promega)

Extraction of DNA from agarose gels, as well as the purification of PCR or other DNA samples (e.g. after dephosphorylation, restriction) were performed with the Wizard® SV Gel and PCR Clean-Up System kit from Promega.

For the extraction of DNA from a gel, the band was isolated from the gel by cutting, followed by adding membrane binding solution at a ratio of 10 µl of solution per 10 mg of agarose gel slice. The mixture was then incubated at 65°C for 10 minutes or until the gel slice was completely dissolved. For purifying PCR or other reaction samples, an equal volume of membrane binding solution was added. One SV minicolumn was placed in a collection tube for each dissolved gel slice or DNA sample. The dissolved gel mixture or prepared DNA sample was transferred to it and incubated for 1 minute at RT. After centrifugation at 13200 rpm for 1 minute, the column was washed by adding 700 µl of membrane wash solution. The centrifugation and washing step was repeated by adding 500 µl of membrane wash solution. After another centrifugation, the collection tube was completely emptied, and the minicolumn was centrifuged at 13200 rpm for 5 minutes. After that the minicolumn was transferred to a clean 1.5 ml microcentrifuge tube and 15 µl – 50 ml dH_2O was added onto the column, incubated for two minutes and centrifuged at 13200 rpm for three minutes. The elution, containing the DNA, could then be stored at – 20°C or used for further experiments.

3.3.8.2 Phenol-chloroform extraction

To remove proteins and other contaminants from DNA 2 µl 0.5 M EDTA pH 8.0 and 100 µl phenol were added (per 100 µl of DNA sample). After that the mixture was vortexed and centrifuged

at 13200 rpm for two minutes. The aqueous phase was transferred to a new eppendorf tube and 100 µl of chloroform was added to the tube. Vortexing, centrifuging and transfer to a new eppendorf tube was repeated as described above. The purified sample was stored for later use at -20°C (DNA) or -80°C (RNA).

3.3.9 PRECIPITATION OF DNA

DNA was precipitated with 1/10 volume of 3M NaOAc to neutralize the charge on the sugar phosphate backbone, making the molecule less hydrophilic and less soluble and 2.5 volumes of 100% ethanol. Sodium acetate is used for routing DNA precipitations, whereas for RNA precipitation ammonium acetate is used, which facilitates also the removal of dNTPs. The precipitation mix was incubated at -80°C for 30 minutes. The tube was then centrifuged at 13200 rpm for 20 minutes the pellet was air-dried and resuspended in 25 µl of dH_2O.

3.3.10 QUANTIFICATION OF DNA/RNA

Concentrations and sample purity (260/280) of DNA and RNA were measured using the NanoDrop from Thermo Scientific.

3.3.11 DNA SEQUENCING

Samples for DNA sequencing were prepared. For sequencing of plasmid DNA, samples with concentrations of 100 ng/µl were needed. For sequencing DNA of PCR reactions a concentration of 40 ng/µl was needed. 4 µl of the appropriate primer (1:30 diluted) was added and the sample was sent to LGC Genomics.

3.4 RNA METHODS

3.4.1 *IN VITRO* TRANSCRIPTION

Producing RNA from DNA was performed using an *in vitro* transcription system with the T7 promoter. First the plasmid DNA was linearized with a restriction enzyme cleaving just downstream of the coding sequence. After purification, DNA was eluted in 36 µl dH_2O.

Transcription reactions were performed in a total volume of 100 µl composed of:

36 µl	DNA
20 µl	5x PO_4/DTT
20 µl	2.5 mM NTPs
20 µl	Spermidine/Mg
3 µl	RNasin® RNase Inhibitor (Promega, 40 u/µl)
1 µl	T7 RNA polymerase
100 µl	

To *in vitro* transcribe DNA into RNA the reaction mix was incubated at 37°C for 120-180 minutes. Template DNA was digested by adding 0.6 µl desoxyribonuclease I (Invitrogen, 251 u/µl) and 1 µl RNasin® RNase Inhibitor (Promega, 40 u/µl) and incubating it again at 37°C for 20 minutes. The RNA was extracted using phenol/chloroform extraction. RNA was precipitated with 1/3 volume of 8M NH_4OAc and 2.5 volumes of 100% ethanol. The precipitation mix was incubated at -80°C for 30 minutes. The tube was then centrifuged at 13200 rpm for 20 minutes, the pellet was air-dried and resuspended in 25 µl of dH_2O.

3.4.2 RNA AGAROSE GEL ELECTROPHORESIS

The quality of the RNA was checked on a 1% agarose gel containing 0.1% (w/v) SDS. 10x loading buffer was added to the RNA samples. To better denature secondary structures, the samples were heated to 70°C for 5 minutes, before putting them on ice for some seconds. After loading, RNA fragments separation was performed at 100 V using the Biorad power pack 300. Before staining the agarose gel in ethidium bromide solution, it was washed two times in dH_2O for 15 minutes. RNA bands were visualized using an UV transilluminator.

3.4.3 *IN VITRO* TRANSLATION

To monitor self-processing of the $2A^{pro}$ *in vitro* translation reactions were performed. Thereby, *in vitro* transcribed mRNA, coding for VP-$2A^{pro}$, was added to rabbit reticulocyte lysate (RRL) and ^{35}S methionine, which was used to build the protein during the reaction and could later be detected. Aliquots of the newly synthesized viral proteins were taken at determined times.

In vitro translation reactions were typically performed in reaction volumes of 10 µl (multiplied depending on how many aliquots are needed to be taken at different time points) at 30°C. The mastermix of a standard reaction was composed out of:

70 µl RRL (rabbit reticulocyte lysate, Promega)
2 µl 1 mM amino acid mix without methionine (Promega)
2 µl RNasin (Promega, 40 u/µl)
4 µl 10 µM ^{35}S methionine (1000 Ci/mmol, Hartmann Analytics)
12 µl dH_2O
90 µl

9 µl of the mastermix were transferred into a new tube containing 1 µl of dH_2O and served as a negative control. After pre-incubation of the translation mix for two minutes at 30°C, the translation was started by the addition of 10 µl *in vitro* transcribed RNA (10ng/µl). 10 µl aliquots were removed after translation start at the following time points: 0, 10, 20, 30, 60, 120 and 180 minutes. The reaction was stopped by transferring the aliquots immediately to 41 µl of ice-cold stop solution.

The translation products were analyzed by the polyacrylamide gel electrophoresis system described by Dasso & Jackson (1989) and fluorography.

Solutions

Stop solution	**2x Laemmli Sample buffer**
1 µl 20 mM Unlabeled methionine/cysteine mix 25 µl 2x Laemmli sample 15 µl H20	20% glycerol 10% β-mercapto-ethanol 6% SDS 0.01% Bromophenol blue pH6.8

3.4.4 SDS PAGE (DASSO AND JACKSON, 1989)

In vitro translated products were analyzed on a 17.5% SDS-PAGE followed by fluorography. A protocol of sodiumdodecylsulfate polyacrylamide electrophoresis (SDS PAGE) of Dasso and Jackson (Dasso and Jackson, 1989) was used to separate protein fragments of smaller size. Composition of both gel parts are listed in table 10.

	17.5 % Separation gel	Stacking gel
30% Polyacrylamide	3.500 ml	0.333 ml
2.5 % Bisacrylamide	0.158 ml	0.104 ml
4 x LGS	1.500 ml	-
4x UGS	-	0.500 ml
dH_2O	0.754 ml	1.060 ml
10% APS	0.050 ml	0.020 ml
TEMED	0.005 ml	0.002 ml

Table 10 Components of separation and stacking gel of SDS PAGE gel (Dasso and Jackson, 1989). LGS: lower gel solution; UGS: upper gel solution; APS: Ammoniumperoxidisulfate; TEMED: N,N,N',N'-tetramethyl-ethane-1,2-diamine.

The separation gel was poured and overlaid with 70% ethanol. After polymerization it was rinsed with H_2O, and the stacking gel was poured on top of the separation gel. Samples were mixed with 2x Laemmli sample buffer and heated to 95°C for 10 minutes. The gel unit was assembled and the tank of a mini-PROTEAN® 3 system from BioRad was filled with running buffer. After loading the samples, protein separation was achieved at 150 V. 5 µl of the ^{14}C-labelled protein marker from Perkin Elmer or of the ^{14}C labeled CFA.626 protein marker from Amersham was used as a size marker.

Solutions

4x Lower gel solution	**4 x Upper gel solution**	**Running buffer (Dasso and Jackson)**	**2x Laemmli Sample buffer**
1.5 M Tris HCl pH8.8 0.4% SDS	0.5 M Tris HCl pH 6.8 0.4% SDS	50 mM Tris/HCl 385 mM Glycine 0.1% (w/v) SDS	20% Glycerol 10% β-mercapto-ethanol 6% SDS 0.01% Bromophenol blue pH6.8

3.4.5 FLUOROGRAPHY

After separation of the ^{35}S-methionine labeled *in vitro* translated proteins on a Dasso & Jackson polyacrylamide gel, the gel was washed two times in enhancer solution for 15 minutes at room temperature. By doing this, the wavelength of radiation is shifted, to increase the sensitivity of the signal by an autoradiography film and to lower the background. After drying with vacuum on Whatman™ 3MM paper, the gel was exposed to a KODAK BioMax MR film for 16 – 24 hours at -80°C. Films were developed on an AGFA Curix 60.

Solutions

Enhancer solution
1 M sodium salicylate 45% methanol

3.5 TISSUE CULTURE

3.5.1 CELL LINES AND VIRUS

Human cervix carcinoma HeLa Ohio, which are particularly suited for growth of human rhinoviruses, were obtained from the Flow Company and used throughout all experiments. HRV1A, and -14 were thankfully provided by Irene Gösler.

3.5.2 MEDIA AND SOLUTIONS

Growth medium: Minimum essential medium (MEM, Gibco) was supplemented with 10% (v/v) fetal calf serum (FCS, Gibco), 1% (v/v) 200 mM L-Glutamine (Gibco), 1% (v/v) 100x penicillin/ streptomycin (Gibco). This medium is used for monolayer culture of HeLa cells.

For virus infectivity assays, MEM was supplemented with 2% (v/v) FCS, 1% (v/v) 200 mM L-Glutamine, 1% (v/v) penicillin/streptomycin and 1% (v/v) 3 M $MgCl_2$.

The buffer used to wash the cells was 1x phosphate buffered saline (PBS) containing 1.4 mM KH_2PO_4, 2.7 mM KCl, 4-3 mM Na_2HPO_4 and 137 mM NaCl dissolved in H_2O.

For plaque purification and plaque assays a semi solid medium was made, containing 2% low melting agarose (Sigma) and 2x Infection medium.

RNA transfection is performed with DEAE dextran solution and 2x LiCl2 buffer. The DEAE dextran stock solution contains 3mg/ml and the 2x $LiCl_2$ buffer contains 0.28 M $LiCl_2$, 2 mM $MgCl_2$, 20 mM HEPES pH 7.5 (adjusted with NaOH).

To dissociate adherent cells from tissue culture dishes a buffered salt solution containing 0.5% (w/v) trypsin and 0.2% (w/v) EDTA is used (PAA Laboratories GmbH).

3.5.3 CULTIVATION OF MAMMALIAN CELLS

Adherent HeLa cells were cultured as monolayers in tissue culture flasks, petri-dishes or micro titer well plates (Nunc, Corning) in MEM supplemented with FCS, glutamine and antibiotics (see chapter 3.5.2) at 37°C in presence of 5% CO_2.

For splitting confluent cells, the petri-dish or flasks had to be washed once with warm 1x PBS to completely remove old media and dead cells and incubated with 3 ml Trypsin/EDTA for 5 minutes at 37°C to dissociate from the surface. Floating cells were then resuspended in growth medium to stop the activity of trypsin/EDTA and were diluted to the preferred density.

6-well plate, 2 ml media per well

96-well plate, 100 µl media per well

T25 cm^2 flask, 50 ml media

T75 cm^2 flask, 50 ml media

3.5.4 DETERMINATION OF CELL NUMBERS

After the cells were detached from the flask surface, they were centrifuged 5000 rpm for 5 minutes and the cells were taken up in a known volume of fresh infection medium. 100 µl of the cell

suspension was mixed with 400 µl trypan blue and loaded onto a thoma haemocytometer. The cells were counted under the light microscope.

3.5.5 FREEZING AND THAWING CELLS

Cells were pelleted by centrifugation for 5 minutes at 1200 rpm and about 10^7 cells were resuspended in 1 ml heat inactivated FCS containing 10% DMSO and were transferred into cryotubes. The tubes were frozen in a cryobox containing isopropanol at -80°C overnight and on the next day transferred into liquid nitrogen (-196°C).

Thawing of the frozen stocks was performed quickly at 37°C, and the cells were resuspended in 10 volumes of appropriate growth medium and centrifuged for 5 minutes at 1200 rpm. Then they were resuspended in fresh growth medium and transferred into a tissue culture flask.

3.5.6 INFECTING CELLS

One day prior to infection HeLa cells were prepared by seeding a determined amount of cells in petri dishes or flasks. Normally cells were seeded in infection medium to obtain a density of 50% on the following day.

Plastic ware	Surface area	Number of HeLa cells
T-175	175 cm^2	$280 \cdot 10^5$ cells
T-75	75 cm^2	$120 \cdot 10^5$ cells
T-25	25 cm^2	$40 \cdot 10^5$ cells
6-well plate	9.4 cm^2/well	$15 \cdot 10^5$ cells/well
12-well plate	4 cm^2/well	$6.4 \cdot 10^5$ cells/well
24-well plate	2 cm^2/well	$3.2 \cdot 10^5$ cells/well
48-well plate	0.8 cm^2/well	$1.3 \cdot 10^5$ cells/well
96-well plate	0.32 cm^2/well	$0.51 \cdot 10^5$ cells/well

Table 11 Tissue culture dishes. Cell number corresponding to the surface of culture flasks/plates used (1 cm^2 ~ $1.6 \cdot 10^5$ HeLa cells)

On the day of infection cells were washed two times with 1x PBS and virus dilution harvested after transfection or infection was added. After incubation for 90 minutes at 34°C and 5% CO_2 the supernatant was removed and the cells were washed two times with 1x PBS and 2 ml fresh infection medium was added and incubated for 48-72 hours.

3.5.7 CELL TRANSFECTION BY DEAE-DEXTRAN

For the introduction of RNA into eukaryotic cells the transient DEAE-dextran mediated transfection was used, which facilitates RNA binding to the cell membranes and entry of the RNA into the cell via endocytosis.

HeLa cells were prepared for transfection by seeding 0.325 10^6 cells per 6-well in 2 ml infection medium. Cells were grown for 18-24 hours at 37°C until a density of 50% was reached.

The transfection mix (for each 6-well) was prepared with the following components: 1.2 µg *in vitro* transcribed RNA diluted in 55 µl, 175 µl 2x $LiCl_2$ and 110 µl 3mg/ml DEAE-dextran. The resulting mix was incubated for 30 minutes on ice. For MOCK transfection 55 µl water was used instead of RNA. Meanwhile cells were washed two times with 1x PBS and 300 µl of transfection/MOCK transfection mix was added to the cells and incubated for 25 minutes at 34°C with light shaking. Then the transfection mix was removed, the cells were washed two times with 1x PBS and 3 ml of fresh infection medium or 3 ml of an 1:1 mix of 2% agarose and 2x infection medium was added and the plate was incubated for 2-3 days at 34°C, 5% CO_2.

3.5.8 CELL TRANSFECTION USING LIPOFECTAMINE 2000 TRANSFECTION REAGENT

Cells were seeded the day prior to infection as described in 3.5.7. On the day of infection 1.2 µg of RNA was mixed with 250 µl OptiMEM (Invitrogen) per well and 8 µl of Lipofectamine 2000 (Invitrogen) was also gently mixed with 250 µl OptiMEM per well and incubated at room temperature for 5 minutes. Then the RNA/OptiMEM was mixed with the Lipofectamine/OptiMEM and left at room temperature for 20 minutes. Meanwhile, cells were rinsed with 1x PBS and 500 µl of warm OptiMEM was added to each well, before distributing the RNA/lipofectamine mixture over the cells. With gentle agitation the plates were incubated at room temperature for 15 minutes, followed by an incubation of 45 minutes at 34°C. Transfection medium was aspirated off, cells were rinsed with 1x PBS and 3 ml of fresh infection medium or 3 ml of a 1:1 mix of 2% agarose and 2x infection medium was added and the plate was incubated for 2-3 days at 34°C, 5% CO_2.

3.5.9 VIRUS INFECTIVITY ASSAYS

3.5.9.1 Viral titer determination by $TCID_{50}$

HeLa cells were seeded in a 96-well plate (1.3 10^4 cells per well in 100 µl infection medium) one day prior to infection to be about 50% dense on the day of infection.

On the day of infection serial dilutions of the virus sample of unknown titer was prepared in 2 ml infection medium. Cells were infected with 100 µl per well of the virus dilutions (12 wells for each of the 8 dilutions). After incubation time of 5 days at 34°C, 5% CO_2 the supernatant was discarded and the remaining cells were stained with 100 µl 0.1% crystal violet in H_2O for about 10 minutes. Staining solution was discarded and the cells were washed with water. Infected wells remained unstained because lysed cells detach from the surface and were washed away, whereas uninfected cells were stained violet. By the number of infected wells in each dilution the tissue culture infective dose 50 ($TCID_{50}$) per ml of the virus sample could be calculated (Blake and O'Connell, 1993).

It has been experimentally determined that 10 $TCID_{50}$ equal approximately 1 plaque forming unit (pfu).

3.5.9.2 Plaque assays

HeLa Ohio cells were seeded in 6-well plates (0.325 10^6 cells per well in 2 ml infection medium) to be about 50% dense on the day of infection.

On the day of infection, virus dilutions were prepared in 1 ml infection medium. The medium from the 6-well plates was aspirated and the wells were washed twice with PBS. Then, 1 ml of virus dilution/MOCK dilution was added and the plates were incubated for 90 minutes at 34°C, 5% CO_2. The virus dilutions were aspirated, the cells were again washed twice with PBS and 3 ml of semi-solid medium (consisting of 1.5 ml of pre-warmed 2x infection medium and 1.5 ml pre-warmed 2% low melting type agarose) was added quickly to each well. The plates were further incubated at 34°C, 5% CO_2 until plaques were visible under the microscope or after three days.

For the isolation of mutant viruses the following procedure was performed: the wells were then stained with 1 ml of a sterile 0.05% neutral red solution in PBS for 1 hour at 34°C. After removing the neutral red solution, plaques were visible as unstained spots in the red cell monolayer. Those plaques were then picked with a Pasteur pipette and resuspended in 1 ml infection medium. Those plaques were then frozen and thawed three times, before starting a new round of plaque purification. For isolation of mutant viral plaques, three rounds of plaque purifications were performed. After the last round the picked plaques were resuspended in 100 µl PBS instead of infection medium before synthesizing cDNA via RT-PCR (see chapter 3.3.1.3).

The overlay medium could then be removed and the underlying cells were then stained with 0.1% crystal violet solution to count the plaques.

3.5.9.3 Growth kinetics

HeLa cells were seeded in lose 6-wells (0.325 10^6 cells per well in infection medium) to be about 50% dense on the day of infection.

On the day of infection medium was aspirated and the cells were washed twice with PBS. 1.5 ml of a virus dilution with an MOI of 1 (6.5 10^5 pfu/ml) was added to each well and the cells were incubated for 90 minutes at 34°C, 5% CO_2. Unbound virus was then removed by aspirating the virus suspension and the cells were washed twice with PBS. 1.5 ml fresh infection medium was added and the wells were then further incubated at 34°C, 5% CO_2. Two samples (intracellular and extracellular virus) was frozen immediately (0 hours post infection). After 3h, 6h, 8h, 24h and 48h the other samples were taken. To distinguish between intracellular and extracellular virus, the supernatant containing the free or extracellular virus was frozen separately. To the cells containing the intracellular virus 1.5 ml of fresh infection medium was added before freezing. After three freeze/thaw cycles, the virus titer of each sample was determined by $TCID_{50}$.

4 RESULTS

4.1 SEQUENCE COMPARISON OF ENTEROVIRAL 2A^{PRO}

The 2A^{pro} of various different *Enteroviruses* is a protein composed of 142 to 149 amino acids. Sequence comparison of the 2A^{pro} of human rhinovirus A (HRVA-1a, HRVA-2), human rhinovirus B (HRVB-14), human rhinovirus C (HRVC-1), poliovirus (PV-1), coxsackievirus B (CVB-4) and enterovirus (EV-71) show only an identity at the amino acid level of about 23% (see Figure 15A).

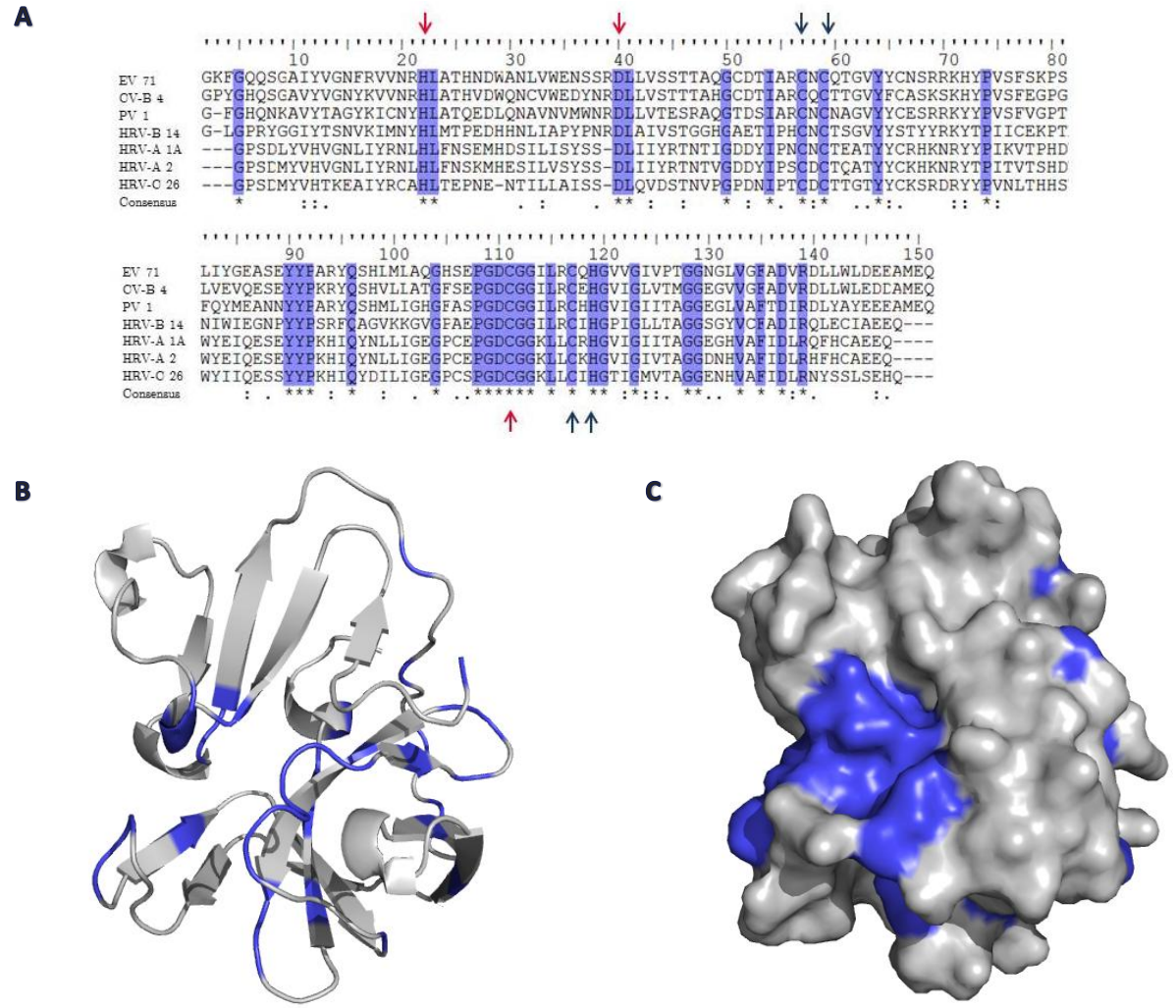

Figure 15 Amino acid sequence alignment of 2A^{pro} of different picornaviruses. A) Conserved residues are represented in blue. The active site residues of HRV2 2A^{pro} are marked with a red arrow: His, Asp, Cys. The residues coordinating the zinc ion are marked with a dark blue arrow. The sequences were taken from the database www.ncbi.nlm.nih.gov**.** Sequence IDs: AY458604 (HRV-A 1a), X02316.1 (HRV-A 2), X01087 (HRV-B 14), EF582387.1 (HRV-C 26) ABV60422 (PV 1), DQ480420 (CV-B 4), U22521.1 (EV 71). The sequence alignment was made online using ClustalW (http://www.ebi.ac.uk/Tools/msa/clustalw2/) and edited with the programme BioEdit. PV poliovirus, CV coxsackievirus, HRV human rhinovirus, EV enterovirus. B) Ribbon diagram and C) surface representations of the 2A^{pro} showing conserved residues from selected picornaviruses identified from the sequence alignment in Figure 15A. Identical residues are colored on the HRV2 2A^{pro} in blue. Non homologous residues are shown in grey. Conserved residues are mainly on the C-terminal part of the protein. Only single residues in the N-terminal part are conserved. Created with Pymol (DeLano, 2002) using the PDB ID code 2HRV2.

The catalytic triad of the active site residues was determined for HRV2 $2A^{pro}$ to consist of His18, Asp35 and Cys106 (Sommergruber et al., 1997; Petersen et al., 1999), for PV $2A^{pro}$ the residues are His20, Asp38 and Cys109 (Yu and Lloyd, 1991). These three residues are conserved in all *Enteroviruses*. On the opposite face of the active site at the beginning of the C-terminal region is the zinc binding site (Peterson 1999), in which a zinc ion is coordinated by three Cys sulfurs (Cys52, Cys54 Cys112) and one His nitrogen (His114) to stabilize the $2A^{pro}$ to form an active enzyme (Voss et al., 1995). These residues are conserved in all shown picornaviral $2A^{pro}$ sequences (Figure 15A, dark blue arrow). Other conserved residues are mainly located on the C-terminal part of the protein and only certain specific residues are identical in the N-terminal part. In Figure 15B and C, HRV2 $2A^{pro}$ is used as a model to show the localization of conserved residues from the sequence alignment.

The self-processing reaction of the $2A^{pro}$ is the first cleavage event during protein synthesis (Toyoda et al., 1986) and leads to a separation of the structural proteins from the non-structural ones. The cleavage site, consisting of at least five residues of the C-terminal part of VP1 (also designated as the P site according to Schechter and Berger, 1967) and at least four residues of the N-terminal part of the $2A^{pro}$ (also designated as the P' site), is recognized by the $2A^{pro}$ and cleaved. Figure 12 (in chapter 1.6.3) gives an overview of some enteroviral serotypes and their respective cleavage sites on the polyprotein. By comparing the cleavage site of different picornaviruses, no appreciable identity between the residues can be seen. The only absolutely conserved residue is the Gly at position P1'. At position P4, sequences shown here contain a Leu or an Ile and an amino acid with a hydrophobic side chain at position P1. All other positions show many diverse residues such as hydrophobic amino acids and amino acids with polar or charged side chains. It was shown for HRV2 $2A^{pro}$ that, upon substrate entry into the binding cleft Thr at the P2 position makes a hydrogen bond to Ser83 from the dityrosine flap, which is thought to compensate for the rotation of Tyr85 away from its original position, stacked upon His18 (Petersen et al., 1999).

Figure 16A shows a comparison of the $2A^{pro}$ sequence of a HRV group A, group B and group C virus. Although the overall sequence of HRV-C group is substantially different from other classified species, the $2A^{pro}$ sequence of HRV-C and HRV-A share some homologies. In fact, Simmonds et al. (2010) showed that the C-terminal domain of HRV-A and HRV-C have undergone interspecies recombination, whereas the N-terminal part is species-specific (McIntyre et al., 2010; Simmonds et al., 2010). Figure 16B, C and D show the cleavage site of all HRV group A, B or group C viruses. In HRV-A group viruses, the C-terminal VP1 part of the cleavage site seems rather amenable to accepting various residues at those positions, whereas the N-terminal $2A^{pro}$ part is nearly completely conserved. The first residues P1' and P2' are the hydrophobic amino acids Gly and Pro, which are conserved in all HRV-A group viruses. In contrast, HRV-B group viruses have three completely conserved residues, two in the C-terminal VP1 part of the cleavage site: Ile at position P4 and Tyr at

position P1. Additionally, the Gly at position P1' in the N-terminal 2A^{pro} part of the cleavage site is also invariable. HRV-C group viruses show a rather similar cleavage site to that of HRV-A group viruses. Gly at position P1' seems to be completely required as it is conserved in all serotypes.

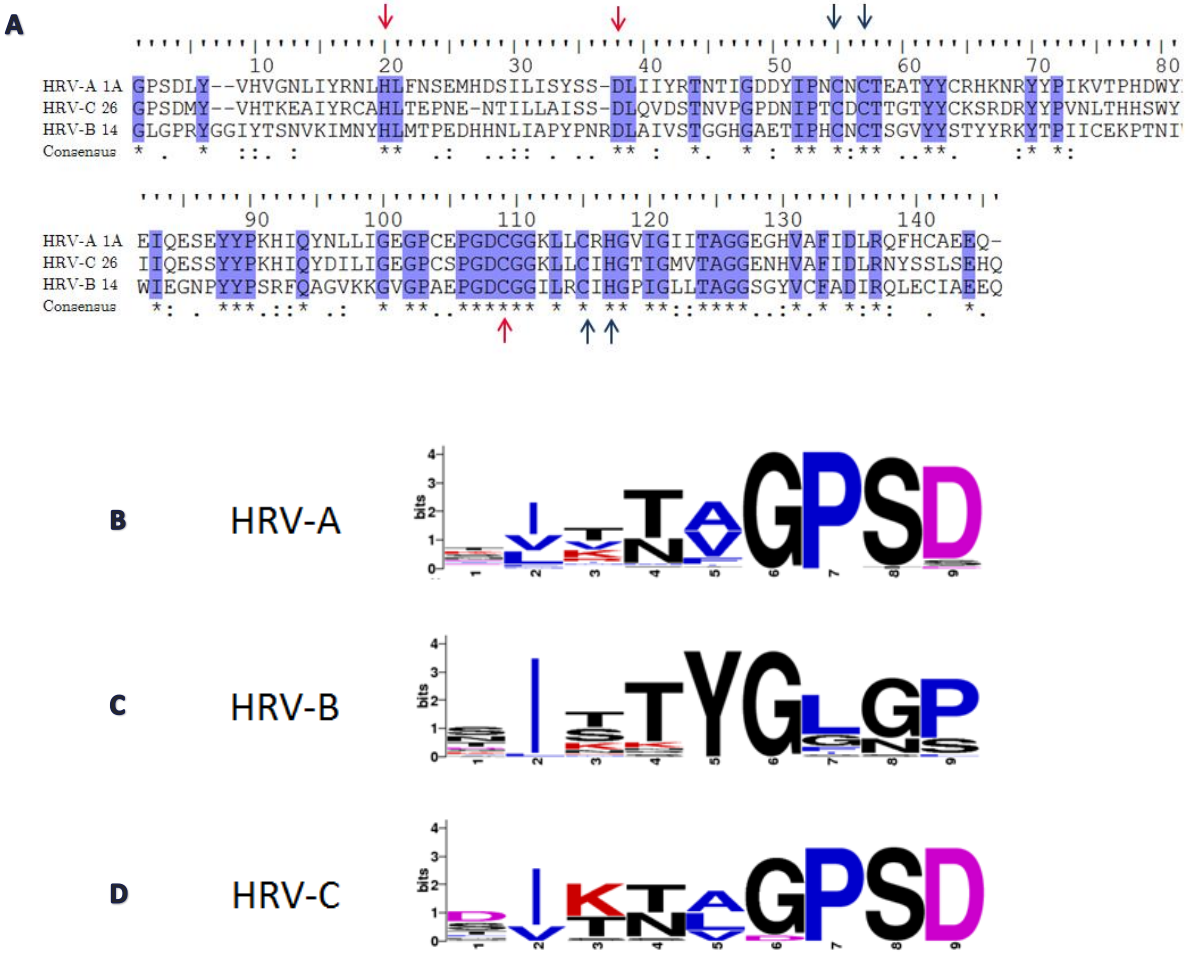

Figure 16 Comparison of the 2A^{pro} sequence and cleavage sites of 2A^{pro} of HRV group A, B and C viruses . A) Sequence alignment of the 2A^{pro} of HRV1A (group A), HRV14 (group B) and HRV26 (group C). The sequences were taken from the database www.ncbi.nlm.nih.gov. Sequence IDs: AY458604 (HRV-A 1a), X01087 (HRV-B 14), EF582387.1 (HRV-C 26). The sequence alignment was made online using ClustalW (http://www.ebi.ac.uk/Tools/ msa/clustalw2/) and edited with the programme BioEdit. HRV human rhinovirus. B) Comparison of cleavage site of all human rhinovirus group A viruses. C) Comparison of cleavage site of all human rhinovirus group B viruses. D) Comparison of the 2A^{pro} cleavage site of all human rhinovirus group C viruses. The P site representing the C-terminus of VP1 is shown as 1-5 here. The P' site representing the N-terminus of 2A^{pro} is shown as 6-9 here. The sequence logo was generated by using WebLogo (Crooks et al., 2004). HRV human rhinovirus.

For the development of an antiviral inhibitor against this protein, it is nevertheless necessary to fully understand how the 2A^{pro} recognizes the cleavage site, which residues are involved in this recognition and which are involved in the cleavage reaction. Experiments in this thesis were aimed towards this goal.

4.2 PROTEOLYTIC ACTIVITY OF WILD TYPE HRV1A 2A^{PRO}

The *cis*-cleavage event of wild type HRV1A 2A^{pro} from its precursor VP1-2A^{pro} occurs as soon as the 2A^{pro} is generated during protein synthesis. In the course of this work, the cleavage was monitored by translating a suitable RNA encoding VP1 and 2A^{pro} in RRLs. The 48 kDa precursor VP1-2A^{pro}, the initial translation product, is cleaved to yield equimolar amounts of 32 kDa VP1 and 16 kDa 2A^{pro} cleavage products.

Figure 17 shows the kinetics of protein translation and self-cleavage of the HRV1A wt 2A^{pro} in a typical experiment. Translation of mRNA into protein is already apparent after 10 minutes, having started between 0 and 10 minutes. After 10 minutes, 50% of the VP1-2A^{pro} precursor is already cleaved; cleavage is nearly complete after 120 minutes. The band of the 2A^{pro} is only weakly detected by fluorography, as it only contains 1 Met residue labeled during protein translation with ^{35}S methionine, whereas VP1 contains eight.

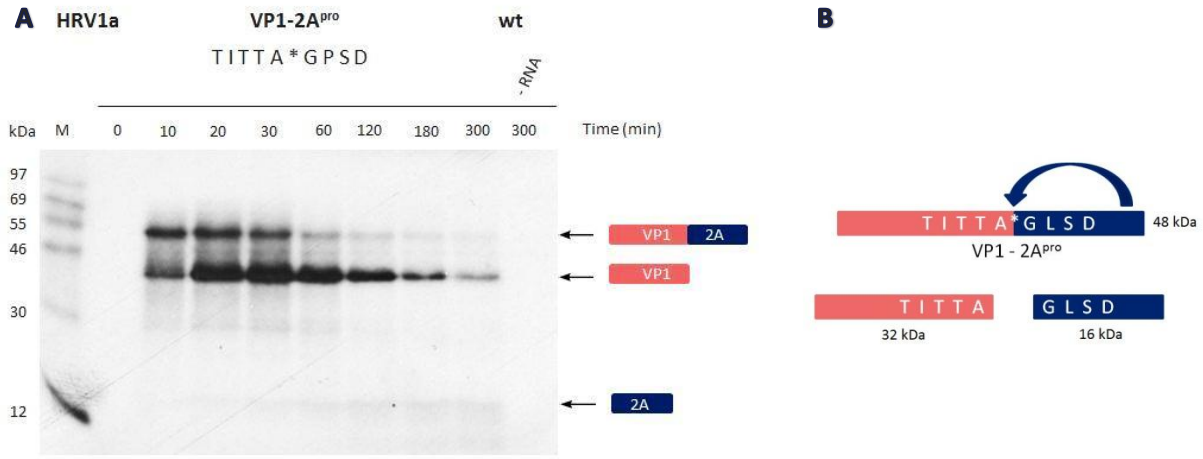

Figure 17 Proteolytic activity of 2A^{pro} wild type. A) Translation into protein was monitored at 30°C by using rabbit reticulocyte lysate which were programmed with RNA (10 ng/µl) coding for VP1-2A^{pro}. As a negative control, water instead of RNA was used. At the indicated time points, 10 µl aliquots were taken and translation reaction were stopped by adding an ice-cold stop solution containing 25 µl 2x Laemmli sample buffer, 15 µl H_2O and 1 µl unlabeled methionine/cysteine (20 mM). Viral proteins were separated on a 17.5% Dasso & Jackson PAA gel and visualized by fluorography after an exposure time of 16 hours. The ^{14}C-methylated protein marker (M) from Perkin Elmer was used and size is shown in kDa. Uncleaved VP1-2A^{pro} and the cleavage products VP1 and 2A^{pro} are marked by arrows. B) Schematic of the cleavage of the initial translation product into VP1 (red) and 2A^{pro} (blue). The cleavage site is indicated.

4.3 CONSTRUCTION OF HRV1A 2A^{PRO} MUTANTS

In the first experiment, the cleavage site of HRV1A VP1-2A^{pro}, T I T T A * G P S D was replaced by the corresponding region of HRV14 VP1-2A^{pro}, D I K S Y * G L G P. HRV1A and HRV14 are serotypes of human rhinoviruses, belonging to genetic groups A and B respectively. As the 2A^{pro} of HRV1A and HRV14 show only 42% identity in their amino acid sequence, we wanted to find out whether the

HRV1A enzyme could cleave at the rather different HRV14 cleavage site. Thus, in Figure 18, the cleavage site of HRV1A, T I T T A * G P S D, was replaced by the corresponding region of HRV14, D I K S Y * G L G P.

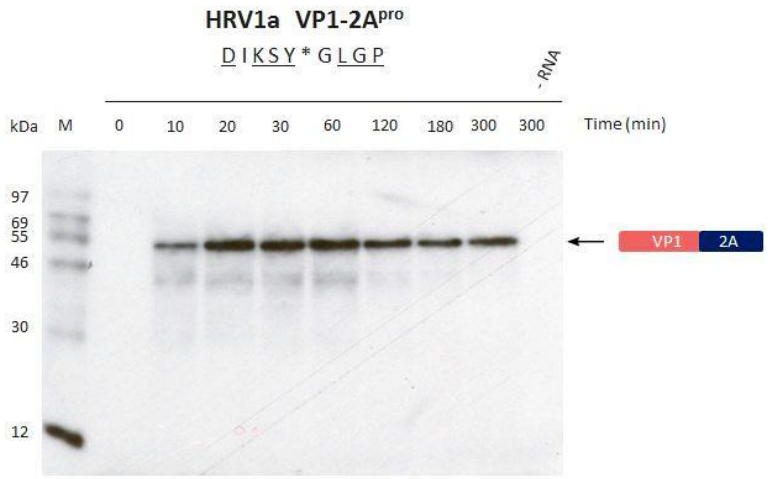

Figure 18 Self-processing of HRV1A 2A^{pro} on cleavage sites containing residues that differ from the wild type cleavage site. In a first attempt the cleavage site was exchanged with the entire cleavage site found in HRV14. Amino acids which differ from the wt HRV1A 2A^{pro} cleavage site are underlined. The procedure is the same as described in Figure 17.

Translation was monitored by autoradiography to investigate whether the 2A^{pro} of HRV1A was still able to recognize the cleavage site of HRV14. Figure 18 shows that no cleavage products were observed within 300 minutes of *in vitro* translation when the whole sequence of the HRV14 cleavage site was exchanged in the HRV1A VP1-2A^{pro}. Therefore, it can be concluded that HRV1A cannot accept the HRV14 cleavage site (D I K S Y * G L G P) in *cis*.

We next wanted to find out which residues of the HRV14 cleavage site could not be recognized by the HRV1A 2A^{pro}. To this end, other constructs with different combinations of amino acids were produced and tested for their ability to perform this cleavage event. Table 12 gives an overview of the mutated cleavage sites used in the HRV1A VP1-2A^{pro} junction.

Serotype	VP1						2A^{pro}			
	P5	P4	P3	P2	P1		P1'	P2'	P3'	P4'
HRV 1a wt	T	I	T	T	A	*	G	P	S	D
HRV 14 wt	D	I	K	S	Y	*	G	L	G	P
HRV 1A mutant 1	D	I	K	S	Y	*	G	P	S	D
HRV 1A mutant 2	T	I	T	T	A	*	G	L	G	P
HRV 1A mutant 3	T	I	K	S	Y	*	G	L	S	D
HRV 1A mutant 4	T	I	T	S	Y	*	G	L	S	D
HRV 1A mutant 5	T	I	T	T	A	*	A	P	S	D

Table 12 Overview of the HRV1A VP1-2A^{pro} constructs with wt and mutated cleavage site of the 2A^{pro}. C-terminus of VP1 and N-terminus of 2A^{pro} are shown. Underlined residues in the HRV1A mutants differ from wild-type sequence and are, except for the last one, all found at equivalent positions at the HRV14 2A^{pro} cleavage site.

The HRV1A VP1-2A^{pro} constructs contained combinations of some HRV14 2A^{pro} residues upstream and downstream of the cleavage junction. In one construct, Gly, which was exclusively found in nearly all picornaviruses at position P1', was replaced by Ala. Alanine, a very abundant amino acid, is only slightly larger than Gly as it possesses a methyl group as side chain in place of a single hydrogen atom.

To monitor *in vitro* cleavage of the 2A^{pro} from the VP1-2A^{pro} precursor containing substituted cleavage sites, these were exchanged by cassette cloning and mutations were confirmed by nucleotide sequence analysis. Following this, the linearized template was transcribed into mRNA and *in vitro* translated into protein.

4.4 CLEAVAGE OF HRV1A VP1-2A^{PRO} CONTAINING SUBSTITUTIONS AT THE CLEAVAGE SITE OF THE 2A^{PRO}

We compared the HRV1A VP1-2A^{pro} wt cleavage with the cleavage of VP1-2A^{pro} constructs where parts of the HRV14 cleavage sites were exchanged: Figure 19A shows the cleavage when T I T T A * G P S D was replaced by only the VP1 part of HRV14, D I K S Y * G P S D (mutant 1). And Figure 19B shows the cleavage, when T I T T A * G P S D was replaced by only the 2A^{pro} part of HRV14, T I T T A * G L S D (mutant 2).

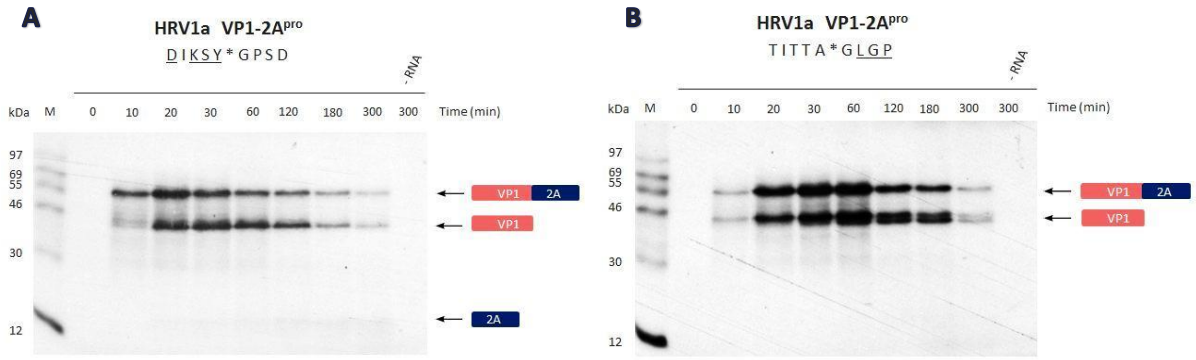

Figure 19 Self-processing of HRV1A 2A^{pro} on cleavage sites containing residues that differ from the wild type cleavage site. Here the cleavage sites were exchanged with parts of the cleavage site of the HRV14 2A^{pro}. A) P5-P1 of the cleavage site mutated to that found in HRV14. B) P1'-P4' of the cleavage site mutated to that found in HRV14. Amino acids which differ from the wt HRV1A 2A^{pro} cleavage site are underlined. The procedure is the same as described in Figure 17.

Different results to that when the full HRV14 wt cleavage site was exchanged, are obtained when only one (either the VP1 or the 2A^{pro}) part was exchanged (Figure 19A and B), where only kinetics of cleavage is slightly delayed. Introduction of the VP1 part of HRV14 (D I K S Y instead of HRV1A T I T T A) into the HRV1A VP1-2A^{pro} cleavage site shows a 50% conversion into the cleavage

product after 20 to 30 minutes, which is slightly slower than with HRV1A wt (compare Figure 17). Complete cleavage was not finished within 300 minutes of translation. Introduction of the 2A part of HRV14 (G L G P instead of HRV1A G P S D) into the HRV1A VP1-2A^{pro} cleavage site shows nearly the same cleavage kinetics with 50 % conversion into the cleavage products being reached after about 30 to 40 minutes. Complete cleavage was also not finished within 300 minutes of translation.

These cleavage results reveal that HRV1A 2A^{pro} is not able to accept the HRV14 cleavage site. Furthermore, the results suggest that mutations upstream and downstream of the cleavage bond will be necessary to completely stop the *cis*-cleavage event of the 2A^{pro}. Mutation of either site alone does not impair the activity of the 2A^{pro}.

As the previous experiments have suggest that mutations upstream and downstream of the cleavage bond are necessary to impair the self-processing of the 2A^{pro}, combinations of single amino acid changes were therefore used to investigate this influence. In Figure 20A, the P3-P1 (T T A) and the P2' (P) amino acids were replaced by the corresponding amino acids of HRV14 cleavage site (K S Y, and L respectively, mutant 3). It shows that cleavage was drastically blocked when amino acids at P3-P1 (T T A) and P2' (P) were replaced by the corresponding residues of HRV14 wt (K S Y and L, respectively), indicating that HRV1A 2A^{pro} is no longer able to process this cleavage site.

Figure 20B shows the cleavage when only P2-P1 (T A) and the P2' (P) amino acids were replaced by the corresponding amino acids of HRV14 cleavage site (S Y and L respectively, mutant 4). Again, cleavage was shown to be blocked with this mutated cleavage site. Although, after 20 minutes of *in vitro* translation, some cleavage products of VP1 could be detected, most amount of precursor VP1-2A^{pro} was not cleaved within the 300 minutes of *in vitro* translation.

This indicates that mutations on both sides are necessary to inhibit the self-processing reaction. Mutations at P2-P1 and additionally mutating Pro at P2' to Leu severely effects cleavage.

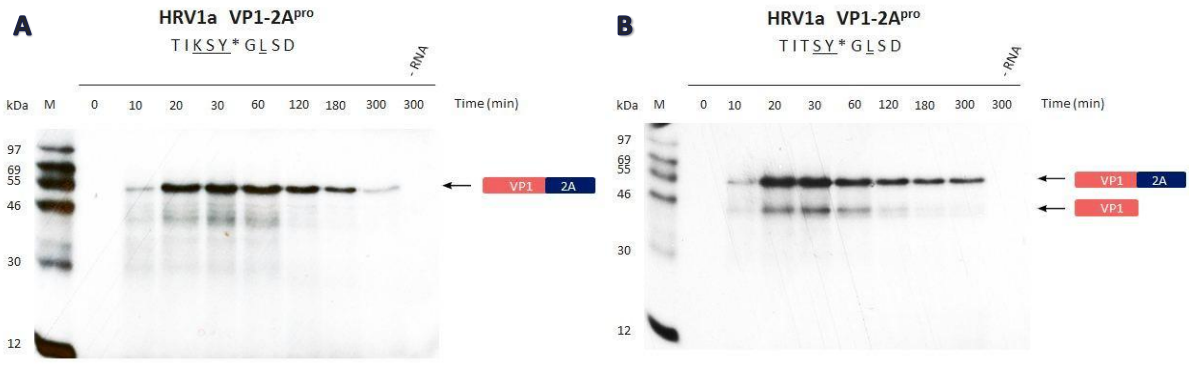

Figure 20 Self-processing of HRV1A 2A^{pro} containing several substitutions at the cleavage site. Parts of the cleavage site of HRV14 2A^{pro} were used. A) P3-P1 amino acids of the cleavage site were exchanged from Thr to Lys, from Thr to Ser and from Ala to Tyr respectively and P2' amino acid was exchanged from Pro to Leu. B) P2-P1 amino acids of the cleavage site were exchanged from Thr to Sere and from Ala to Tyr respectively and P2' amino acid was exchanged from Pro to Leu. Amino acids which differ from the wt HRV1A 2A^{pro} are underlined. The procedure is the same as described in Figure 17.

Gly, as the only totally conserved residue in the cleavage site of picornaviruses seems to be indispensable for the self-processing reaction of the $2A^{pro}$. Several amino acid changes at this P1' (Glu, Lys, Thr, Trp, Phe, Asp) completely blocked the self-cleavage process (Skern et al., 1991; Sommergruber et al., 1992) suggesting the strong requirement of Gly at this site. Nevertheless, it was tested whether the single addition of a methyl group was able to totally disrupt self-processing by replacing the Gly at position P1' with Ala (mutant 5). The presence of Ala led to a total disruption of self-processing activity (Figure 21).

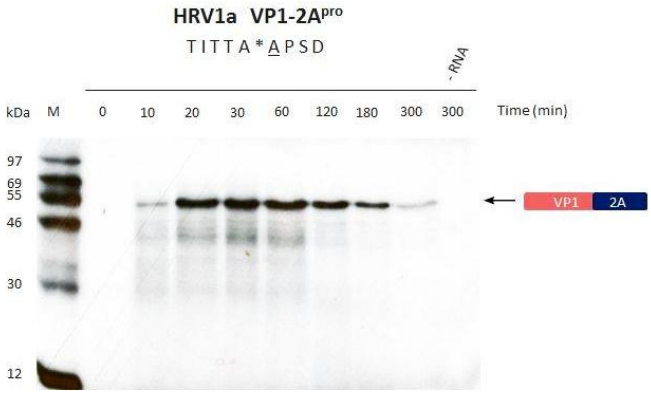

Figure 21 Self-processing of HRV1A $2A^{pro}$ containing only one substitution at the cleavage site. P1' amino acid was changed from Gly to Ala. The procedure is the same as described in Figure 17.

In Table 13, results of the self-processing reactions of HRV1A $2A^{pro}$ cleavage site mutants are summarized.

Serotype	VP1						$2A^{pro}$				Cleavage efficiency
	P5	P4	P3	P2	P1		P1'	P2'	P3'	P4'	
HRV 1a wt	T	I	T	T	A	*	G	P	S	D	++
HRV 14 wt	D	I	K	S	Y	*	G	L	G	P	-
HRV 1A mutant 1	D	I	K	S	Y	*	G	P	S	D	+
HRV 1A mutant 2	T	I	T	T	A	*	G	L	G	P	+
HRV 1A mutant 3	T	I	K	S	Y	*	G	L	S	D	-
HRV 1A mutant 4	T	I	T	S	Y	*	G	L	S	D	-
HRV 1A mutant 5	T	I	T	T	A	*	A	P	S	D	-

Table 13 Overview of the cleavage efficiency of the HRV1A VP1-$2A^{pro}$ constructs. *In vitro* translation experiments are summarized and the results of their cleavage efficiency are shown. (++) indicates wild type cleavage; (+) indicates good cleavage and (-) indicates no cleavage during *in vitro* translation.

4.5 ISOLATION AND CHARACTERIZATION OF HRV1A SECOND SITE REVERTANTS

For transfection into HeLa cells, three different cleavage site mutants were chosen and cloned into the full length clone of HRV1A via cassette cloning:

1) Full HRV14 cleavage site exchanged (D I K S Y * G L G P); this cleavage site was chosen because cleavage was completely blocked by these multiple changes in the cleavage site. Therefore, we were interested to see whether virus is able to cope with many mutations in the cleavage site, and might be able to evolve in order to recover $2A^{pro}$ function.
2) Combinations of mutations upstream and downstream of the cleavage bond by HRV14 amino acids (T I T S Y * G L S D); this hybrid HRV2/HRV14 cleavage site was chosen because it was the lowest combination of changes on both sides of the cleavage site that were shown to inhibit HRV1A $2A^{pro}$ self-processing (Table 13). As we were interested in isolating escape mutants, we thought that the fewer mutations necessary to change for the virus to regain functionality of the $2A^{pro}$, the more multiple second site revertants would be obtained.
3) The single addition of methyl group at the P1' position (T I T T A * A P S D); this single mutation was chosen as Gly, as the only completely conserved residue in *Enteroviruses*, had previously been shown *in vitro* to be irreplaceable. We therefore wanted to investigate whether virus is able to introduce a second site mutation in order to keep the Ala at this position or whether it would change Ala back to the wt Gly.

During these studies we wanted to isolate second site revertants that should help us to identify structural changes in the mutant and non-functional $2A^{pro}$ that have recovered their biological activity. There are two possible pathways the virus can proceed in order to regain functionality. Both pathways rely on the high mutation rate of RNA viruses. One is when the specific defect in the primary mutant is changed back to the original amino acid; the other is when a mutation elsewhere in the protein is introduced (called a second site revertant). Second site revertants might reveal structurally important residues that could be positioned in the cleavage site or active site of the $2A^{pro}$.

4.7.1 GROWTH PHENOTYPE OF HRV1A CLEAVAGE SITE MUTANTS

HeLa cells were transfected with HRV1A wt RNA as well as those from the three cleavage site mutants. After incubation at 34°C for 2-3 days, plaques were visible under the agar on HeLa monolayers in some of the wells (see Figure 22). The transfection well with HRV1A wt was already stained after two days; therefore wt plaque sizes are not comparable with those of HRV1A cleavage site mutants, which were stained after three days.

When the HRV1a VP1-$2A^{pro}$ junction was replaced by corresponding amino acids from HRV14 (D I K S Y * G L G P), no plaques were obtained. Thus, these mutations do not only severely impair

self-processing *in vitro*; probably, there would also be too many changes necessary to restore cleavage activity.

However, plaques were detected after the transfection with HRV1A genome containing combinations of the HRV14 cleavage site (T I T S Y * G L S D) as well as after the transfection with HRV1A genome containing only the single addition of a methyl group in the P1' position (T I T T A * A P S D).

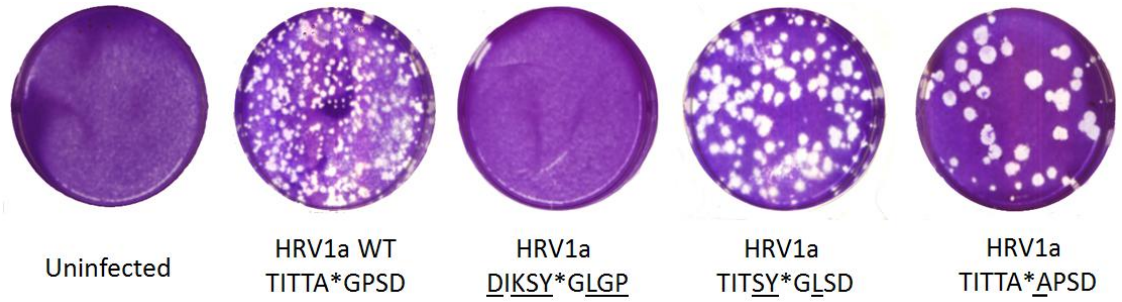

Figure 22 Effect of mutations on HRV1A growth and spread. Plaque phenotypes on HeLa cells of HRV1A wt and mutant viruses with exchanged cleavage sites of the $2A^{pro}$ are shown. HeLa cells were seeded one day prior to transfection. 1200 ng RNA for wt and 8000 ng RNA for mutants was transfected at 34°C for 25 minutes and incubated at 34°C for 2-3 days under agar overlay: an uninfected well, cells transfected with HRV1A wt (only two days of incubation), HRV1A with a cleavage site of the $2A^{pro}$ consisting of DIKSY*GLGP, HRV1A with a cleavage site of the $2A^{pro}$ consisting of TITSY*GLSD and HRV1A with a cleavage site of the $2A^{pro}$ consisting of TITTA*APSD are shown. Residues different to wt residues are underlined.

4.7.2 ISOLATION OF VIRAL PLAQUES

Plaques were then isolated from the HRV1A viruses with the cleavage sites T I T S Y * G L G P and T I T T A * A P S D. This was done by overlaying the cells with a semi-solid medium after transfection, which prevents the virus from spreading indiscriminately. A viral plaque is formed when one cell is infected within the fixed cell monolayer, lyses after infection and spreads the infection only to adjacent cells where the infection to lysis cycle is repeated. Plaques are therefore an area of infected cells surrounded by uninfected cells, and are considered to display only one population of virus. This is important for the later identification of the sequence of the cDNA of isolated virus.

Plaques isolated after the transfection were supposed to still carry the mutated cleavage site but should have also introduced a second site mutation somewhere in the cleavage site or the $2A^{pro}$ to restore cleavage activity and therefore be able to infect surrounding cells. To investigate this, after three rounds of plaque purification, viral RNA was reverse transcribed into cDNA by RT and the cDNA amplified by PCR. The PCR product synthesized completely covers the $2A^{pro}$ and short regions of the neighboring VP1 and 2B protein.

4.7.3 LOCALIZATION OF MUTATIONS IN THE SECOND SITE REVERTANTS

Sequences of plaques of the HRV1A cleavage site mutant carrying combinations of the HRV14 cleavage site (T I T S Y * G L S D) revealed three different outcomes (Table 14).

Amount of same sequences identified	Cleavage site
Original cleavage site mutant	T I T S Y * G L S D
6	T I T S C * G L S D
1	T I T S Y * G L S D
3	T I T S Y * G P S D

Table 14 Sequence of second site revertants isolated by plaque purification; after three rounds plaques isolated were reverse transcribed and amplified by RT-PCR and sent for sequencing. Amino acids changed from the original sequence are shown in red.

Six out of ten sequences identified contained a Cys in the P1 position. As Tyr is a rather bulky amino acid compared to the original Ala residue in the HRV1A P1 position, which may hinder self-processing due to steric hindrance, it was not greatly surprising that this amino acid was changed to a smaller one. By looking in detail at the simplest single base transition possible in this region, Cys was identified as being the most likely amino acid change in this P1 position (Table 15). Mutation of only one purine base change (A→G) is required to change Tyr into Cys.

Base transition	DNA sequence	Amino acid
Original mutated	T A T	Tyrosine
Single	T G T	Cysteine
	C A T	Histidine
	T A C	Tyrosine
Double	C G T	Arginine
	T G C	Cysteine
	C A C	Histidine
Triple	C G C	Arginine

Table 15 Base transitions possible in the P1 position of HRV1A cleavage site mutant containing combinations of amino acid residues from HRV14 $2A^{pro}$ cleavage site (T I T S Y * G L S D). Tyr in the P1 position was exchanged for Cys, which was identified to be the smallest amino acid possible where only a single base transition was performed. However, double base transitions would also yield Cys as the smallest amino acid possible in this position.

Three further sequences contained a Pro at position P2' instead of Leu, which was the original amino acid in the HRV1A wt cleavage site. As shown previously (see Figure 18, 19A and B), modified residues upstream and downstream of the cleavage bond are necessary to completely stop activity of the $2A^{pro}$. A single base transition in this P2' position yields Pro as the simplest amino acid possible (Table 16). To replace Leu by Ser in this P2' position, two base transitions would be necessary.

Base transition	DNA sequence	Amino acid
Original mutated	C T A	Leucine
Single	C C A	Proline
	T T A	Leucine
	C T G	Leucine
Double	T C A	Serine
	C C G	Proline
	T T G	Leucine
Triple	T C G	Serine

Table 16 Base transition possible in the P2' position of HRV1A cleavage site mutant containing combinations of amino acid residues from the HRV14 **(T I T S Y * G L S D)**. Leu in the P2' position was changed back to the original amino acid Pro, which was identified as being the smallest amino acid possible in which only a single base transition was performed.

One sequence was identified that carried the original exchanged cleavage site (T I T S Y * G L S D), but had no additional second site mutation elsewhere in the $2A^{pro}$ or 2B. When comparing *in vitro* cleavage data (Figure 20B), it can be seen that cleavage of the precursor VP1-$2A^{pro}$ is carried out to a very small extent by the HRV1A $2A^{pro}$. This suggests that, although it is not very likely that self-processing by the $2A^{pro}$ happens with this mutated cleavage site, it is in a few cases sufficient. However, compensatory mutations outside the VP1/2A/2B region cannot of course be ruled out.

Sequences of plaques of the HRV1A cleavage site mutant carrying an Ala in the P1' position instead of Gly revealed that all viruses isolated had changed the Ala mutation back to the original amino acid Gly. Changing Ala back to Gly in the P1' position needs one transition and one transversion reaction (Table 17).

DNA sequence	Amino acid
G C A	Alanine
G G G	Glycine

Table 17 Reactions necessary to change Ala back to the original amino acid Gly: Transition (A ←→ G) and transversion (C ←→ T) reaction.

4.6 INFLUENCE OF VP1 Y289R MUTATION AND 2B I94N MUTATION ON HRV14 $2A^{PRO}$ CLEAVAGE

In another approach, experiments for HRV14, a human rhinovirus of the group B, were performed to obtain second site revertants that could reactivate non-functional $2A^{pro}$. The rationale was that HRV14 transfection efficiency in HeLa cells is higher than with HRV1A possibly leading to an increase in the efficiency of revertant isolation.

Previous results have shown that substitution of residues surrounding the HRV14 VP1-$2A^{pro}$ scissile bond (D I K S Y * G L G P) affect autocatalytic cleavage by the $2A^{pro}$. Thus, HRV14 $2A^{pro}$ cannot accept an Arg (in place of Tyr) in the P1 position of the cleavage site (Sousa et al., 2006). This was

examined by studying autocatalytic cleavage reaction of the eIF4GI cleavage site of HRV2 $2A^{pro}$ (T L S T R * G P P R), which is not recognized by the HRV14 $2A^{pro}$. During investigation of these substitutions, Arg was determined to be responsible for the lack of cleavage of the eIF4GI cleavage site by the HRV14 $2A^{pro}$ (Sousa et al., 2006).

In another approach, recent results from Karla Kirkegaard and David Neubauer (both pers.comm.) suggest that the activity of $2A^{pro}$ may also be influenced by the 2B protein. Several PV1 escape mutants, which showed resistance to the specific $2A^{pro}$ inhibitor zVAM.fmk, were identified as mapping to a mutation in the 2B (Kirkegaard, pers.comm.). Furthermore, HRV14 VP1-$2A^{pro}$-2B containing a single mutation (Ile to Asn at position 94 in 2B) in the C-terminal region of the 2B was unable to perform the *cis*-cleavage event (Neubauer, pers. comm., Figure 23).

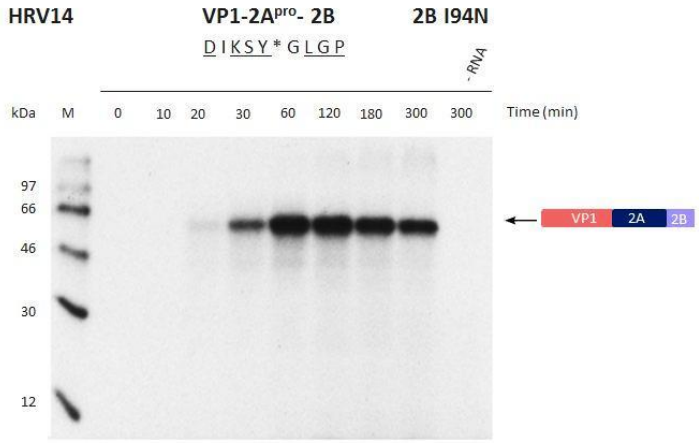

Figure 23 Proteolytic activity of HRV14 VP1-2A-2B with the mutation I94N in the 2B. Translation into protein was monitored at 30°C by using rabbit reticulocyte lysate which were programmed with RNA (10 ng/µl) coding for VP1-$2A^{pro}$. As a negative control water instead of RNA was used. At indicated time points 10 µl aliquots were taken and translation reaction were stopped by adding an ice-cold stop solution containing 25 µl 2x Laemmli sample buffer, 15 µl H_2O and 1 µl unlabeled methionine/cysteine (20 mM). Viral proteins were separated on a 17.5% Dasso & Jackson PAA gel and visualized by fluorography after an exposure time of 16 hours. ^{14}C labeled CFA.626 (Amersham) was used as a size marker (M) and size is shown in kDa. Uncleaved VP1-$2A^{pro}$ and the cleavage products VP1 and $2A^{pro}$ are marked by arrows. This experiment was performed by David Neubauer.

These findings strongly support the idea that at least *in vitro* not only the C-terminal part of the VP1 (cleavage site of the $2A^{pro}$) plays an important role in the proteolytic activity of the HRV14 $2A^{pro}$, but that also the adjacent protein on the polyprotein, 2B, may also influence the properties of the $2A^{pro}$. Figure 24 shows localization of the VP1 Y289R and the 2B I94N mutation on the HRV14 genome.

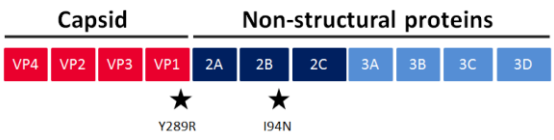

Figure 24 Location of the mutations VP1 Y289R and 2B I94N on the HRV14 genome. Mutations are indicated by an asterisk. VP1 belongs to the structural proteins (P1, red), whereas 2B belongs to the non-structural proteins at the P2 region (dark blue). P3 is shown here in light blue. Picture made with Photoshop.

4.7 ISOLATION AND CHARACTERIZATION OF HRV14 SECOND SITE REVERTANTS

To monitor the effect of the VP1 Y289R and 2B I94N mutation *in vivo*, HeLa cells were transfected with HRV14 full length constructs containing one of these two mutations. Plasmids with the full length constructs and mutations were provided by David Neubauer. As described in chapter 4.5, structurally important residues in the $2A^{pro}$ should be identified which restore the proteolytic activity of the $2A^{pro}$.

4.7.4 GROWTH PHENOTYPE OF HRV14 VP1 Y289R AND 2B I94N MUTANT VIRUS AFTER TRANSFECTION

After the transfection of HeLa cells with HRV14 wt and maintaining both mutants at 34°C for three days, plaques were visible under the agar on HeLa monolayers.

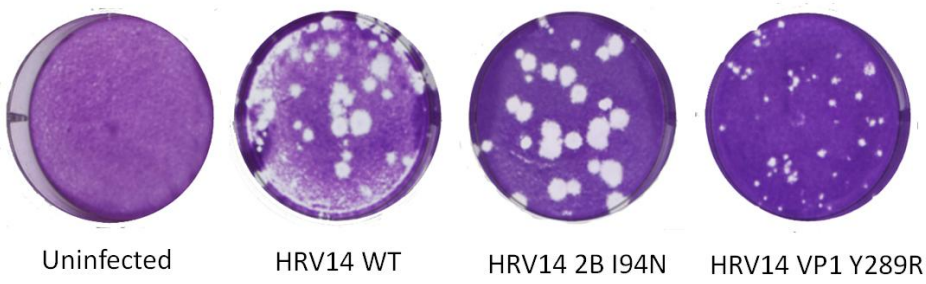

Figure 25 Effect of mutations on HRV14 growth and spread. Plaque phenotypes on HeLa cells of HRV14 wt and mutant viruses are shown. HeLa cells were seeded one day prior to transfection. 1200 ng RNA was transfected at 34°C for 25 minutes and incubated at 34°C for three days under agar overlay: an uninfected well, cells transfected with HRV14 wt, HRV14 2B I94N or HRV14 VP1 Y289R are shown.

As can be seen in Figure 25, the 2B I94N virus displayed plaques which are about equal in size to those formed by the wild-type HRV14. However, the mutant that contained the VP1 Y289R mutation consistently produced smaller plaques than the wild type after the first transfection.

4.7.5 LOCALIZATION OF SECOND SITE REVERTANTS OF THE HRV14 2B I94N MUTANT

Plaques were then isolated from both mutant viruses and the VP1-2A-2B region sequenced as described in 4.5.2. Nearly all plaques isolated contained the previously substituted amino acid change: VP1 Y289R or 2B I94N. This experiment shows that viruses carrying one of these mutations

are able to self-process the polyprotein by the $2A^{pro}$ *in vivo* and therefore replicated in HeLa cells. No second site revertants could be identified for the HRV14 VP1 Y289R. In the case of HRV14 2B I94N, two second site revertants in $2A^{pro}$ (M17T and P4H) could be isolated by plaque purification. On the basis of the HRV2 $2A^{pro}$ structure (Petersen et al., 1999), the mutated residues identified from the isolated plaques were mapped. Sequence alignment show Arg15 (HRV2) as the corresponding residue to Met17 (HRV14) and Asp4 (HRV2) as the corresponding residue to Pro4 (HRV14). The locations of the second site revertants on the HRV2 $2A^{pro}$ are shown in Figure 26.

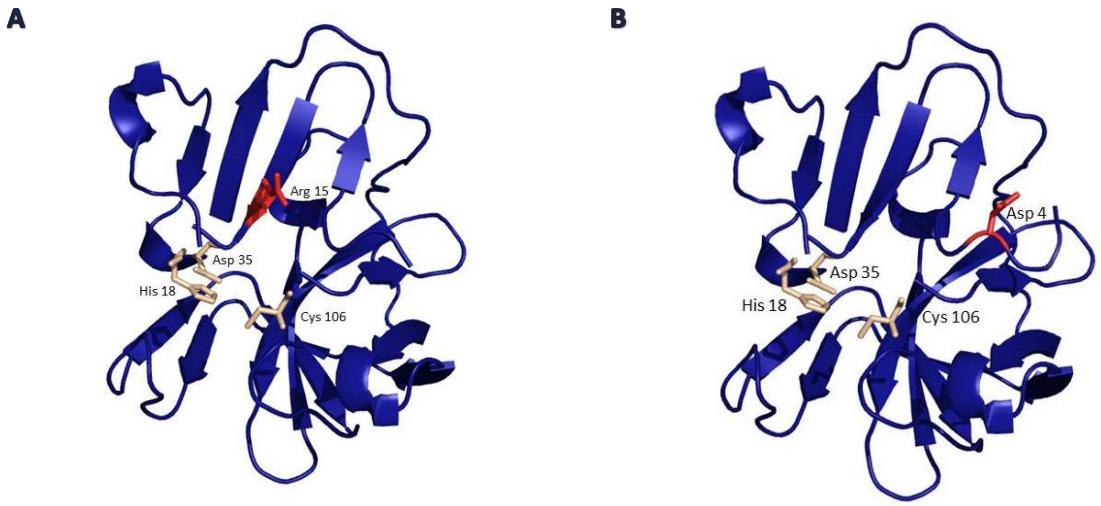

Figure 26 Locations of second site revertants in the $2A^{pro}$ from the HRV14 2B I94N mutant. HeLa cells were infected with HRV14 2B I94N, which was unable to self-process itself *in vitro*. After the infection period of 90 minutes, cells were overlayed with a semi-solid agarose medium, which should inhibit spreading of virus from one location to the other and incubated for three days. Plaques were then isolated and used to infect a new population of cells. After three rounds of plaque purification, RNA was reverse transcribed by Superscript III Reverse Transcriptase and cDNA was sent for sequencing. Two second site revertants in the $2A^{pro}$ could be identified. Here, the crystal structure of HRV2 was used for modeling of the mutations identified. A) $2A^{pro}$ M17T: Here R15 of the HRV2 structure is thought to correspond to the M17 of the HRV14 structure and is highlighted in red. B) $2A^{pro}$ P4H: Here D4 of the HRV2 structure is thought to correspond to the P4 of the HRV14 structure and is highlighted in red. The active site residues: His18, Asp35 and Cys106 are shown in light yellow. Created with PyMol (DeLano, 2002) using the PDB ID code 2HRV.

Met at position 17 in the HRV14 $2A^{pro}$ is not a highly conserved residue; the corresponding position is occupied by an Arg in other rhinoviruses, a Cys in poliovirus and a Val in coxsackievirus. In this second site revertant, it was changed to Thr. This mutation is a single base transition mutation, where A T G is converted into A C G (underlined residue shows the mutated base).

In the second mutant, Pro at position P4' of the cleavage site was changed to His. Poliovirus and coxsackievirus both contain His at position P4' of the cleavage site as well. However, these viruses have also a different amino acid at position 94 in the 2B protein; poliovirus encodes a Val and coxsackievirus an Ala at this site. This mutation is a single base transversion mutation, where C C T is converted into C A T.

4.8 KINETICS FOR VIRUS GROWTH FOR SELECTED HRV14 VP1 Y289R AND 2B I94N MUTANTS AND SECOND SITE REVERTANTS

As shown *in vitro* (see Figure 23), the presence of a single mutation in an adjacent protein on the polyprotein is able to completely abrogate the activity of HRV14 $2A^{pro}$. Thus, the substitution of Tyr to Arg at residues 289 in the VP1 protein and the substitution of Ile for Asn at residue 94 in the 2B protein both influence the properties of the $2A^{pro}$ *in vitro*. However, *in vivo* data suggests that viruses bearing one of these mutations are capable of replication in cells and are also able to infect surrounding cells. Although $2A^{pro}$ of virus carrying the mutation I94N in the 2B protein seems to be able to cleave itself off the polyprotein as several plaques could be isolated carrying the mutation, two mutants were identified carrying an additional mutation in the $2A^{pro}$ protein. In a further experiment, we wanted to monitor and compare growth kinetics of the wt HRV14 virus, the single site mutants and the mutants carrying an additional second site mutation.

The kinetics viral growth of HRV 14 wild type, mutant (2B I94N or VP1 Y289R) and second site revertants (2A M17T 2B I94N and 2A P4H 2B I94N) are shown in Figure 27 - 31. For each time point and each viral mutant, three individual experiments were performed and the mean values and standard deviations were calculated from those results. The titer of extracellular or intracellular virus of each mutant at indicated time points after the infection was compared to that for wt HRV14 to see whether the mutations have any influence on the replication rate and on the maximal yield of viral infection.

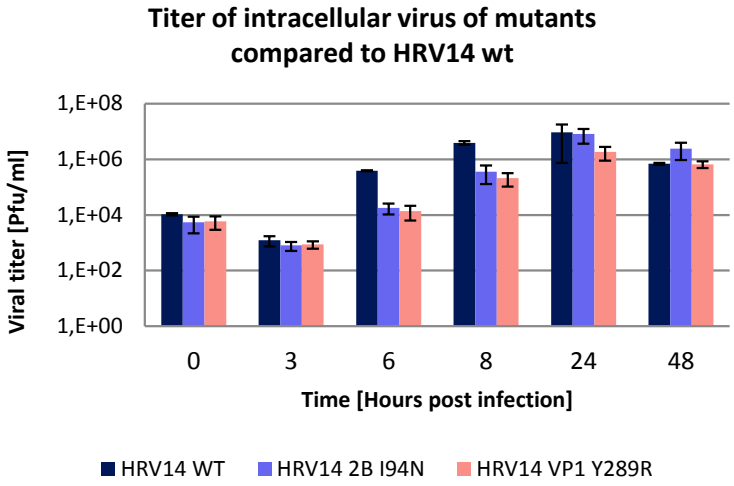

Figure 27 Kinetics of intracellular virus growth for HRV14 single mutants and HRV14 wt. HeLa cells were infected at a multiplicity of infection of 1 with HRV14 encoding wt or the mutant VP1 (Y289R) or the mutant 2B protein (I94N). The cells were incubated at 34°C for 0, 3, 6, 8, 24 and 48 hours post-infection. At indicated time points, virus supernatant containing extracellular virus was transferred to a new tube. To the remaining cells, fresh infection medium was added, and virus was harvested by three repeated freeze/thaw cycles to break up the cells and to release intracellular virus. Virus titers (pfu/ml) were measured by performing a TCID50 and were plotted as a function of time post-infection. Viral titers were measured for each virus and each time points three times and the mean values and the standard deviations were calculated.

Figure 27 shows the growth kinetics of intracellular wt and single mutant viruses. The titer at the first two time points (0 and 3 hours) is very slightly reduced for the mutant viruses compared to HRV14 wt. As no replication has taken place in this early phase of infection, the titer only comes from virus originally bound to the cells in the 90 minutes of infection or attachment period. After about 6 hours viral replications is visible. Here, wt virus shows a titer more than 1 log higher than both of the mutant viruses. After 24 hours, the maximal titers are reached. No apparent difference between wt (black) and the 2B mutant (dots) could be detected here. However, the VP1 mutant (hatched) shows a reduced viral growth compared to that of the wild type. Viral titers of VP1 mutants reached about 1 log less than wt virus. Afterwards the titer started to decrease again. The reason for this is that, when all cells are lysed, no further replication of the virus is possible and at 34°C the newly synthesized virus particles are unstable and/or are degraded. The maximal yield is nearly the same for the 2B mutant as for wild-type, so replication *in vivo* itself does not seem to be affected by that mutations. Viral titers for the VP1 Y289R mutant showed a small decrease in viral replication. However, this decreased rate cannot explain the very small plaque sizes of these viruses (compare with Figure 25).

The titer of extracellular virus is shown from intracellular virus in Figure 28. In the case of the extracellular virus, the difference between HRV14 wt and mutant levels is even less apparent than in the case of intracellular virus, suggesting that after the replication has started, approximately the same amount of virus is produced and replication *in vivo* is not greatly affected by the mutations.

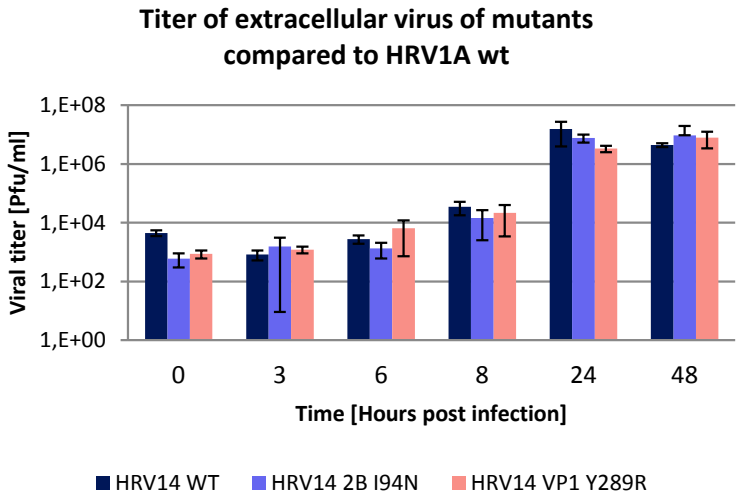

Figure 28 Kinetics of extracellular virus growth for HRV14 single mutants and HRV14 wt. HeLa cells were infected at a multiplicity of infection of 1 with HRV14 encoding wt or the mutant VP1 (Y289R) or the mutant 2B (I94N). The cells were incubated at 34°C for 0, 3, 6, 8, 24 and 48 hours post-infection. At indicated time points virus supernatant containing extracellular virus was separated from cells containing intracellular virus. Virus titers were measured by performing TCID50's. Viral titer (pfu/ml) was plotted as a function of time post-infection. The mean value and the standard deviation were calculated from three independent measurements.

In the next step, the growth kinetics of the second site revertants bearing the 2B I94N mutation and one additional mutation in the $2A^{pro}$ genome (M17T or P4H) in comparison to the

original 2B I94N single mutant and to the HRV14 wt were measured. The results of this comparison are shown in Figure 29 and 30.

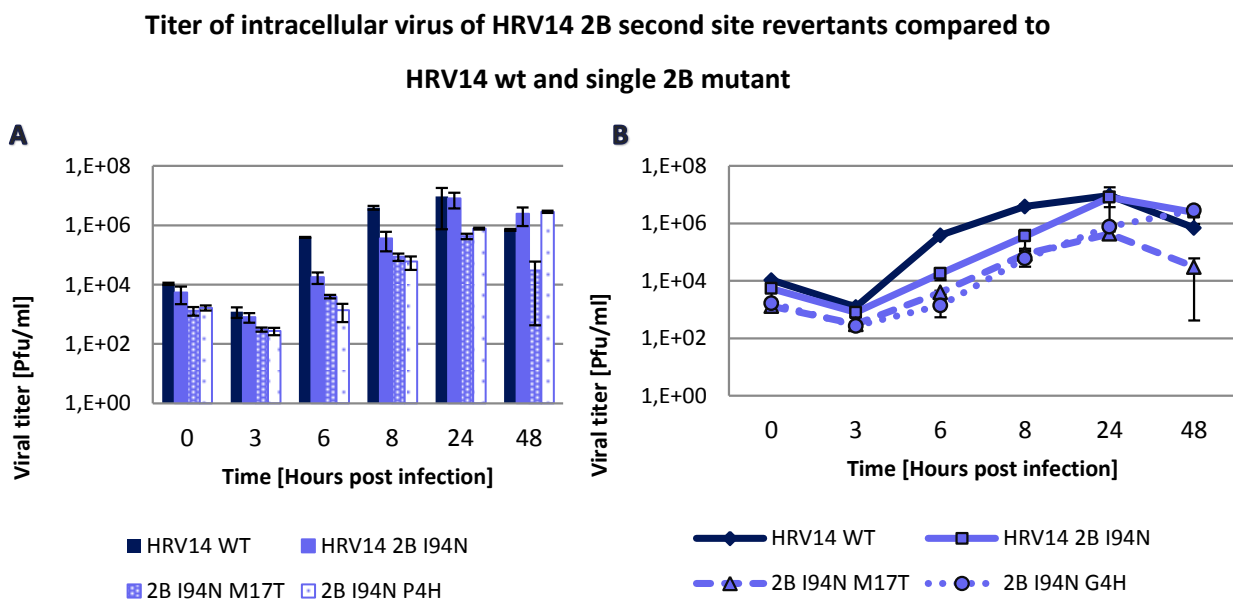

Figure 29 Kinetics of intracellular virus growth for HRV14 mutants carrying a second site mutation in the genome compared to the HRV14 2B I94N single mutation and the HRV14 wt. HeLa cells were infected at a multiplicity of infection of 1 with HRV14 encoding wt, the mutant 2B (I94N) or one of the two HRV14 2B I94N mutations bearing a second mutation in the $2A^{pro}$: Met to Thr at position 17 of the $2A^{pro}$ and Pro to His at position 4 of the $2A^{pro}$. Same procedure as described in Figure 27. A) Bar chart and B) line chart.

It was expected that the second site revertants show a similar kinetic pattern than HRV14 wt or at least replicate faster than the single mutant. However, the results of the growth kinetics differed from the expected outcome. Interestingly, kinetics shows that viral titers in all time points (except for the time points of 48 hours after post-infection) are about 1 to 1.5 logs higher for HRV14 wt than for HRV14 2B I94N second site revertants bearing a mutation in the $2A^{pro}$: Met to Thr at position 17 of the $2A^{pro}$ and Pro to His at position 4 of the $2A^{pro}$. In addition, also by comparing kinetics of the second site revertant to the 2B I94N starting mutant, it can be seen that the single mutant replicates to higher yields than the second site revertants. Thus, no positive effect on the viral replication by these second site revertants could be identified. We therefore concluded that the second site mutations were not introduced as a response to the 2B I94N mutation.

For a better comparison, the kinetics of growth of intracellular virus for HRV14 mutants carrying a second site mutation in the genome compared to wt HRV14 and the original HRV14 2B I94N mutant is shown as linear graph in Figure 29B.

Titer of extracellular virus is shown separately from intracellular virus in Figure 30.

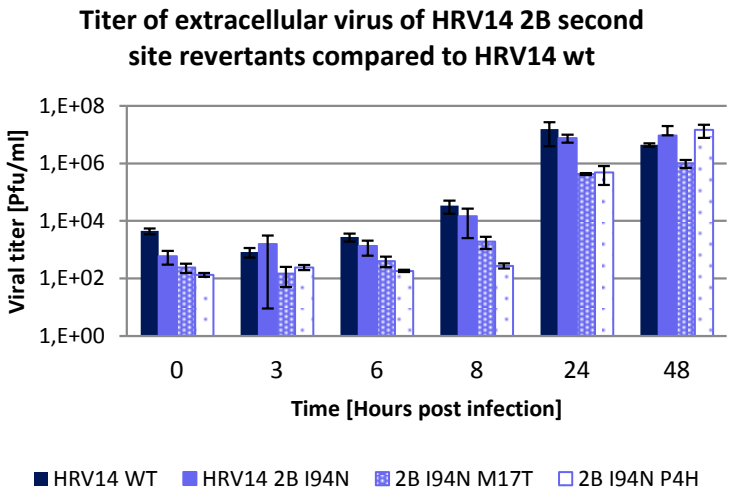

Figure 30 Kinetics of extracellular virus growth for HRV14 mutants carrying a second site mutation in the genome compared to the HRV14 2B I94N single mutation and the HRV14 wt. HeLa cells were infected at a multiplicity of infection of 1 with HRV14 encoding wt, the mutant 2B (I94N) or one of the two HRV14 2B I94N mutations bearing a second mutation in the $2A^{pro}$: Met to Thr at position 17 of the $2A^{pro}$ and Pro to His at position 4 of the $2A^{pro}$. Same procedure as described in Figure 28.

Again some unbound virus is present at the first three time points (0, 3 and 6 hours post-infection), but titers of extracellular virus do not rise, suggesting that no new virus is produced in this time span. Titers of extracellular virus carrying a second site mutation in the $2A^{pro}$ after 24 hours post-infection are still 1 to 1.5 logs lower than HRV14 wt or single mutant. After 48 hours, the mutant 2B I94N 2A P4H has achieved the same titer as the original mutant whereas 2B I94N 2A M17T is still one log lower.

Although we were hoping to isolate second site revertants bearing an additional mutation in the $2A^{pro}$ that has a positive effect on the proteolytic activity, this was not the case. We suppose that these isolated second site revertants have probably not been introduced as a response to the $2A^{pro}$ cleavage inhibition due to the 2B I94N mutation but either due to random introduction of a mutation by the error prone RNA polymerase and/or because multiple continuous passages also might reduce fitness through random mutations (Domingo and Holland, 1997).

5 DISCUSSION

About 30% of all common colds are caused by HRV. Moreover, it is one of the most frequently and recurring infectious diseases in humans with a major economic impact. Although infections are normally relatively mild, billions are spent every year for treatment of the common cold (Monto and Sullivan, 1993). However, little progress in the generation of vaccines or anti-viral compounds has been made until now, due to the large variety of HRV serotypes. This makes it rather difficult to produce a vaccine against HRVs. Antibodies against one serotype are often not able to neutralize another serotype (Whitton et al., 2005). Another option would be the development of antiviral inhibitors against one or more of the non-structural proteins of HRVs. The $2A^{pro}$ of *Enteroviruses* seem to be potential targets as they perform a highly conserved cleavage process during infection. Although the cleavage event is rather conserved, the proteins responsible for it nevertheless vary greatly among the different serotypes. Therefore, no consensus sequence of these cleavage sites could be determined for HRV $2A^{pro}$. However, some positions could be determined to be rather conserved. Gly at position P1' seems to be absolutely required for the cleavage process. Another highly preferred residue is Thr at position P2, forming a hydrogen bond to Ser83 which leads to an important rotation of Tyr85 and therefore to substrate binding. These identified requirements provide the basis to state that the $2A^{pro}$ is a specific proteinase. Understanding substrate specificity of rhinoviral $2A^{pro}$ would be of great importance for the development of effective inhibitors.

The work in this thesis was made to gain deeper insight in the $2A^{pro}$ cleavage event of HRV1A and HRV14. Mutational analysis of the cleavage site of HRV1A should lead to the identification of residues important for the cleavage process. The generation of second site revertants should help to further identify structurally important positions that allow the recovery of functionality and also shed light on the substrate requirements of the $2A^{pro}$ of human rhinoviruses.

5.1 PROTEOLYTIC SELF-PROCESSING PERFORMED BY HRV1A $2A^{PRO}$

The first part of this thesis centered on illuminating the substrate specificity of the HRV1A $2A^{pro}$ and therefore which residues were required to perform the autocatalytic cleavage between the C-terminus of VP1 and its own N-terminus. The HRV1A $2A^{pro}$ cleaves its own polyprotein at T I T T A * G P S D, whereas HRV14 $2A^{pro}$ cleaves at D I K S Y * G L G P. Therefore cleavage sites of these two rhinoviruses differ strongly at position P5, P3, P1, P2'-P4'. The exchange of the wild type residues at the VP1-$2A^{pro}$ cleavage junction of HRV1A with the corresponding residues of the HRV14 cleavage site led to a complete abrogation of proteolytic activity (Figure 18). The HRV1A $2A^{pro}$ is therefore not able to accept the VP1-$2A^{pro}$ cleavage site of HRV14. We then tried to determine which part was

responsible for this discrimination. However, neither the introduction of the HRV14 VP1 part (P5-P1), nor mutating the 2A^{pro} part (P2'-P4') alone stopped the self-processing reaction; it was only slightly delayed (Figure 19A and B). We therefore concluded that combination of mutations on both sides of the cleavage junction are necessary to stop the HRV1A 2A^{pro} in performing this *cis*-cleavage event. As a consequence we tried to mutate combinations on both sides of the cleavage junctions in HRV1A 2A^{pro}. To choose the appropriate residues for these changes, we first had a closer look at the residues present in the HRV14 VP1-2A^{pro} cleavage junction in comparison with those of HRV1A.

Several substrate specificity studies have been performed with the HRV2 2A^{pro} (Skern et al., 1991; Sommergruber et al., 1992), which is assumed to be similar to the HRV1A 2A^{pro}, as it shows a sequence identity of 88% and a positive score of 96% (indicates how many amino acids are at least similar). This is shown in Figure 31A. The HRV14 2A^{pro}, however, shares only a sequence identity of 43% to the HRV1A 2A^{pro} sequence (Figure 31 B).

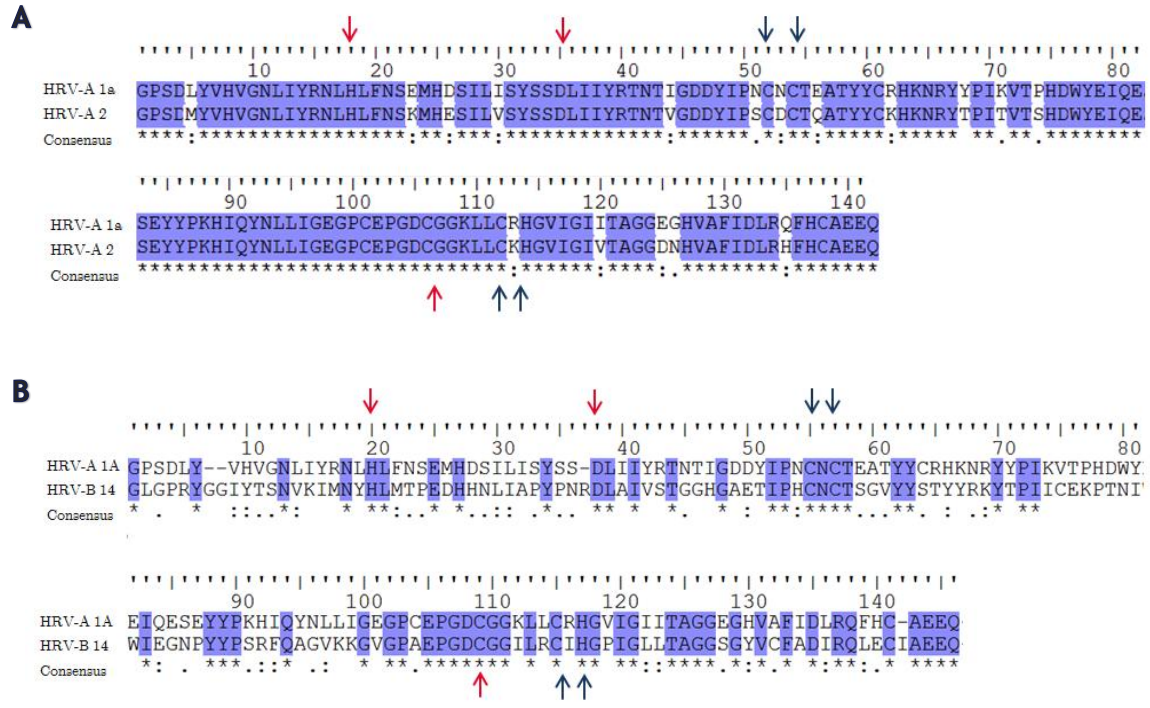

Figure 31 Comparison of the 2A^{pro} of HRV1A with HRV2 and HRV14. A) HRV1A and HRV2, both from the human rhinoviruses group A share an amino acid sequence identity of 88%. B) HRV1A compared to HRV14, which belongs to the group B of human rhinoviruses share only a sequence identity of 43%. The active site residues of HRV2 2A^{pro} are marked with a red arrow: His, Asp, Cys. The residues coordinating the zinc ion are marked with a dark blue arrow. The sequences were taken from the database www.ncbi.nlm.nih.gov. Sequence IDs: AY458604 (HRV-A 1a), X02316.1 (HRV-A 2), X01087 (HRV-B 14). The sequence alignment was made online using ClustalW (http://www.ebi.ac.uk/Tools/ msa/clustalw2/) and edited with the programme BioEdit.

The cleavage site of HRV1A 2A^{pro} differs from HRV2 2A^{pro} by only one amino acid, a Thr at position P5 instead of an Ile (Figure 12 in chapter 1.6.3). The contribution of various amino acids to the substrate specificity of the HRV2 2A^{pro} has been extensively studied. These revealed that HRV2

$2A^{pro}$ has an absolute requirement for Gly at position P1' and a strong requirement for Thr at position P2.

Amino acids at position P2 of a synthetic peptide, such as Ala, Val, Lys, Ile, Phe, Gly, Tyr, Asp, Glu were shown to be not processed at all and mutating this site to Ser, Pro, Asn, Gln, Lys, Arg or His resulted in a highly reduced cleavage efficiency (Sommergruber et al., 1992). Therefore, we concluded that the Ser at position P2, which is present in the HRV14 $2A^{pro}$ wt cleavage site and replaces Thr in the HRV1A constructs, is maybe one reason for the lack of cleavage. Petersen et al. (1999) provided an explanation for this, as Thr in HRV2 was found to form a hydrogen bond with Ser83 and thereby facilitate in a rotation of Tyr85 away from its original position, where it was stacked upon His18. This leads to the formation of an S2 site. This hydrogen bond seems to compensate for this rotation after the substrate has bound (Petersen et al., 1999).

It was further shown that the HRV2 $2A^{pro}$ cleaved substrates with a Tyr at position P1 even better than with the wt Ala. Met at this position resulted in an even higher relative cleavage efficiency in respect to the peptide with the wt cleavage sequence. Besides this, several other residues were shown to be accepted at this position, such as Phe, Thr, Lys, Arg, even though not as wt Ala (Sommergruber et al., 1992). Other residues, such as Pro, Asp, Glu, Val, Asn and Gln were not accepted at this position. Tyr at position P1 seems therefore not to be responsible for the cleavage inhibition.

Substrates with a Lys at position P3 were shown to be cleaved when a Thr at P2 was also present (Skern et al., 1991). However, substrates with a Lys at P3 were not cleaved when a Ser or Asn instead of a Thr were present at P2 (Sommergruber et al., 1992).

The role of the conserved residues in the P' region has also been examined by mutagenesis. Although Gly at P1' position is conserved in all *Enteroviruses*, it has been shown that poliovirus $2A^{pro}$ is able to accept Ala and Ser in the P1' position of the cleavage site (Hellen et al., 1992). However, many studies have shown that HRV2 $2A^{pro}$ is not able to accept any substrate/peptide with an amino acid P1' substitution. Amino acids tested included Phe, Thr, Asp, Lys, Glu, Trp (Skern et al., 1991; Sommergruber et al., 1992).

In addition, it has been shown that peptides with Asp, Phe Thr, Lys at position P2' are cleaved with a two to five fold less efficiency than with a Pro at this site (Sommergruber et al., 1992). Thus, a negative influence of the exchanged Leu at this P2' site could be very likely.

On the basis of these considerations, we decided that residues at position P3, P2, P1 on the one side and P1' and P2' on the other side were the most important residues. To this end, we aimed to determine the exact residues exchanged which were required to be mutated to stop proteolytic activity of the HRV1A $2A^{pro}$. We therefore exchanged residues on both sites of the VP1-$2A^{pro}$ cleavage junction, either mutating P3-P1 (ThrThrAla to LysSerTyr) in addition to mutating Pro at P2' with Leu

or only P2-P1 (ThrAla to SerTyr) in combination with P2' (Pro to Leu). These mutations were determined to severely impair self-processing (Figure 20A and B). As a very slight cleavage could be monitored with the mutant 4 (P2-P1 and P1'), we concluded that Lys at position P3 might be responsible for a slight decrease in self-processing efficiency. However, Ser at P2 and Leu at P2' seem to be important to abrogate cleavage. This leads us to the assumption that Thr at P2 and Pro at P2', are important substrate requirements for the HRV1A 2A^{pro}, in addition to the completely conserved Gly at P1'.

We further wanted to investigate whether it was possible to exchange Gly at position P1' with a slightly larger amino acid, Ala. Ala has a methyl group as side chain in place of a single hydrogen atom. In our *in vitro* studies, we found that HRV1A 2A^{pro} is not able to process the polyprotein when the cleavage sequence contains an Ala at the P1' position. Petersen et al. (1999) explained that this absolute requirement of Gly at P1' could be due to Leu19 that blocks the access of any residues other than Gly to the S1' site (Petersen et al., 1999). However, by modeling a substrate into the binding cleft of HRV2 2A^{pro} and changing the side chain of Gly to the side chain of Ala we can see that Leu19 is too far away to block the access of Ala. Figure 32A shows a model of an oligopeptide substrate occupying subside S4-S1'. This peptide, consisting of five residues, corresponds to the sequence of the polyprotein at the junction of VP1 and 2A^{pro} of HRV2 (ITTA*G). Figure 32B shows a substrate where the Gly at the P1' position was replaced by Ala.

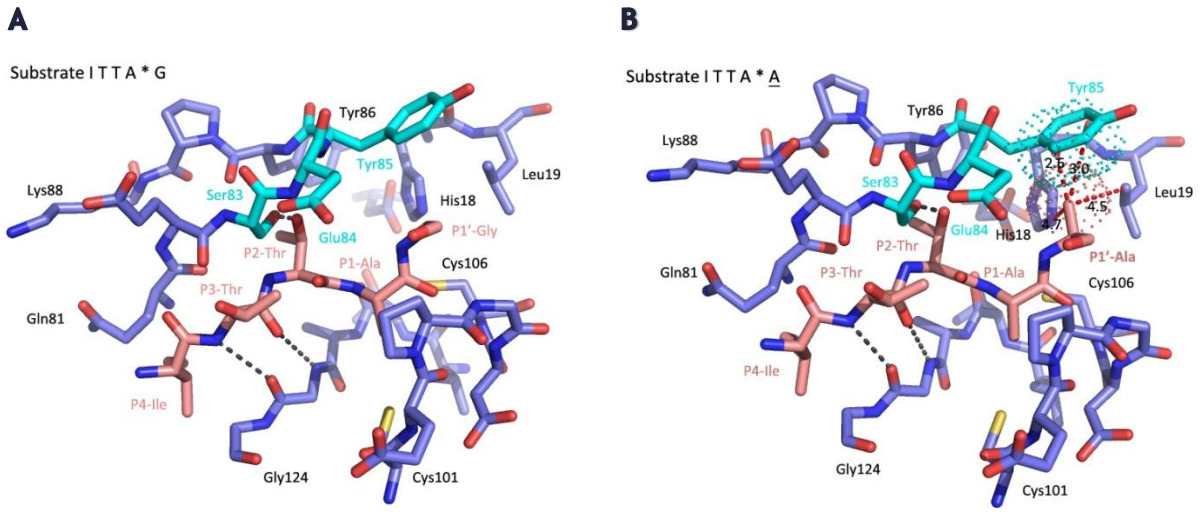

Figure 32 Substrate modeled into the HRV2 2A^{pro} binding site. The atomic color coding for the enzyme is light blue for the main chain, dark blue for the nitrogen and red for the oxygen. For the substrate, color coding is rose for the main chain, dark blue for the nitrogen and red for the oxygen. Tyr85 of the enzyme which has been rotated out of the binding site after the formation of a hydrogen bond between Thr at P2 (substrate) and Ser83 (enzyme) is shown in turquoise. Hydrogen bonds are designated by dashed, grey lines between donor and acceptor atoms. A) Drawing showing a pentapeptide with corresponding wt residues (I T T A * G) bound to the subside S4-S1' of the HRV2 2A^{pro} binding cleft. B) Drawing showing a mutated oligopeptide where the Gly at position P1' is exchanged by Ala (I T T A * A). The dots in this figure show the area including hydrogen atoms of the residues Tyr85 and the P1' Ala to see that whether they sterically hinder each other. This explains why Ala at the P1' is not accepted by the HRV1A 2A^{pro}. The distance between some adjacent molecules was calculated and shown by dashed, red lines. Model was generated with the program PyMol (DeLano, 2002). Precise explanation of how the model was generated is described in the text.

This model was generated as described by Petersen et al. 1999. Briefly, this was produced on the basis of the *Streptomyces griseus* proteinase B (SGPB) in complex with the third domain of the turkey ovomucoid inhibitor OMTKY3 (Read et al., 1983). This proteinase shows a chymotrypsin-like proteinase fold, and although sequence identity between SGPB and HRV2 $2A^{pro}$ is less than 20%, it was chosen as a representative structure of the canonical substrate binding. Indeed, the structure of the SGPB differs from the HRV2 $2A^{pro}$ only in the N-terminal part. The binding of the SGBP to the OMTKY3 involves an antiparallel β-strand interaction between P2-P4 from the inhibitor with the eII strand from the proteinase, typical for chymotrypsin-related proteinases (Bode and Huber, 1992). The interaction of the HRV2 $2A^{pro}$ is thought to be similar.

To design the substrate binding site, residues of the HRV2 $2A^{pro}$ were structurally aligned with those of SGBP via the pair fitting mode of PyMol (DeLano, 2002). To this end, residues 101-106 (oxyanion hole) and residues 120-124 (eII strand) of the HRV2 $2A^{pro}$ (PDB code: 2HRV) were aligned with residues 192-198 and residues 212-216, respectively, of the SGPB-OMTKY3 complex (PDB code: 3SGB). Residues 14-19 from the OMTKY3 inhibitor correspond to the P4-P1' site; side chains of this residues were replaced with the side chains of the HRV1A $2A^{pro}$ substrate and side chains of mutated substrates.

According to the measurement in PyMol, the methyl group of Ala at the P1' position of the substrate is not blocked by Leu19 as it is 4.5 Å distant. However, in the modeling in Figure 32B, it can be seen that Tyr85, which was rotated out of the substrate binding site to form the S2 pocket is rather close to the side chain of the P1-Ala. The distance between the Cβ atom of the methyl group of Ala to the C5 and C6 atom of Tyr85 was calculated to be 2.6Å and 3.0Å. With the dotted structure, in which also hydrogen atoms are considered, it can be seen that these structures overlap.

We therefore predict that not Leu19, but rather Tyr85 is responsible for the discrimination of any larger amino acid than Gly. As Tyr85 is rotated out because the Thr at position P2 forms a hydrogen bond with Ser83, the question arises whether Ala would be accepted when Thr at position P2 was mutated to another amino acid. However, as described above, nearly all amino acids exchanged at this site were shown to inhibit the self-processing of the HRV2 $2A^{pro}$. In fact, residues larger than Ala would also be blocked by Leu19. PV $2A^{pro}$ is in contrast able to accept an Ala and several other smaller residues, such as Ser at P1' (Hellen et al., 1992). In addition, several amino acids are also accepted by the PV $2A^{pro}$ at position P2, such as Ala, Ser, Asn, Gln and Pro. However, Tyr85 is also conserved in PV. This suggests that substrate recognition does differ between HRV and PV.

On the contrary, the $2A^{pro}$ of HRV2 was able to perform *trans*-cleavage of Nup62 when an Ala was present at P1' (Park et al., 2010). However, none of these cleavage sites contained in addition Thr at P2. This could indicate that Ala can be accepted at P1' when no hydrogen bond between the substrate (Thr at P2) and the enzyme (Ser83) is formed and therefore no rotation of Tyr85 is

accomplished. However, the question remains whether the hydrogen bond formation and subsequent rotation of Tyr85 is vital for the substrate binding. To determine if Tyr85 is required to rotate out of the substrate binding site, a crystal structure will be needed that shows whether a hydrogen bond is formed with a different amino acids (such as Thr or Asn), which are also able to participate in a hydrogen bond. Indeed, the hydrogen bond with Tyr85 has not even been shown.

In short, we identified several residues in the cleavage site of the HRV1a VP1-2A^{pro} junction as being detrimental for carrying out the self-processing reaction. These residues are summarized in Table 18. Cleavage sites, which were chosen for the further experimental procedures, are marked with an arrow.

Serotype	VP1 P5	P4	P3	P2	P1		2A^{pro} P1'	P2'	P3'	P4'	Cleavage efficiency	
HRV 1a wt	T	I	T	T	A	*	G	P	S	D	++	
HRV 14 wt	D	I	K	S	Y	*	G	L	G	P	-	←
HRV 1A mutant 1	D	I	K	S	Y	*	G	P	S	D	+	
HRV 1A mutant 2	T	I	T	T	A	*	G	L	G	P	+	
HRV 1A mutant 3	T	I	K	S	Y	*	G	L	S	D	-	
HRV 1A mutant 4	T	I	T	S	Y	*	G	L	S	D	-	←
HRV 1A mutant 5	T	I	T	T	A	*	A	P	S	D	-	←

Table 18 Cleavage sites which were shown *in vitro* to inhibit self-processing of HRV1A 2A^{pro}. Arrows indicate cleavage sites which were further introduced into the full length HRV1A clone for transfection of HeLa cells.

5.2 STRUCTURAL CHANGES OF HRV1A ESCAPE MUTANTS

Three different cleavage sites were introduced into the full length HRV1A clone: D I K S Y * G L G P, T I T S Y*G L S D and T I T T A * A P S D. All of these sites were previously shown to inhibit the self-processing reaction of the HRV1A 2A^{pro}. By transfecting HeLa cells with viral RNA containing the desired mutations, virus with second site revertants should be generated from viral offspring. Virus could be isolated from viral plaques from all RNAs except for the virus carrying the full wt cleavage site of the HRV14 2A^{pro}. This full HRV14 2A^{pro} cleavage site mutation does not only severely impair self-processing *in vitro*; there are probably also too many changes necessary to restore cleavage activity.

In the case in which combinations of the HRV14 2A^{pro} cleavage site were exchanged (T I T S Y*G L S D), several viral plaques were isolated. We could deduce three reactions of how the virus reacted to the mutated cleavage sites that *in vitro* had inhibited the self-processing of the 2A^{pro} (see Table 14).

Six out of ten isolated viral plaques changed the Tyr at position P1 to Cys. This was rather surprising, as Tyr at position P1 (alone) was shown to be cleaved even better by HRV2 2A^{pro}

(Sommergruber et al., 1992). Figure 33A shows a representation of a model of the previously mutated substrate occupying subside S4-S1' (I T S T * G). Although Leu at position P2', which replaced the wt Pro, plays also a role in the inhibition of substrate binding, it is not shown in the model. Figure 33B shows the substrate when the Tyr at P1 was mutated to Cys by escape mutants. This second site mutation was isolated several times in independent experiments. Hence, the presence of Cys at P1 (instead of Tyr) is possibly compensating the harmful effect of Ser at P2 and Leu at P2'. By looking at detail at the single nucleotide bases, we identified Cys as being the most likely amino acid possible by a single base transition mutation. Mutation of only one purine base change (TAT→TGT) is required to change Tyr into Cys (Table 15).

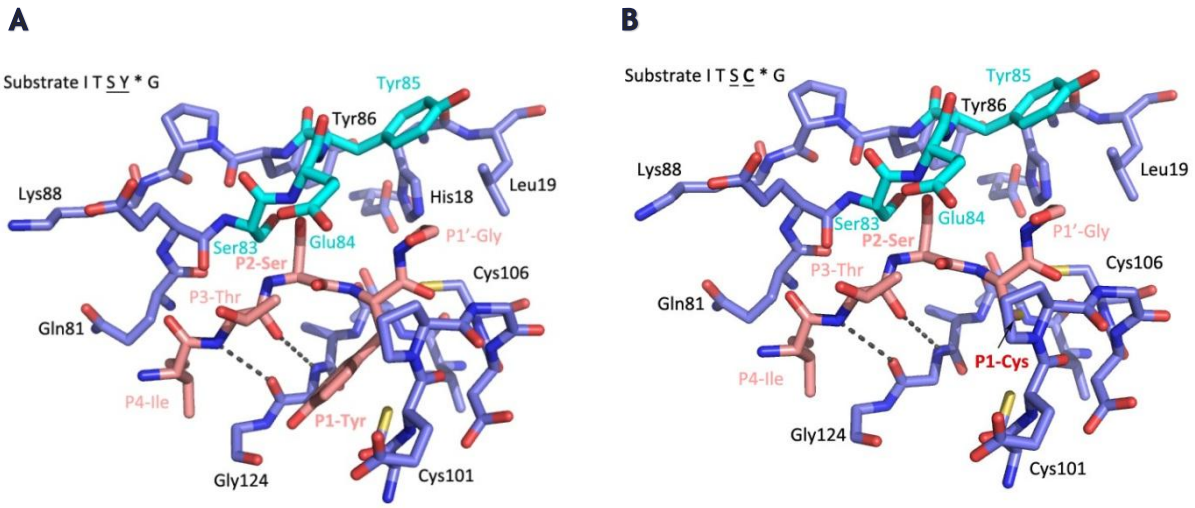

Figure 33 Drawing of a mutated substrate modeled into the HRV2 2A^{pro} binding site. The atomic color coding is the same as in Figure 32. Although there is no crystal structure with a different amino acid than Thr at P2, we indicate here that a hydrogen bond is also formed between Ser at P2 and Ser83 that subsequently leads to the rotation of Tyr85. A) Drawing showing a mutated oligopeptide with corresponding residues I T S Y * G. B) Drawing showing the second site revertant, where the Tyr at P1 was changed to Cys (shown in dark red).The sulfhydryl group of this Cys is marked by an arrow as it is hard to see. Precise explanation of how the model was generated is described in the text.

The final residue of the VP1 thus becomes Cys and not Tyr in this mutant. VP1 is one of the outer capsid proteins and is assembled in the cytosol of the infected cell. Figure 34A and B shows the location of the mutated Cys in the 5S protomer structure of HRV1A. In Figure 34C and D, the originally mutated Tyr at position 289 in the VP1 protein (instead of the wt Ala) is compared to the mutated Cys at position 289 as isolated by several escape mutants.

As it is the last residue (C-terminus of VP1) it is at a particularly flexible region. Although we do not think it is very likely to happen, as the cytosol, a reducing environment, destabilizes disulfide bonds, we could nevertheless imagine that the Cys forms a disulfide bridge with another Cys of a VP1 molecule of a neighboring particle. However, this would probably lead to an inhibition of viral release.

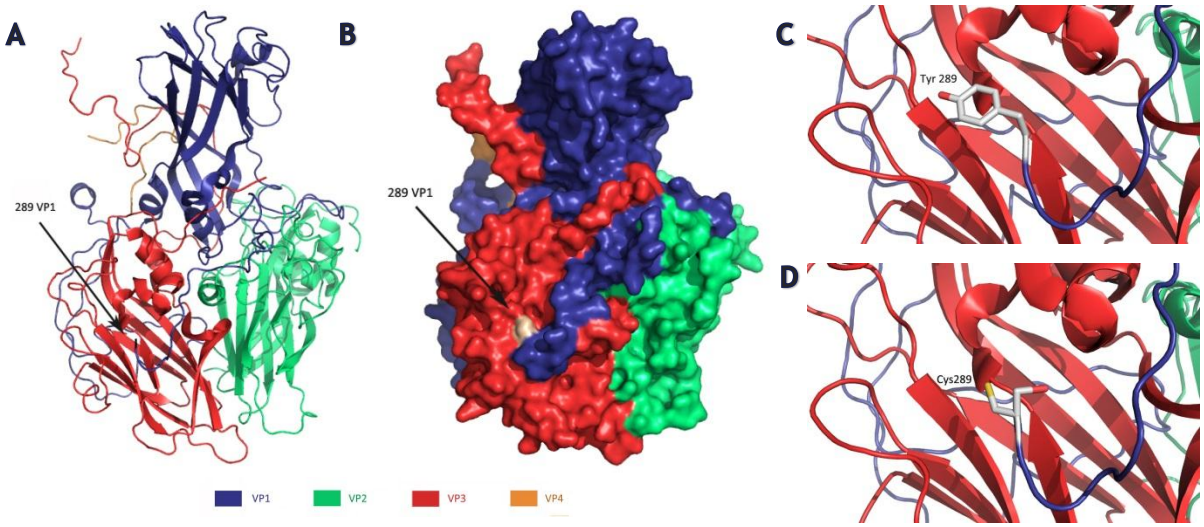

Figure 34 Location of the mutated Cys 289 of VP1 in the 5S protomer structure of HRV1A. A) Ribbon diagram and B) surface representations of the 5S protomer; position 289 on VP1 (last residue before the cleavage junction) is marked by an arrow. The color for this residue is black in A and grey in B, C and D. C) Drawing of the mutated Tyr (instead of the wt Ala). D) Drawing of the mutated Cys as isolated by several escape mutants. Color coding: VP1 (blue), VP2 (green), VP3 (red) and VP4 (light orange). Created with PyMol (DeLano, 2002) using the PDB ID code 1R1A .

The second way the virus reacted to the exchanged cleavage site (T I T S Y * G L S D) was by mutating the Leu at P2' back to the wt Pro, maintaining the Ser at P2 and Tyr at P1. This is also a single base transition mutation from CTA to CCA. This is not a particularly unexpected result, as it was shown *in vitro* that combinations of mutations on both sides of the cleavage junction are necessary to inhibit cleavage (Figure 19A and B). Therefore, mutating Leu back to the original Pro will recover self-processing as the P' side now has the wt sequence.

For the third way, we isolated one virus which carried the original mutated cleavage site. Thus, we concluded, that although cleavage is not very likely to happen, the $2A^{pro}$ is not 100% inhibited by these changes. This was also shown *in vitro* (Figure 20B). In addition, compensatory mutations outside the VP1/2A/2B region cannot be excluded.

As a summary, identified viruses had either a second site mutation in the cleavage site (Tyr at P1 to Cys), changed an amino acid back to the original sequence (Leu at P2' to Pro) or carried the original mutant cleavage site (T I T S Y * G L G P).

In future experiments, we would like to look at the *in vitro* cleavage to see whether these escape mutants are able to cleave VP1-$2A^{pro}$ during *in vitro* translation. Furthermore, we would like to investigate whether Ala would be accepted at the P1' if the Thr at P2 was changed to a different residue, which is not able to facilitate in a hydrogen bond with Ser83. In addition, we would like to monitor growth kinetics of the isolated escape mutants, to investigate whether there is a difference in replication efficiency to wt HRV1A $2A^{pro}$.

We can only speculate why it is easier for the virus to mutate residues in the cleavage site than somewhere in the active site or substrate binding site. Possibly, to change the mechanism in the

active site, several mutations and probably also base transversions must occur. Single base transition happen more frequently than multiple base transitions or transversions. In the case in which the full cleavage site was replaced by the corresponding amino acids of HRV14, the virus was not able to introduce any successful mutation(s), probably due to the multiple mutations that would be necessary to perform the self-processing reaction.

Several viral plaques were also isolated after infecting cells with the TI T T A * A P S D cleavage site mutant. All of the sequences showed that the Ala at P1' was mutated back to the original Gly. As described in Figure 32A and B, we suppose that Ala is blocked by the rotated Tyr85 (see chapter 5.1). We therefore conclude that Gly at the P1' position is an absolute requirement for performing the self-processing reaction of rhinoviral $2A^{pro}$ in *cis*.

5.3 INVESTIGATING THE HRV14 $2A^{PRO}$

As described in results, the mutations in the protein VP1 (Y289R) and in the 2B (I94N) were shown to prevent the HRV14 $2A^{pro}$ from cleaving itself off from VP1-$2A^{pro}$ *in vitro* (Sousa et al., 2006; Neubauer et al., 2009).

Again, viral RNA carrying the desired mutations was transfected into HeLa cells and viral offspring was isolated. Sequence analysis revealed that, although self-processing was inhibited *in vitro*, it did not have such a detrimental effect *in vivo*, since several viral plaques were isolated carrying only the introduced mutation. One difference could however be detected in the plaque size of virus carrying the VP1 Y289R mutation. Viral plaque size of these viruses was about three times smaller than compared to that of wt HRV14 (Figure 25). Therefore, we first supposed that although the VP1 Y289R mutations, which is the last residue before the cleavage junction (P1), is able to be cleaved by the HRV14 $2A^{pro}$ *in vivo*, it leads to a reduced efficiency of cleavage and therefore a growth defect of this virus. However, by monitoring growth kinetics only a delay and slight growth defect could be determined (Figure 27 and 28). However, this slight growth defect can not explain the small plaque size. One explanation could be that these viruses have a defect in spreading or lysis, as virus is obviously produced. Furthermore, the defect in spreading could explain why mutant VP1 Y289R virus could replicate better in liquid medium, where virus is easier transmitted to another cell instead in a semi-solid medium.

Although mutating the Arg at position 289 back to Tyr would only need two base transition mutations, no escape mutants were isolated. Figure 35 shows the location of the mutated Arg 289 in the VP1 protein of the HRV14 in the viral 5S protomer (Figure 35A and B) and compares the wt Tyr at position 289 of VP1 (Figure 35C) to the mutated Arg at position 289 (Figure 35D).

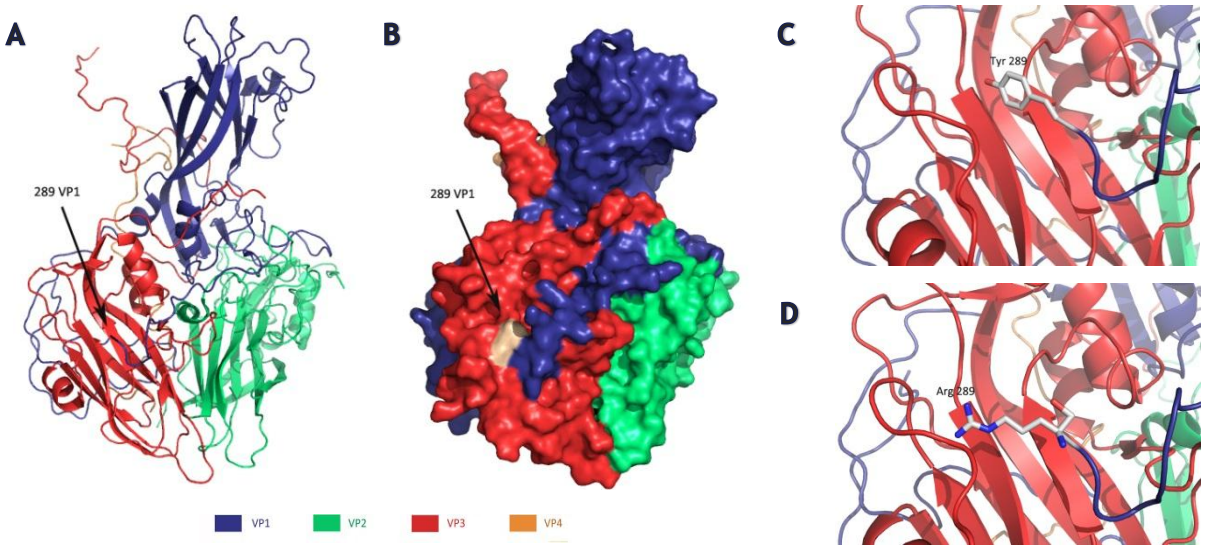

Figure 35 Location of the mutated Arg 289 of VP1 in the 5S protomer structure of HRV14. A) Ribbon diagram and B) surface representation of the 5S protomer; position 289 on the VP1 protein (last residue before the cleavage junction) is marked by an arrow. C) Drawing of the wt Tyr at position 289 in HRV14. D) Drawing of the mutated Arg at position 289 in HRV14 mutants. Color coding is the same as in Figure 34. Created with PyMol (DeLano, 2002) using the PDB ID code 4RHV.

The influence on the growth kinetics of the 2B I94N mutations was even less than for the VP1 mutation. Kinetics of growth showed a slightly decreased rate in the beginning, but maximum yield of virus, which was reached after about 24 hours showed, nearly the same pfu/ml than for wt HRV14. Although recent results suggest that the protein 2B is involved in the cleavage event of $2A^{pro}$ (Kirkegaard, pers.comm.; Neubauer et al., 2009), our results show that the self-processing reaction of the HRV14 $2A^{pro}$ is not inhibited in HeLa cells. It was surprising that two different escape mutants, bearing an additional mutation in the $2A^{pro}$, were isolated. One second site mutant changed the Pro at position P4 to His, the other changed Met at position 17 to Arg (Figure 26). Although our growth kinetics of the 2B mutant did not show any defect, we also monitored the kinetics of the escape mutants. Unexpectedly, these mutants grew slower and to a lower yield of maximum virus than both the wt HRV14 and the single mutant 2B virus (Figure 29 and 30). This led us to conclude that these additional mutations identified in the $2A^{pro}$ have probably nothing to do with the mutations in the 2B and were not introduced to recover proteolytic activity. The quasispecies theory suggests that mutations are constantly introduced during viral evolution in the fitness landscape (Wilke et al., 2001). As RNA viruses replicate with a high mutation rate, they will after some generations develop a diverse mutant repertoire (Lauring and Andino, 2010). Darwin stated that this is done to optimize fitness and thereby generating an organism which fits, survives and reproduces “better” in the existing environment (Orr, 2009). However, Domingo and Holland stated that RNA viruses undergo fitness changes during continuous passages, thereby reducing fitness (Domingo and Holland, 1997). This may have happened to our second site revertants.

The results of this thesis are one step further in the investigation of the exact substrate requirement of enteroviral $2A^{pro}$. It was demonstrated that inhibition of the intramolecular cleavage of the HRV1A $2A^{pro}$ was achieved by exchanging combinations of residues on both side of the cleavage junction. Exchanging only one side resulted solely in a slightly delayed cleavage kinetics. However, *in vivo* experiments, in which escape mutants were isolated, have shown that the replacement of one side is enough to recover proteolytic activity of the HRV1A $2A^{pro}$. We showed that the HRV1A $2A^{pro}$ accepts a cysteine at the position P1 of the cleavage junction *in vivo* as several escape mutants bearing this change could be isolated. Although the VP1 Y289R mutation was shown to inhibit proteolytic cleavage of the HRV14 $2A^{pro}$ *in vitro*, we show that this is different *in vivo*. Even though virus with this VP1 mutation could replicate *in vivo*, we observed a small plaque phenotype, which might be due to the presence of the arginine at the P1 position of the cleavage junction of the HRV14 $2A^{pro}$. These experiments suggest that substrate requirements for HRV1A and HRV14 $2A^{pro}$ are rather different; therefore the development of specific inhibitors against either protease will be required. Thus, further investigations in the substrate specificity of the $2A^{pro}$ of HRV-A, -B and -C viruses will be necessary.

6 APPENDIX

6.1 LIST OF AMINO ACIDS

A	Ala	Alanine
C	Cys	Cysteine
D	Asp	Aspartic acid
E	Glu	Glutamic acid
F	Phe	Phenylalanine
G	Gly	Glycine
H	His	Histidine
I	Ile	Isoleucine
K	Lys	Lysine
L	Leu	Leucine
M	Met	Methionine
N	Asn	Asparagine
P	Pro	Proline
Q	Gln	Glutamine
R	Arg	Arginine
S	Ser	Serine
T	Thr	Threonine
V	Val	Valine
W	Trp	Tryptophan
Y	Tyr	Tyrosine

6.2 LIST OF ABBREVIATIONS

$2A^{pro}$	Proteinase 2A
Å	Angström
°C	Degrees celsius
µl	Microliter
µg	Microgram
aa	Amino acid
Amp	Ampicillin
APS	Ammonium peroxidisulfate
ATP	Adenosine triphosphate
bp	Base pair
cDNA	Complementary DNA
CIP	Calf intestine phosphatase
CITE	Cap-independent translation enhancer
cre	*Cis* responsive element
CV	Coxsackievirus
dH_2O	Deionized water
DMSO	Dimethyl sulfoxide
DNA	Deoxyribonucleic acid
dNTP	Deoxynucleotide triphosphate
DTT	Dithiothreitol
EDTA	Ethylenediaminetetraacetic acid
eIF	Eukaryotic initiation factor
EMCV	Encephalomyocarditis virus
FCS	Fetal calf serum

FMDV	Foot-and-mouth disease virus
g	Gram
h	Hour
HAV	Hepatitis A virus
HeLa	Henrietta Lacks' cells
Hpi	Hours post infection
HRV	Human rhinovirus
ICAM-1	Intercellular adhesion molecule 1
ICTV	International committee on taxonomy of viruses
IRES	Internal ribosomal entry site
kb	Kilobases
kDa	Kilo Dalton
l	Liter
L^{pro}	Leader protease
LB	Luria Bertani
LDL	Low-density-lipoprotein
LDLR	Low-density-lipoprotein receptor
LGS	Lower gel solution
M	Molar
Min	Minutes
ml	Milliliter
mM	Milimolar
mRNA	Messenger RNA
nt	Nucleotide
NTP	Nucleotide triphosphate
NUP	Nuclear pore complex protein
ORF	Open reading frame
PABP	PolyA-binding protein
PAGE	Polyacrylamide gel electrophoresis
PBS	Phosphate buffered saline
PCR	Polymerase chain reaction
PDB	Protein Data Bank
Pfu	Plaque forming unit
PNK	Polynucleotide kinase
PolyA	Poly adenylation
PV	Poliovirus
RNA	Ribonucleic acid
RNase	Ribonuclease
Rpm	Rotations per minute
RRL	Rabbit reticulocyte lysate
RT	Room temperature
SDS	Sodiumdodecylsulfate
SGPB	*Streptomyces griseus* proteinase B
TAE	Tris-acetate-EDTA
TE	Tris-EDTA
TEMED	Tetramethylethylenediamine
UTR	Untranslated region
UV	Ultraviolet
VLDLR	Very low density lipoprotein receptor
VP	Viral protein
VPg	Viral protein genome linked
Wt	Wild type
zVAD.fmk	Benzyloxycarbonyl-Val-Ala-Asp-fluoromethylketone
zVAM.fmk	Benzyloxycarbonyl-Val-Ala-Met-fluoromethylketone

REFERENCES

Aldabe, R., Barco, A., and Carrasco, L. (1996). Membrane permeabilization by poliovirus proteins 2B and 2BC. The Journal of Biological Chemistry *271*, 23134-23137.

Ambros, V., and Baltimore, D. (1980). Purification and properties of a HeLa cell enzyme able to remove the 5'-terminal protein from poliovirus RNA. The Journal of Biological Chemistry *255*, 6739-6744.

Badorff, C., Lee, G.-H., J., L.B., Martone, M.E., Campbell, K.P., Rhoads, R.E., and Knowlton, K.U. (1999). Enteroviral protease 2A cleaves dystrophin: evidence of cytoskeletal disruption in an acquired cardiomyopathy. Nature Medicine *5*, 320-326.

Basavappa, R., Syed, R., Flore, O., Icenogle, J.P., Fileman, D.J., and Hogle, J.M. (1994). Role and mechanism of the maturation cleavage of VP0 in polioviurs assembly: structure of the empty capsid assembly intermediate at 2.9 A resolution. Protein Science *3*, 1651-1669.

Baxter, N., Roetzer, A., Liebig, H.-D., Sedelnikova, S.E., Hounslow, A.M., Skern, T., and P., W.J. (2006). Structure and dynamics of coxsackievirus B4 2A proteinase, an enzyme involved in the etiology of heart diseases. Journal of virology *80*.

Bazan, J.F., and Fletterick, R.J. (1988). Viral cysteine proteases are homologous to the trypsin-like family of serine proteases: structural and functional implications. Proceedings of the National Academy of Sciences of the United States of America *85*, 7872-7876.

Bella, J., and Rossmann, M.G. (1999). Review: rhinovirus and their ICAM receptors. Journal of Structural Biology *128*, 69-74.

Bella, J., and Rossmann, M.G. (2000). ICAM-1 receptors and cold viruses. Pharmaceutica Acta Helvetiae *74*, 291-297.

Bienz, K., Egger, D., Pfister, T., and Troxler, M. (1992). Structural and functional characterization of poliovirus replication complex. Journal of virology *66*, 2740-3747.

Blake, K., and O'Connell, S. (1993). Virus culture (West Smithfield, Londong EC1a 7BE, UK: Blackwell Scientific Publications).

Bode, W., and Huber, R. (1992). Natural protein proteinase inhibitors and their interaction with proteinases. European journal of biochemistry / FEBS *204*, 433-451.

Borman, A.M., Baillyl, J.-H., Girard, M., and Kean, K.M. (1995). Picornavirus internal ribosome entry segments: comparison of translation efficiency and the requirements for optimal internal initiation of translation *in vitro*. Nucleic acids research *23*, 3656-3663.

Borman, A.M., and Kean, K.M. (1997). Intact eukaryotic initiation factor 4G is required for hepatitis A virus internal initiation of translation. Virology *237*, 129-136.

Borman, A.M., Kirchweger, R., Ziegler, E., Rhoads, R.E., Skern, T., and Kean, K.M. (1997). eIF4G and its proteolytic cleavage products: effect on initiation of protein synthesis from capped, uncapped, and IRES-containing mRNAs. RNA *3*, 186-196.

Branden, C., and Tooze, J. (1999). Introduction to protein structure (New York: Garland Publishing).

Buenz, E.J., and Howe, C.L. (2006). Picornaviruses and cell death. Trends in microbiology *14*, 28-36.

Cameron, C.E., Götte, M., and Raney, K.D. (2009). Viral genome replication (Springer).

Castello, A., Alvarez, E., and Carrasco, L. (2011). The multifaceted poliovirus 2A protease: regulation of gene expression by picornavirus proteases. Journal of biomedicine & biotechnology *2011*, 369648.

Cordey, S., Gerlach, D., Junier, T., Zdobnov, E.M., Kaiser, L., and Tapparel, C. (2008). The *cis*-acting replication elements define human enterovirus and rhinovirus species. RNA *14*, 1568-1578.

Crooks, G.E., Hon, G., Chandonia, J.M., and Brenner, S.E. (2004). WebLogo: a sequence logo generator. Genome research *14*, 1188-1190.

Crowder, S., and Kirkegaard, K. (2005). Trans-dominant inhibition of RNA viral replication can slow growth of drug-resistant viruses. Nature genetics *37*, 701-709.

Dasso, M.C., and Jackson, R.J. (1989). On the fidelity of mRNA translation in the nuclease-treated rabbit reticulocyte lysate system. Nucleic acids research *17*, 3129-3144.

DeLano, W.L. (2002). The PyMOL Molecular Graphics System, D. Scientific, ed. (San Carlos, CA, USA).

Domingo, E., and Holland, J.J. (1997). RNA virus mutations and fitness for survival. Annual review of microbiology *51*, 151-178.

Donnelly, M.L., Hughes, L.E., Luke, G., Mendoza, H., ten Dam, E., Gani, D., and Ryan, M.D. (2001). The 'cleavage' activities of foot-and-mouth disease virus 2A site-directed mutants and naturally occurring '2A-like' sequences. The Journal of general virology *82*, 1027-1041.

Egger, D., Teterina, N., Ehrenfeld, E., and Bienz, K. (2000). Formation of the poliovirus replication complex requires coupled viral translation, vesicle production, and viral RNA synthesis. Journal of virology *74*, 6570-6580.

Ehrenfeld, E., Domingo, E., and Roos, R.P. (2010). The picornaviruses (Washington, DC: ASM Press).

Etchison, D., and Fout, S. (1985). Human rhinovirus 14 infection of HeLa cells results in the proteolytic cleavage of the p220 cap-binding complex subunit and inactivates globin mRNA translation *in vitro*. Journal of virology *54*, 634-638.

Etchison, D., Milburn, S.C., Edery, I., Sonenberg, N., and Hershey, J.W. (1982). Inhibition of HeLa cell protein synthesis following poliovirus infection correlates with the proteolysis of a 220,000-dalton polypeptide associated with eucaryotic initiation factor 3 and a cap binding protein complex. J Biol Chem *257*, 14806-14810.

Flanegan, J.B., Petterson, R.F., Ambros, V., Hewlett, N.J., and Baltimore, D. (1977). Covalent linkage of a protein to a defined nucleotide sequence at the 5'-terminus of virion and replicative intermediate RNAs of poliovirus. Proceedings of the National Academy of Sciences of the United States of America *74*, 961-965.

Flint, S.J., Enquist, L.W., Racaniello, V.R., and Skalka, A.M. (2009). Principles of virology: molecular biology, pathogenesis and control of animal viruses (Washington, DC: ASM Press).

Foeger, N., Glaser, W., and Skern, T. (2002). Recognition of eukaryotic initiation factor 4G isoforms by picornaviral proteinases. The Journal of Biological Chemistry *277*, 44300-44309.

Foeger, N., Schmid, E.M., and Skern, T. (2000). Human Rhinovirus 2 $2A^{pro}$ recognition of eukaryotic initiation factor 4GI. The Journal of Biological Chemistry *278*, 33200-33207.

Gamarnik, A.V., and Andino, R. (1998). Switch from translation to RNA replication in a positive-stranded RNA virus. Genes & development *12*, 2293-2304.

Gingras, A.C., Raught, B., and Sonenberg, N. (1999). eIF4 initiation factors: effectors of mRNA recruitment to ribosomes and regulators of translation. Annual review of biochemistry *68*, 913-963.

Gradi, A., Imataka, H., Svitkin, Y.V., Rom, E., Raught, B., Morino, S., and Sonenberg, N. (1998). A novel functional human eukaryotic translation initiation factor 4G. Molecular and cellular biology *18*, 334-342.

Gradi, A., Svitkin, Y.V., Sommergruber, W., Imataka, H., Morino, S., Skern, T., and Sonenberg, N. (2003). Human rhinovirus 2A proteinase cleavage sites in eukaryotic initiation factors (eIF) 4GI and eIF4GII are different. Journal of virology *77*, 5026-5029.

Greve, J.M., Davis, G., Meyer, A.M., Forte, C.P., Yost, S.C., Marlor, C.W., Kamarck, M.E., and McClelland, A. (1989). The major human rhinovirus receptor is ICAM-1. Cell *56*, 839-847.

Gustin, K.E., and Sarnow, P. (2001). Effects of poliovirus infection on nucleo-cytoplasmic trafficking and nuclear pore complex composition. The EMBO journal *20*, 240-249.

Haghighat, A., Svitkin, Y., Novoa, I., Kuechler, E., Skern, T., and Sonenberg, N. (1996). The eIF4G-eIF4E complex is the target for direct cleavage by the rhinovirus 2A proteinase. Journal of virology *70*, 8444-8450.

Hanecak, R., Semler, B.L., Anderson, C.W., and Wimmer, E. (1982). Proteolytic processing of poliovirus polypeptides: antibodies to polypeptide P3-7c inhibit cleavage at glutamine-glycine pairs. Proceedings of the National Academy of Sciences of the United States of America *79*, 3973-3977.

Hellen, C.U., Lee, C.K., and Wimmer, E. (1992). Determinants of substrate recognition by poliovirus 2A proteinase. Journal of virology *66*, 3330-3338.

Herdy, B., Snyers, L., Reithmayer, M., Hinterdorfer, P., and Blaas, D. (2004). Identification of the human rhinovirus serotype 1A binding site on the murine low-density lipoprotein receptor by using human-mouse receptor chimeras. Journal of virology *78*, 6766-6774.

Hewat, E.A., Neumann, E., Conway, J.F., Moser, R., Ronacher, B., Marlovits, T.C., and Blaas, D. (2000). The cellular receptor to human rhinovirus 2 binds around the 5-fold axis and not in the canyon: a structural view. The EMBO journal *19*, 6317-6325.

Hofer, F., Gruenberger, M., Kowalski, H., Machat, H., Huettinger, M., Kuechler, E., and Blaas, D. (1994). Members of the low density lipoprotein receptor family mediate cell entry of a minor-group common cold virus. Proceedings of the National Academy of Sciences of the United States of America *91*, 1839-1842.

Holland, J.J., and Kiehn, E.D. (1968). Specific cleavage of viral proteins as steps in the synthesis and maturation of enteroviruses. Proceedings of the National Academy of Sciences of the United States of America *60*, 1015-1022.

ICTV (2009). International committee on taxonomy of viruses (www.ictvdb.org).

Imataka, H., Gradi, A., and Sonenberg, N. (1998). A newly identified N-terminal amino acid sequence of human eIF4G binds poly(A)-binding protein and functions in poly(A)-dependent translation. The EMBO journal *17*, 7480-7489.

Jackson, R.J., and Kaminski, A. (1995). Internal initiation of translation in eukaryotes: the picornavirus paradigm and beyond. RNA *1*, 985-1000.

Jacobson, M.F., and Baltimore, D. (1968). Morphogenesis of poliovirus. I. Association of the viral RNA with coat protein. Journal of molecular biology *33*, 369-378.

Janner, A. (2006). Crystallographic structural organization of human rhinovirus serotype 16, 14, 3, 2 and 1A. Acta crystallographica Section A, Foundations of crystallography *62*, 270-286.

Joachims, M., Van Breugel, P.C., and Lloyd, R.E. (1999). Cleavage of poly(A)-binding protein by enterovirus proteases concurrent with inhibition of translation *in vitro*. Journal of virology *73*, 718-727.

Johnston, S.L. (2005). Overview of virus-induced airway disease. Proceedings of the American Thoracic Society *2*, 150-156.

Jore, J., De Geus, B., Jackson, R.J., Pouwels, P.H., and Enger-Valk, B.E. (1988). Poliovirus protein 3CD is the active protease for processing of the precursor protein P1 *in vitro*. The Journal of general virology *69 (Pt 7)*, 1627-1636.

Kaminsky, A., Poyry, T.A.A., Skene, P.J., and Jackson, R.J. (2010). Mechanism of initiation site selection promoted by the human rhinovirus 2 internal ribosome entry site. Journal of virology *84*, 6578-6589.

Kerekatte, V., Keiper, B.D., Badorff, C., Cai, A., Knowlton, K.U., and Rhoads, R.E. (1999). Cleavage of Poly(A)-binding protein by coxsackievirus 2A protease *in vitro* and *in vivo*: another mechanism for host protein synthesis shutoff? Journal of virology *73*, 709-717.

Kim, S.S., Smith, T.J., Chapman, M.S., Rossmann, M.C., Pevear, D.C., Dutko, F.J., Felock, P.J., Diana, G.D., and McKinlay, M.A. (1989). Crystal structure of human rhinovirus serotype 1A (HRV1A). Journal of molecular biology *210*, 91-111.

Kistler, A., Avila, P.C., Rouskin, S., Wang, D., Ward, T., Yagi, S., Schnurr, D., Ganem, D., DeRisi, J.L., and Boushey, H.A. (2007). Pan-viral screening of respiratory tract infections in adults with and without asthma reveals unexpected human coronavirus and human rhinovirus diversity. The Journal of infectious diseases *196*, 817-825.

Kitamura, N., Semler, B.L., Rothberg, P.G., Larsen, G.R., Adler, C.J., Dorner, A.J., Emini, E.A., Hanecak, R., Lee, J.J., van der Werf, S.*, et al.* (1981). Primary structure, gene organization and polypeptide expression of poliovirus RNA. Nature *291*, 547-553.

Knowles, N.J., Hovi, T., Hyypiä, T., King, A.M.Q., Lindberg, M., Pallansch, M.A., Palmenberg, A.C., Simmonds, P., Skern, T., Stanway, G.*, et al.* (2011). Picornaviridae (Oxford: Elsevier).

Konig, H., and Rosenwirth, B. (1988). Purification and partial characterization of poliovirus protease 2A by means of a functional assay. Journal of virology *62*, 1243-1250.

Kuyumcu-Martinez, N.M., Joachims, M., and Lloyd, R.E. (2002). Efficient cleavage of ribosome-associated poly(A)-binding protein by enterovirus 3C protease. Journal of virology *76*, 2062-2074.

Kuyumcu-Martinez, N.M., Van Eden, M.E., Younan, P., and Lloyd, R.E. (2004). Cleavage of poly(A)-binding protein by poliovirus 3C protease inhibits host cell translation: a novel mechanism for host translation shutoff. Molecular and cellular biology *24*, 1779-1790.

Laine, P., Blomqvist, S., Savolainen, C., Andries, K., and Hovi, T. (2006). Alignment of capsid protein VP1 sequences of all human rhinovirus prototype strains: conserved motifs and functional domains. The Journal of general virology *87*, 129-138.

Lamphear, B.J., Yan, R., Yang, F., Waters, D., Liebig, H.D., Klump, H., Kuechler, E., Skern, T., and Rhoads, R.E. (1993). Mapping the cleavage site in protein synthesis initiation factor eIF-4 gamma of the 2A proteases from human Coxsackievirus and rhinovirus. J Biol Chem *268*, 19200-19203.

Lamson, D., Renwick, N., Kapoor, V., Liu, Z., Palacios, G., Ju, J., Dean, A., St George, K., Briese, T., and Lipkin, W.I. (2006). MassTag polymerase-chain-reaction detection of respiratory pathogens, including a new rhinovirus genotype, that caused influenza-like illness in New York State during 2004-2005. The Journal of infectious diseases *194*, 1398-1402.

Lau, S.K., Yip, C.C., Lin, A.W., Lee, R.A., So, L.Y., Lau, Y.L., Chan, K.H., Woo, P.C., and Yuen, K.Y. (2009). Clinical and molecular epidemiology of human rhinovirus C in children and adults in Hong Kong reveals a possible distinct human rhinovirus C subgroup. The Journal of infectious diseases *200*, 1096-1103.

Lauring, A.S., and Andino, R. (2010). Quasispecies theory and the behavior of RNA viruses. PLoS pathogens *6*, e1001005.

Lee, W.M., Kiesner, C., Pappas, T., Lee, I., Grindle, K., Jartti, T., Jakiela, B., Lemanske, R.F., Jr., Shult, P.A., and Gern, J.E. (2007). A diverse group of previously unrecognized human rhinoviruses are common causes of respiratory illnesses in infants. PloS one *2*, e966.

Lee, Y.F., Nomoto, A., Detjen, B.M., and Wimmer, E. (1977). A protein covalently linked to poliovirus genome RNA. Proceedings of the National Academy of Sciences of the United States of America *74*, 59-63.

Leong, L.E.C., Cornell, C.T., and Semler, B.L. (2002). Processing determinants and functions of cleavage products of picornavirus polyproteins. In Molecular Biology of Picornaviruses, B.L. Semler, and E. Wimmer, eds. (Washington, DC: ASM Press).

Lin, J.Y., Chen, T.C., Weng, K.F., Chang, S.C., Chen, L.L., and Shih, S.R. (2009). Viral and host proteins involved in picornavirus life cycle. Journal of biomedical science *16*, 103.

Lloyd, R.E. (2006). Translational control by viral proteinases. Virus research *119*, 76-88.

Makela, M.J., Puhakka, T., Ruuskanen, O., Leinonen, M., Saikku, P., Kimpimaki, M., Blomqvist, S., Hyypia, T., and Arstila, P. (1998). Viruses and bacteria in the etiology of the common cold. Journal of clinical microbiology *36*, 539-542.

Malcolm, B.A. (1995). The picornaviral 3C proteinases: cysteine nucleophiles in serine proteinase folds. Protein science : a publication of the Protein Society *4*, 1439-1445.

McIntyre, C.L., McWilliam Leitch, E.C., Savolainen-Kopra, C., Hovi, T., and Simmonds, P. (2010). Analysis of genetic diversity and sites of recombination in human rhinovirus species C. Journal of virology *84*, 10297-10310.

Monto, A.S., and Sullivan, K.M. (1993). Acute respiratory illness in the community. Frequency of illness and the agents involved. Epidemiology and infection *110*, 145-160.

Neubauer, D., Steinberger, J., and Skern, T. (2009). Picornaviruses (Springer).

Nicholson, K.G., Kent, J., and Ireland, D.C. (1993). Respiratory viruses and exacerbations of asthma in adults. BMJ *307*, 982-986.

Norder, H., De Palma, A.M., Selisko, B., Costenaro, L., Papageorgiou, N., Arnan, C., Coutard, B., Lantez, V., De Lamballerie, X., Baronti, C.*, et al.* (2011). Picornavirus non-structural proteins as targets for new anti-virals with broad activity. Antiviral research *89*, 204-218.

Novak, J.E., and Kirkegaard, K. (1991). Improved method for detecting poliovirus negative strands used to demonstrate specificity of positive-strand encapsidation and the ratio of positive to negative strands in infected cells. Journal of virology *65*, 3384-3387.

Nugent, C.I., and Kirkegaard, K. (1995). RNA binding properties of poliovirus subviral particles. Journal of virology *69*, 13-22.

Olson, N.H., Kolatkar, P.R., Oliveira, M.A., Cheng, R.H., Greve, J.M., McClelland, A., Baker, T.S., and Rossmann, M.G. (1993). Structure of a human rhinovirus complexed with its receptor molecule. Proceedings of the National Academy of Sciences of the United States of America *90*, 507-511.

Orr, H.A. (2009). Fitness and its role in evolutionary genetics. Nature reviews Genetics *10*, 531-539.

Pain, V.M. (1996). Initiation of protein synthesis in eukaryotic cells. European journal of biochemistry / FEBS *236*, 747-771.

Palmenberg, A.C. (1982). *In vitro* synthesis and assembly of picornaviral capsid intermediate structures. Journal of virology *44*, 900-906.

Palmenberg, A.C. (1990). Proteolytic processing of picornaviral polyprotein. Annual review of microbiology *44*, 603-623.

Palmenberg, A.C., Rathe, J.A., and Liggett, S.B. (2010). Analysis of the complete genome sequences of human rhinovirus. The Journal of allergy and clinical immunology *125*, 1190-1199; quiz 1200-1191.

Palmenberg, A.C., Spiro, D., Kuzmickas, R., Wang, S., Djikeng, A., Rathe, J.A., Fraser-Liggett, C.M., and Liggett, S.B. (2009). Sequencing and analyses of all known human rhinovirus genomes reveal structure and evolution. Science *324*, 55-59.

Papi, A., and Contoli, M. (2011). Rhinovirus vaccination: the case against. The European respiratory journal : official journal of the European Society for Clinical Respiratory Physiology *37*, 5-7.

Park, N., Katikaneni, P., Skern, T., and Gustin, K.E. (2008). Differential targeting of nuclear pore complex proteins in poliovirus-infected cells. Journal of virology *82*, 1647-1655.

Park, N., Skern, T., and Gustin, K.E. (2010). Specific cleavage of the nuclear pore complex protein Nup62 by a viral protease. J Biol Chem *285*, 28796-28805.

Paul, A.V., van Boom, J.H., Filippov, D., and Wimmer, E. (1998). Protein-primed RNA synthesis by purified poliovirus RNA polymerase. Nature *393*, 280-284.

Petersen, J.F., Cherney, M.M., Liebig, H.D., Skern, T., Kuechler, E., and James, M.N. (1999). The structure of the 2A proteinase from a common cold virus: a proteinase responsible for the shut-off of host-cell protein synthesis. The EMBO journal *18*, 5463-5475.

Porter, A.G. (1993). Picornavirus nonstructural proteins: emerging roles in virus replication and inhibition of host cell functions. Journal of virology *67*, 6917-6921.

Prchla, E., Kuechler, E., Blaas, D., and Fuchs, R. (1994). Uncoating of human rhinovirus serotype 2 from late endosomes. Journal of virology *68*, 3713-3723.

Racaniello, V.R. (2007). Picornaviridae: the viruses and their replication (Philadelphia: Lippincott Williams & Wilkins).

Read, R.J., Fujinaga, M., Sielecki, A.R., and James, M.N. (1983). Structure of the complex of Streptomyces griseus protease B and the third domain of the turkey ovomucoid inhibitor at 1.8-A resolution. Biochemistry *22*, 4420-4433.

Reithmayer, M., Reischl, A., Snyers, L., and Blaas, D. (2002). Species-specific receptor recognition by a minor-group human rhinovirus (HRV): HRV serotype 1A distinguishes between the murine and the human low-density lipoprotein receptor. Journal of virology *76*, 6957-6965.

Renwick, N., Schweiger, B., Kapoor, V., Liu, Z., Villari, J., Bullmann, R., Miething, R., Briese, T., and Lipkin, W.I. (2007). A recently identified rhinovirus genotype is associated with severe respiratory-tract infection in children in Germany. The Journal of infectious diseases *196*, 1754-1760.

Rohll, J.B., Percy, N., Ley, R., Evans, D.J., Almond, J.W., and Barclay, W.S. (1994). The 5' untranslated regions of picornavirus RNAs contain independent functional domains essential for RNA replication and translation. Journal of virology *68*, 4383-4391.

Rossmann, M.G. (1994). Viral cell recognition and entry. Protein science : a publication of the Protein Society *3*, 1712-1725.

Rossmann, M.G., Arnold, E., Erickson, J.W., Frankenberger, E.A., Griffith, J.P., Hecht, H.J., Johnson, J.E., Kamer, G., Luo, M., Mosser, A.G., *et al.* (1985). Structure of a human common cold virus and functional relationship to other picornaviruses. Nature *317*, 145-153.

Rotbart, H.A. (1995). Human enterovirus infections (Washington, DC: ASM Press).

Sarkany, Z., Skern, T., and Polgar, L. (2000). Characterization of the active site thiol group of rhinovirus 2A proteinase. FEBS letters *481*, 289-292.

Savolainen, C., Blomqvist, S., and Hovi, T. (2003). Human rhinoviruses. Paediatric respiratory reviews *4*, 91-98.

Schechter, I., and Berger, A. (1967). On the size of the active site in proteases. I. Papain. Biochemical and biophysical research communications *27*, 157-162.

Seipelt, J., Liebig, H.D., Sommergruber, W., Gerner, C., and Kuechler, E. (2000). 2A proteinase of human rhinovirus cleaves cytokeratin 8 in infected HeLa cells. J Biol Chem *275*, 20084-20089.

Semler, B.L., and Wimmer, E. (2002). Molecular biology of picornaviruses (Washington, DC: ASM Press).

Simmonds, P., McIntyre, C., Savolainen-Kopra, C., Tapparel, C., Mackay, I.M., and Hovi, T. (2010). Proposals for the classification of human rhinovirus species C into genotypically assigned types. The Journal of general virology *91*, 2409-2419.

Skern, T., Sommergruber, W., Auer, H., Volkmann, P., Zorn, M., Liebig, H.D., Fessl, F., Blaas, D., and Kuechler, E. (1991). Substrate requirements of a human rhinoviral 2A proteinase. Virology *181*, 46-54.

Smyth, M.S., and Martin, J.H. (2002). Picornavirus uncoating. Molecular pathology : MP *55*, 214-219.

Sommergruber, W., Ahorn, H., Zophel, A., Maurer-Fogy, I., Fessl, F., Schnorrenberg, G., Liebig, H.D., Blaas, D., Kuechler, E., and Skern, T. (1992). Cleavage specificity on synthetic peptide substrates of human rhinovirus 2 proteinase 2A. J Biol Chem *267*, 22639-22644.

Sommergruber, W., Casari, G., Fessl, F., Seipelt, J., and Skern, T. (1994). The 2A proteinase of human rhinovirus is a zinc containing enzyme. Virology *204*, 815-818.

Sommergruber, W., Seipelt, J., Fessl, F., Skern, T., Liebig, H.D., and Casari, G. (1997). Mutational analyses support a model for the HRV2 2A proteinase. Virology *234*, 203-214.

Sonenberg, N., Morgan, M.A., Merrick, W.C., and Shatkin, A.J. (1978). A polypeptide in eukaryotic initiation factors that crosslinks specifically to the 5'-terminal cap in mRNA. Proceedings of the National Academy of Sciences of the United States of America *75*, 4843-4847.

Sousa, C., Schmid, E.M., and Skern, T. (2006). Defining residues involved in human rhinovirus 2A proteinase substrate recognition. FEBS letters *580*, 5713-5717.

Staunton, D.E., Merluzzi, V.J., Rothlein, R., Barton, R., Marlin, S.D., and Springer, T.A. (1989). A cell adhesion molecule, ICAM-1, is the major surface receptor for rhinoviruses. Cell *56*, 849-853.

Steil, B.P., and Barton, D.J. (2009). *Cis*-active RNA elements (CREs) and picornavirus RNA replication. Virus research *139*, 240-252.

Strebel, K., and Beck, E. (1986). A second protease of foot-and-mouth disease virus. Journal of virology *58*, 893-899.

Svitkin, Y.V., Herdy, B., Costa-Mattioli, M., Gingras, A.C., Raught, B., and Sonenberg, N. (2005). Eukaryotic translation initiation factor 4E availability controls the switch between cap-dependent and internal ribosomal entry site-mediated translation. Molecular and cellular biology *25*, 10556-10565.

Toyoda, H., Nicklin, M.J., Murray, M.G., Anderson, C.W., Dunn, J.J., Studier, F.W., and Wimmer, E. (1986). A second virus-encoded proteinase involved in proteolytic processing of poliovirus polyprotein. Cell *45*, 761-770.

Verdaguer, N., Fita, I., Reithmayer, M., Moser, R., and Blaas, D. (2004). X-ray structure of a minor group human rhinovirus bound to a fragment of its cellular receptor protein. Nature structural & molecular biology *11*, 429-434.

Verlinden, Y., Cuconati, A., Wimmer, E., and Rombaut, B. (2000). Cell-free synthesis of poliovirus: 14S subunits are the key intermediates in the encapsidation of poliovirus RNA. The Journal of general virology *81*, 2751-2754.

Vlasak, M., Blomqvist, S., Hovi, T., Hewat, E., and Blaas, D. (2003). Sequence and structure of human rhinoviruses reveal the basis of receptor discrimination. Journal of virology *77*, 6923-6930.

Voss, T., Meyer, R., and Sommergruber, W. (1995). Spectroscopic characterization of rhinoviral protease 2A: Zn is essential for the structural integrity. Protein science : a publication of the Protein Society *4*, 2526-2531.

Wang, Q.M., Johnson, R.B., Sommergruber, W., and Shepherd, T.A. (1998). Development of *in vitro* peptide substrates for human rhinovirus-14 2A protease. Archives of biochemistry and biophysics *356*, 12-18.

Whitton, J.L., Cornell, C.T., and Feuer, R. (2005). Host and virus determinants of picornavirus pathogenesis and tropism. Nature reviews Microbiology *3*, 765-776.

Wilke, C.O., Wang, J.L., Ofria, C., Lenski, R.E., and Adami, C. (2001). Evolution of digital organisms at high mutation rates leads to survival of the flattest. Nature *412*, 331-333.

Yu, S.F., and Lloyd, R.E. (1991). Identification of essential amino acid residues in the functional activity of poliovirus 2A protease. Virology *182*, 615-625.

[1] Skern's lecture on Virology (http://www.univie.ac.at/Medbch/)

CURRICULUM VITAE

PERSONAL INFORMATION

Name	Martina Aumayr
Date of Birth	February 16th, 1988
Address	Mahlergasse 4, 3100 St. Pölten
Nationality	Austrian
Mobile number	0650/4146124
E-mail	martina.aumayr@gmx.at

EDUCATION

1994-1998	Primary school Englische Fräulein in St. Pölten
1998-2002	Gymnasium der Englischen Fräulein St. Pölten
2002-2006	BRG/BORG St. Pölten with focus on natural sciences
2006-2009	Bachelor Programme in "Medical and Pharmaceutical Biotechnology" at the University of Applied Science (IMC FH Krems)
2009-2012	Master Programme in "Molecular Microbiology and Immune Biology" at the University of Vienna

PRACTICAL EXPERIENCE

August 2007	Summer internship at Vienna University of Technology in collaboration with Medical University of Vienna
July 2008 – Januayr 2009	Practical Training at Baxter Inc. Orth an der Donau (Bachelor thesis)
June 2010 – July 2010	Summer internship at Marinomed Company
November 2010 – January 2012	Master thesis at Vienna University (Department of medical biochemistry, Group of Prof. Tim Skern)

PUBLICATION

Gebeshuber, I.C., Aumayr, M., Hekele, O., Sommer, R., Goesselsberger, C.G., Grünberger, C., Gruber, P., Borowan, E., Rosic, A., and Aumayr, F. (2010). Bacilli, green algae, diatoms and red blood cells - How nano-biotechnological research inspires architecture. Chapter IX in Bio-inspired Nanomaterials and Nanotechnology, Y. Zhou, ed. (Nova Science Publisher), pp. 207-243, ISBN: 978-1-60876-105-0; (2011) Chapter X in Diatoms: Ecology and Life Cycle, C. James, ed. (Nova Science Publisher), New York, pp. 265-300, ISBN: 978-1-61761-979-3